IDENTIFICATION AND CHARACTERISATION OF ENDOGLYCOSIDASE ACTIVITIES TOWARDS DERMATAN SULPHATE BY TANDEM MASS SPECTROMETRY

A thesis presented for the degree of

DOCTOR OF PHILOSOPHY

by

Timothy C. Nielsen BSc(Hons)

Discipline of Paediatrics
The University of Adelaide
Adelaide, South Australia

Lysosomal Diseases Research Unit
Department of Genetic Medicine
Children, Youth and Women's Health Service
Adelaide, South Australia

July, 2009

CONTENTS

SUMMARY

Dermatan sulphate (DS) is a sulphated glycosaminoglycan (GAG) that is widely distributed as proteoglycan throughout the extracellular matrix and at cell surfaces where it plays an important role in many key biological processes. The intra-cellular catabolism of DS commences with endohydrolysis of the polysaccharide chains to oligosaccharides, which are then sequentially degraded from the non-reducing terminus by lysosomal exoenzymes to monosaccharides and inorganic sulphate for transport out of the lysosome and re-utilisation by the cell. Both endo-β-*N*-acetylhexosaminidase (Hyal-1 hyaluronidase) and endo-β-glucuronidase activities towards DS have been proposed. The present study was undertaken to: 1) determine the substrate specificities and sub-cellular locations of these endoglycosidase activities; and 2) compare endoglycosidase activities and substrate specificities in the mucopolysaccharidoses, where a defect in one of the lysosomal exoenzymes required to degrade DS results in the lysosomal accumulation of partially degraded DS oligosaccharide fragments. To this end, a series of oligosaccharide substrates designed to represent aspects of the physiological substrate was prepared, and an assay was developed to measure endoglycosidase activities and determine their substrate specificities by quantifying specific oligosaccharide products.

Assay substrates rich in glucuronic acid (GlcA) or iduronic acid (IdoA) were prepared by limited chondroitinase ABC digestion of chondroitin sulphate A and DS, respectively. The resulting tetra- to hexadecasaccharides were separated by size-exclusion chromatography and characterised by electrospray ionisation-tandem mass spectrometry (ESI-MS/MS). These substrates, which were not susceptible to degradation by lysosomal exoenzymes, were then incubated with Chinese hamster ovary (CHO)-K1 cell homogenate (source of endoglycosidase activity), and the oligosaccharide products generated from the non-reducing end of the substrate were measured by ESI-MS/MS. Endo-β-*N*-acetylhexosaminidase and endohexuronidase activities were detected towards the oligosaccharide substrates, with both activities preferentially degrading the GlcA-rich substrates and only minor activity observed towards IdoA-rich substrate. The endo-β-*N*-acetylhexosaminidase activity had a minimum-sized substrate requirement of a hexasaccharide and was observed to sequentially remove tetrasaccharides from the non-reducing end of oligosaccharides, whereas the

endohexuronidase activity had a minimum substrate of an octasaccharide, acted randomly and was comparatively low. The activities displayed the same acidic pH optimum and responded in the same manner to changes in buffer composition and substrate concentration, and to the presence of divalent cations, NaCl, detergent and protease inhibitors. Both activities were modestly affected by the hyaluronidase inhibitor, apigenin. Percoll density gradient sub-cellular fractionation confirmed that the activities were primarily in the lysosomes and late endosomes. The endo-β-*N*-acetylhexosaminidase and endohexuronidase activities detected here in CHO-K1 cells are consistent with the Hyal-1 and endo-β-glucuronidase enzymes described previously. These data suggest that Hyal-1 and endo-β-glucuronidase are predominantly lysosomal enzymes that act in concert to degrade the low-sulphate, GlcA-rich domains of DS, but are less active towards the highly sulphated regions containing IdoA.

To test the hypothesis that endoglycosidase activities are altered in the mucopolysaccharidoses, an attempt was made to compare Hyal-1- and endo-β-glucuronidase-like activities and their substrate specificities in mucopolysaccharidosis (MPS)-affected and unaffected control skin fibroblasts. However, no activity was detected towards octa- to hexadecasaccharide substrates in control fibroblast homogenates, and in homogenates of MPS fibroblasts deficient in the lysosomal exoenzymes α-L-iduronidase and *N*-acetylgalactosamine-4-sulphatase, despite the fact that: 1) what appear to be the products of Hyal-1 and endo-β-glucuronidase activities towards endogenous DS could be detected in the lysosomes of the MPS cells by sub-cellular fractionation; and 2) the ESI-MS/MS assay was demonstrated sensitive enough to detect endoglycosidase activities in homogenates of a number of different mouse tissues (including whole skin). We hypothesise that this absence of detectable endoglycosidase activity in skin fibroblasts results from enzyme non-recognition of the exogenous assay substrates tested, and hence that these cells contain heretofore undescribed Hyal-1 and endo-β-glucuronidase isoforms with unique substrate specificities.

In conclusion, the development of an ESI-MS/MS assay to measure the products of endoglycosidase activities has enabled the characterisation of these activities towards DS. This strategy may be useful for the future study of endoglycosidase activities towards a variety of other GAGs such as heparan sulphate, where particular oligosaccharide structures have been shown to possess unique biological activities.

DECLARATION

This thesis contains no material which has been accepted for the award of any other degree or diploma in any university or other tertiary institution and, to the best of my knowledge and belief, contains no material previously published or written by another person, except where due reference has been made in the text.

I give consent to this copy of my thesis, when deposited in the University Library, being made available for loan and photocopying, subject to the provisions of the Copyright Act 1968.

I also give permission for the digital version of my thesis to be made available on the web, via the University's digital research repository, the Library catalogue, the Australasian Digital Theses Program (ADTP) and also through web search engines, unless permission has been granted by the University to restrict access for a period of time.

……..

TC NIELSEN

July, 2009

ACKNOWLEDGEMENTS

I would like to sincerely thank the following people for their support over the last few years:

- Dr Maria Fuller, my principal supervisor, for her absolute dedication to the research undertaken, her continued concern for my professional development, and in particular for her rapid feedback and encouragement during the writing phase.

- Prof. John Hopwood, co-supervisor, whose vast experience in the field of glycosaminoglycan biochemistry was a priceless resource in guiding the overall direction of the project and providing a "bigger picture" perspective.

- Assoc. Prof. Peter Meikle, co-supervisor, whose influence is apparent in chapters three and four of this thesis.

- All the members of the LDRU, 2005-2009, who provided not only professional but also emotional support throughout, often while completely unaware that they were doing so. A big thank you to the "Blue Lab" in particular, who could always be relied upon to provide a welcome distraction when required. I'm sure I'm in danger of missing someone out, but here goes: Philippa Davey, Karissa Phillis, Dr Mark Prodoehl, Dr Emma Parkinson-Lawrence, Glenn Borlace, Chris Turner and Dr Anthony Fedele. Thanks also to the guys upstairs, Stephen Duplock and Troy Stomski, and to Prof. Doug Brooks.

- Special thanks to Dr Tomas Rozek, who spent much of his own time showing me the ropes on the mass spec, developing methods and trying to figure out where all those product ions came from!

- Sophie Lazenkas, for her thorough proof-reading of this manuscript.

- My family, whose support in the form of babysitting and other sundries made life a bit easier.

…and finally, my wife, Mara, who deserves an award of some kind for sitting this out with me. Perhaps one day I will be able to repay you. Until then, I can only say: thankyou.

ΔUA	unsaturated uronic acid
amu	atomic mass units
AUX	auxiliary gas
BME	basal modified eagle's medium
BSA	bovine serum albumin
BTH	bovine testicular hyaluronidase
CAD	collision gas
CE	collision energy
CHO	Chinese hamster ovary
CNS	central nervous system
CS	chondroitin sulphate
CUR	curtain gas
CXP	collision cell exit potential
Da	Dalton
DMG	3,3-dimethylglutaric acid
DMSO	dimethylsulphoxide
DNA	deoxyribonucleic acid
DP	declustering potential
DS	dermatan sulphate
DSPG	dermatan sulphate proteoglycan
ECM	extra-cellular matrix
EP	entrance potential
ER	endoplasmic reticulum
ESI	electrospray ionisation
FCS	foetal calf serum
FGF	fibroblast growth factor
FP	focussing potential
GAG	glycosaminoglycan
Gal	galactose
GalNAc	*N*-acetylgalactosamine
GlcA	glucuronic acid
GlcN	glucosamine
GlcNAc	*N*-acetylglucosamine
GPI	glycosylphosphatidylinositol

HC II	heparin cofactor II
HNAc	*N*-acetylhexosamine
HPLC	high performance liquid chromatography
IdoA	iduronic acid
IS	ion spray voltage
ISTD	internal standard
MPS	mucopolysaccharidosis
MPSs	mucopolysaccharidoses
MRM	multiple reaction monitoring
MS	mass spectrometry
MS/MS	tandem mass spectrometry
m/z	mass-to-charge ratio
NEB	nebuliser gas
PBS	phosphate-buffered saline
PG	proteoglycan
PMP	1-phenyl-3-methyl-5-pyrazolone
PMSF	phenylmethanesulphonylfluoride
RHhyal-1	recombinant human Hyal-1
S	sulphate
SPAM-1	sperm adhesion molecule-1
TEM	temperature
UA	uronic acid
UDP	uridine diphosphate
UV	ultraviolet
V_0	void volume
V_t	total volume
Xyl	xylose

LIST OF FIGURES

CHAPTER ONE

CHAPTER THREE

CHAPTER FOUR

CHAPTER FIVE

LIST OF TABLES

PUBLICATIONS

The following publications resulted from the work described in this thesis:

Peer-reviewed journals

Nielsen, T.C., Meikle, P.J., Hopwood, J.J. and Fuller, M. (2008) Minimum substrate requirements of endoglycosidase activities towards dermatan sulfate by electrospray-ionization tandem mass spectrometry *Glycobiology* **18(12)**: 1119-1128

Conference abstracts

Nielsen, T.C., Meikle, P.J., Hopwood, J.J. and Fuller, M. A method to measure endohydrolase products by mass spectrometry *Proceedings of the Australian Health and Medical Research Congress 2006* (abstract #1525)

.....for Isabella

"I cannot express strongly enough my unbounded admiration for the greatness of mind of these men who conceived [the heliocentric system] and held it to be true….in violent opposition to the evidence of their own senses….."

- Galileo, *Dialogue concerning Two Principal Systems of the World (Third Day)*

CHAPTER ONE

INTRODUCTION

1.1 GLYCOSAMINOGLYCANS

Glycosaminoglycans (GAGs) are linear, unbranched anionic polysaccharides generally characterised by a backbone of repeating disaccharide subunits containing an amino sugar (either D-glucosamine, *N*-acetyl-D-glucosamine or the C-4 epimer *N*-acetyl-D-galactosamine) linked to a uronic acid (UA) residue (either D-glucuronic acid or the C5 epimer L-iduronic acid). The exception is keratan sulphate, which contains D-galactose in place of UA (Taylor and Gallo 2006). The five main GAG subtypes, hyaluronan, chondroitin sulphate, dermatan sulphate, heparan sulphate/heparin and keratan sulphate, are distinguished by the composition of their disaccharide subunits, the types of glycosidic linkages between the monosaccharide residues, and also by their degree of modification by sulphation, de acetylation and epimerisation reactions. With the exception of hyaluronan (Tsiganos *et al.* 1986), GAGs are attached to core proteins as proteoglycan (PG), and are widely distributed throughout the extra-cellular matrix (ECM) and at cell surfaces in this form. GAGs play an important role in many key biological processes, including cell adhesion, growth factor signalling, wound repair, infection and tumour metastasis, primarily by interacting with proteins and influencing their activities (Bernfield *et al.* 1999, Trowbridge and Gallo 2002).

1.2 DERMATAN SULPHATE

The GAG, dermatan sulphate (DS), is composed of repeating disaccharide subunits of UA alternating with β-linked (1,4) D-*N*-acetylgalactosamine (GalNAc) residues that may be *O*-sulphated at C4 and/or C6 (referred to as GalNAc(4S), GalNAc(6S) and GalNAc(4S, 6S)). The UA may be α-linked (1,3) iduronic acid (IdoA) or β-linked (1,3) glucuronic acid (GlcA), unsulphated or 2-*O* sulphated (referred to as IdoA(2S) and GlcA(2S)) (Figure 1.1A). DS is also known as chondroitin sulphate (CS)-B, based upon the presence of GalNAc; the presence of variable amounts of IdoA distinguishes DS from CS-A and CS-C, which contain GlcA and 4- and 6-*O* sulphated GalNAc units, respectively (Trowbridge and Gallo 2002). DS forms

block structures with domains of IdoA and high sulphation ("IdoA-rich domains"), and poorly sulphated domains where GlcA prevails ("GlcA-rich domains") (Mitropoulou *et al.* 2001) (Figure 1.1B). DS is found covalently linked to specific serine residues of a core protein *via* the common GAG-core protein linkage tetrasaccharide (xylose, galactose, galactose and GlcA) to form dermatan sulphate proteoglycans (DSPG), where the DS chains of the DSPG extend perpendicularly from the core protein to form a brush-like structure (Figure 1.2). DSPG are produced by most, if not all, vertebrate cells as major components of the ECM, and are also found at the cell surface and basement membranes, and in intra-cellular granules of certain cells (Kjellen and Lindahl 1991, Iozzo 1998, Gowda *et al.* 1990). The overall structure of a DS chain, in terms of length (40-100 disaccharide units), backbone chemical structure and organisation into domains, varies widely according to the tissue and DSPG of origin (Cheng *et al.* 1994).

It should be noted that although DS is by definition distinguished from CS by the presence of IdoA, there is some confusion in the literature concerning the precise classification of a GAG structure that contains both GlcA-GalNAc and IdoA-GalNAc disaccharides. Such GAGs have alternatively been classed as either "DS, with GlcA-rich and IdoA-rich domains", as detailed above (Mitropoulou *et al.* 2001, Fuller *et al.* 2004a), or "CS/DS hybrids" containing "CS-like" (i.e. GlcA-GalNAc) and "DS-like" (i.e. IdoA-GalNAc) sequences (Bao *et al.* 2005, Li *et al.* 2007). For the purposes of this thesis, a GAG chain containing both GlcA-GalNAc and IdoA-GalNAc disaccharides shall be classed explicitly as DS, with the GlcA-GalNAc and IdoA-GalNAc sequences referred to as the "GlcA-rich" and "IdoA-rich" domains of DS, respectively.

1.3 BIOSYNTHESIS OF DERMATAN SULPHATE

The initiating event in DS biosynthesis is the formation of the GAG-core protein linkage tetrasaccharide, which involves the sequential addition of the four monosaccharides (xylose,

A

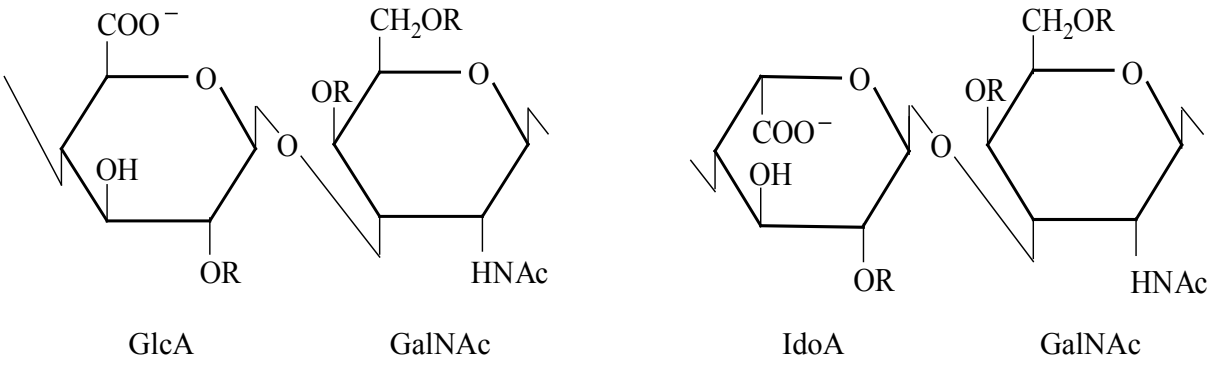

B

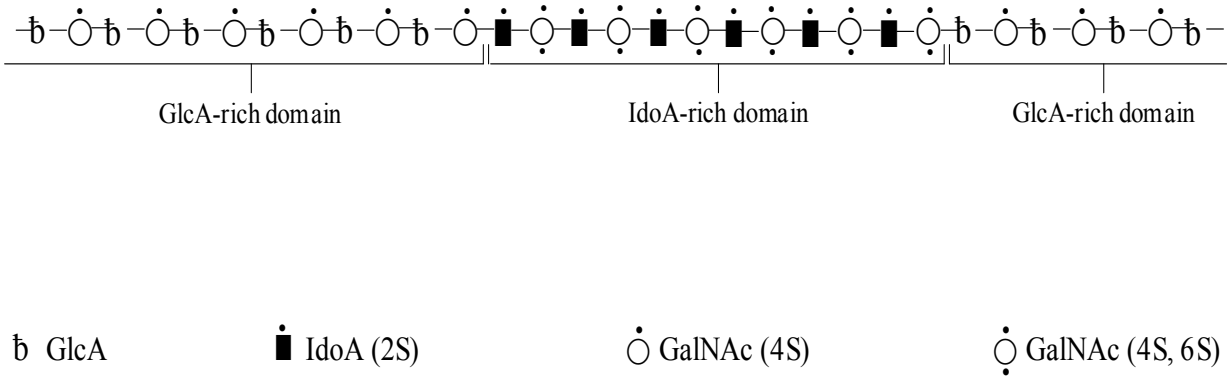

Figure 1.1 Composition of DS

DS is composed of repeating disaccharide subunits containing either glucuronic acid (GlcA) and *N*-acetylgalactosamine (GalNAc), or iduronic acid (IdoA) and GalNAc. Panel A shows the structures of these disaccharide subunits of DS chains (R=H or SO_3^-). Panel B represents the domain structure of DS, where blocks of poorly sulphated GlcA-GalNAc disaccharides (GlcA-rich domains) alternate with blocks of highly sulphated IdoA-GalNAc disaccharides (IdoA-rich domains). The symbols used are defined beneath the figure.

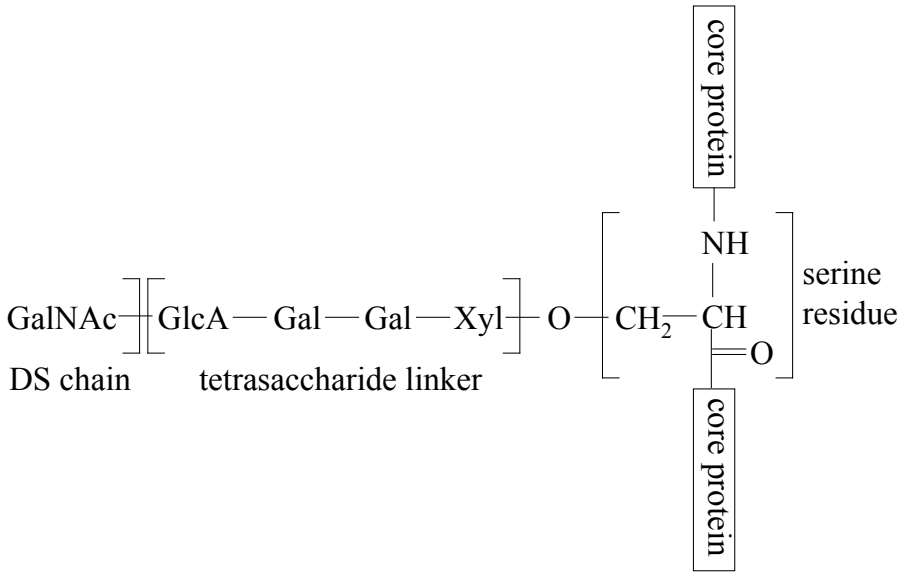

Figure 1.2 Structure of the DS-core protein linkage region in DSPG

Schematic illustrating the structure of the DS-core protein linkage region in DSPG, which comprises a specific tetrasaccharide composed of one xylose residue, two galactose residues and a GlcA residue. This tetrasaccharide linker is coupled at the reducing end to the core protein through an *O*-glycosidic bond between the xylose residue and a specific serine residue in the protein. The DS chain extends from the non-reducing end of the tetrasaccharide linker through a glycosidic linkage between the GlcA residue of the linker and the first GalNAc residue of the DS chain. GalNAc, *N*-acetylgalactosamine; GlcA, glucuronic acid; Gal, galactose; Xyl, xylose.

galactose, galactose and GlcA) to serine residues in the core protein. Xylosylation commences in a late endoplasmic reticulum (ER) compartment and continues into intermediate compartments, perhaps including the *cis*-Golgi (Kearns *et al.* 1993, Vertel *et al.* 1993). The two galactose units are then added by separate membrane-bound transferases, which localise to different sub-regions of the Golgi (Sugumaran *et al.* 1992, Etchison *et al.* 1995). Construction of the tetrasaccharide is completed by the addition of a GlcA by GlcA transferase I, which occurs close to the site of backbone polymer synthesis in the *medial-/trans*-Golgi, but distal from the location of the Gal transferases (Sugumaran *et al.* 1998). At this point, a sulphate may be added to C4 of one or both Gal residues, possibly by the same enzyme that adds sulphate to the GalNAc residues of the DS polymer (Sugahara and Kitagawa 2000, Sugahara *et al.* 1991). Phosphorylation of the linkage tetrasaccharide has also been observed in DS and is believed to occur in the ER and/or Golgi (Prydz and Dalen 2000). While phosphorylation is a stable modification in some DS species, it is a transient phenomenon in others. In the DSPG, decorin, for example, phosphorylation of the linkage sequence gradually increases as each of the first three monosaccharides is added, but the subsequent addition of GlcA leads to a rapid de-phosphorylation (Moses *et al.* 1997 and 1999). It has been suggested that this transient phosphorylation of the linkage tetrasaccharide acts as a signal during intra-cellular trafficking of PG, and/or in the control of modification to the glycan chain (Prydz and Dalen 2000).

Synthesis of the linkage tetrasaccharide is followed by the alternate addition of GalNAc and GlcA from uridine diphosphate (UDP)-activated precursors to the non-reducing end of the nascent oligosaccharide in the *medial-/trans*-Golgi, resulting in the formation of a backbone polymer chain of up to 70 kDa (Silbert and Sugumaran 2002, Velasco *et al.* 1988). Elongation of this backbone appears to be mediated by distinct GlcA- and GalNAc-transferases (Silbert and Reppucci 1976, Sugumaran *et al.* 1997) and is concomitant with a series of enzymatic reactions that modify the individual monosaccharide components. These

modifications may include: *O*-sulphation of GalNAc residues at C 4 and/or C 6; C 5 epimerisation of GlcA residues to IdoA; and *O*-sulphation of the GlcA and IdoA residues at C2. Although the precise order of these events is unclear, 6-*O* sulphation of GalNAc in the *medial-/trans*-Golgi by GalNAc 6-*O* sulphotransferase is probably the first. This is believed to stimulate some 2-*O* sulphation of the adjacent GlcA residues by uronyl 2-*O* sulphotransferase (Silbert and Sugumaran 2002). Four-*O* sulphation of GalNAc by GalNAc 4-*O* sulphotransferase occurs in a later *trans*-Golgi region, and encourages epimerisation of some adjoining GlcA residues to IdoA by uronyl C5 epimerase. The IdoA residues may, in turn, become a substrate for the transfer of sulphate by uronyl 2-*O* sulphotransferase (Silbert *et al.* 1991, Kobayashi *et al.* 1999). As the latter reaction requires a sulphated and epimerised substrate, it is likely to be the final step in DS biosynthesis and therefore occur in a late Golgi compartment.

Although the biosynthetic modification of the individual disaccharide subunits of DS is not uniform, such that some are highly modified and others unmodified, the highly specific nature of the DS biosynthetic enzymes leads to clustering of the modified disaccharides containing high sulphation and IdoA into the regions referred to as "IdoA-rich domains" along the DS backbone (Mitropoulou *et al.* 2001). Chain termination appears to be precipitated by the presence of specific sulphation patterns towards the non-reducing end of the polymer and, in particular, from the proportion of GalNAc(4S) and GalNAc(4S, 6S) units in this region (Kitagawa *et al.* 1997a and b, Otsu *et al.* 1985).

1.4 BIOLOGICAL FUNCTIONS OF DERMATAN SULPHATE

DS has a wide variety of important biological functions that are imparted by the complexities of its composition, from its overall macromolecular shape to the intricacies of its fine structure. For example, as a result of their rigid linear configuration and hydrophilic nature, DS chains adopt extended conformations in the ECM that occupy a huge volume relative to

their mass, and form highly hydrated gels that resist compressive forces upon the matrix while providing mechanical support to tissues (Culav *et al.* 1999). DS also binds to a diverse range of biologically important molecules including (but not limited to) matrix molecules, growth factors, protease inhibitors, cytokines, chemokines, and pathogen virulence factors (Table 1.1). These binding interactions result from electrostatic attractions between the binding partner and particular structural sequences on the DS strand. Interaction with DS may contribute to or modify the biological functions of the binding partner (Trowbridge and Gallo 2002).

The ability of DS to modulate the function of bioactive molecules is exemplified by its interaction with heparin cofactor II (HCII), a homologue of antithrombin III that acts by inhibiting the pro-coagulative effect of thrombin. This effect is enhanced 1000-fold in the presence of DS, possibly due to the formation of a stable ternary complex in which both HCII and thrombin bind *via* ionic attraction to a single DS chain (Liaw *et al.* 2001). HCII binding appears to be influenced by the overall sulphation of the DS chain and by the presence of IdoA(2S)-GalNAc(4S) and IdoA(2S)-GalNAc(4S,6S) disaccharides in particular (Halldorsdottir *et al.* 2006, Denti *et al.* 1995). Another well-studied DS binding interaction occurs with the fibroblast growth factors (FGFs), which are key players in the wound repair process. DS has been shown to bind and promote FGF-2 and -7-dependent cellular proliferation, with the most active DS structures rich in monosulphated (primarily 4-*O* sulphated) disaccharides and IdoA (Penc *et al.* 1998, Taylor *et al.* 2005). Further elucidation of the DS sequences that make up the binding sites in these and other biologically relevant associations may lead to the development of inhibitors and/or modulators of these interactions.

Table 1.1 Binding interactions of DS

Binding protein	Binding sequence[a]	Physiological effect
heparin cofactor II	-IdoA(2S)-GalNAc(4S)-hexasaccharide	enzymatic inactivation of thrombin
thrombin	n.d.	anti-coagulation
activated protein C	n.d.	anti-coagulation
protein C inhibitor	n.d.	stimulates serpin activity
platelet factor 4	n.d.	unknown
tenascin-x	binds GAG chain	collagen matrix stability
α-defensin	n.d.	increased infectivity
RANTES	n.d.	modulation of inflammatory response
interferon-γ	n.d.	receptor for INF-γ
FGF-1 and -2	n.d.	cellular proliferation *via* tyrosine kinase activation
low-density lipoprotein	n.d.	atherosclerotic plaque stabilisation
hepatocyte growth factor/scatter factor	-IdoA-GalNAc(4S)-octasaccharide	cellular proliferation, organogenesis, tumourigenesis

[a] IdoA, iduronic acid; GalNAc, *N*-acetylgalactosamine; S, sulphate; n.d., not determined

Table adapted from Trowbridge and Gallo (2002)

1.5 DEGRADATION OF DERMATAN SULPHATE

Degradation of DS chains occurs as part of the normal cellular recycling of DSPG, which is initiated by the binding of the intact DSPG molecule to specific receptors on the cell surface. The DSPG-receptor complex is internalised into clathrin-coated pits and traverses a mildly acidic endocytic network thought to comprise at least two distinct compartments, the early endosome and the prelysosome (late endosome), during which time extensive proteolysis of the DSPG core protein occurs to liberate single DS chains bound to peptides as intermediates (Feugaing *et al.* 2007, Hoppe *et al.* 1988, Griffiths and Gruenberg 1991). The peptide-DS intermediates are ultimately trafficked to the lysosome, where endoenzymes (endo-β-galactosidase, endo-β-xylosidase and endo-β-glucuronidase) first cleave within the linkage tetrasaccharide to clip the DS chain from the peptide (Takagaki *et al.* 1988a and b). Finally,

the free DS chains are sequentially degraded from the non-reducing terminus by a series of exoenzyme activities to produce monosaccharides and inorganic sulphate for transport out of the lysosome and re-utilisation by the cell. In addition, endoglycosidases cleave the internal bonds of the DS chains, increasing the number of target sites available for the exoenzymes (Neufeld and Muenzer 2001).

1.5.1 Endodegradation of dermatan sulphate

The catabolism of DS chains commences with endohydrolysis of the polysaccharides to oligosaccharides. A number of endoglycosidases with the capacity to cleave the internal glycosidic linkages of DS have been identified that may participate in this process. The hyaluronidases are a family of endo-β-*N*-acetylhexosaminidases that principally degrade hyaluronan, but have also demonstrated the limited ability to cleave internal β-linked (1,4) glycosidic linkages between GalNAc and GlcA in CS (Kreil 1995), and it is predicted that the corresponding linkages in DS would also be susceptible. In the human genome there are six known genes coding for hyaluronidase sequences, all of which have a high degree of homology: the *HYAL-1*, *HYAL-2* and *HYAL-3* genes are clustered on chromosome 3p31.3 and code for the Hyal-1, Hyal-2 and Hyal-3 proteins, respectively; *HYAL-4* (coding for Hyal-4), *PH-20/SPAM-1* (coding for PH20), and the pseudogene, *PHYAL-1*, are similarly clustered on chromosome 7q31.3 (Csóka *et al.* 2001). As two deletions in the human *PHYAL-1* sequence cause premature stop codons, the gene does not encode an active DS-degrading hyaluronidase (Csóka *et al.* 1999). However, a full-length expression sequence of *PHYAL-1* has been identified from a mouse testis cDNA library that does not contain any mutations, indicating that this gene may encode an active hyaluronidase enzyme in other mammals (Csóka *et al.* 2001).

Hyal-1 is generally considered the major intra-cellular hyaluronidase of the somatic tissues (Stern 2003) and has been isolated from various sources, including plasma (Frost *et al.*

1997), serum (Afify *et al.* 1993), urine (Csóka *et al.* 1997), liver (Gold 1982) and placenta (Yamada *et al.* 1977). The product of the *HYAL-1* gene is a 57 kD a single polypeptide glycoprotein (Frost *et al.* 1997), however, the broad range of molecular sizes attributed to purified Hyal-1 (from 45- to 76 kDa for that purified from urine and liver, respectively) points to the existence of multiple isoforms. Nevertheless, the aforementioned studies consistently report a pH optimum of 3.8, with no enzymatic activity observed at neutral pH, which strongly infers that any Hyal-1 activity towards DS is confined to the lysosome.

The substrate specificity and other catalytic properties of Hyal-1 have been studied in some detail. Since hyaluronan is the primary physiological substrate, almost all of these studies have been conducted using hyaluronan, an extremely simple GAG composed entirely of repeating unsulphated disaccharide units containing β-linked GlcA and *N*-acetylglucosamine. However, as mentioned above, the hyaluronidases are also able to degrade the β-linked GalNAc-GlcA linkages of CS, albeit at a slower rate (Stern 2003), and hence their mode of action towards hyaluronan should also apply to the GlcA-rich domains of DS where GalNAc-GlcA bonds are concentrated. Analysis of the catabolic products of a recombinant human hyal-1 (RHhyal-1) recently produced in an insect cell expression system revealed a minimum-sized substrate requirement of an octasaccharide (Hofinger *et al.* 2007a). A continuous degradation of high-molecular-weight hyaluronan to smaller fragments and finally to oligosaccharides (di- to octasaccharides) by RHhyal-1 was observed, with hexasaccharides as the main reaction products (Hofinger *et al.* 2008). This contrasts with previous studies reporting the end product of placenta- and chick embryo fibroblast-derived Hyal-1 as a tetrasaccharide (Yamada *et al.* 1977, Orkin and Toole 1980). Degradation by Hyal-1, as with all the human hyaluronidases, is believed to occur through an endolytic, "random-bite" (i.e. non-processive) mechanism, whereby the catabolic products leave the active site of the enzyme after each cleavage reaction to become substrates for further cleavage (Stern and Jedrzejas 2006). A central aim of this thesis was to characterise the

substrate specificities and catalytic mechanisms of Hyal-1 as they apply to the specific degradation of DS oligosaccharides.

Hyal-2 mRNA and protein are found in many human and mouse tissues (Lepperdinger *et al.* 1998). The enzyme has an acidic pH optimum and is found in the lysosome, however, the very low activity of Hyal-2 relative to other hyaluronidases such as PH20 and Hyal-1 (Lepperdinger *et al.* 2001) indicates that its role in DS turnover is likely to be limited. Hyal-2 has an unusual substrate specificity, degrading high-molecular-weight hyaluronan to intermediate-sized fragments of approximately 20 kDa, or 50 disaccharide units (Lepperdinger *et al.* 2001). This raises the proposition that endodegradation of DS (and other GAGs susceptible to cleavage by the hyaluronidases) may in fact be a two-step process, whereby Hyal-2 makes initial cleavages in the macromolecular chain to produce polysaccharide fragments, which are further digested to oligosaccharides by Hyal-1. A portion of Hyal-2 is also found tethered to the plasma membrane *via* a glycosylphosphatidylinositol (GPI) link where it serves as the cell entry receptor for the lung cancer-inducing jaagsiekte sheep retrovirus (Rai *et al.* 2001), but the hyaluronidase function of the protein is unlikely to be active in the pH-neutral extra-cellular milieu.

Hyal-3 and Hyal-4 are poorly characterised, and their roles in DS degradation are not well understood. Hyal-3 is widely expressed throughout the somatic tissues at very low levels (Shuttleworth *et al.* 2002). The mouse *HYAL-3* gene product has recently been expressed in baby hamster kidney cells and found to comprise a 45- to 56 kDa glycoprotein that appears to lack hyaluronidase activity *per se*, but may augment the hyaluronidase activity of Hyal-1 (Hemming *et al.* 2008). This suggests that any role for Hyal-3 in the degradation of DS is likely to be peripheral, for example by serving as an intra-cellular DS binding protein or by stabilising the Hyal-1 enzyme during transport through intra-cellular compartments (Hemming *et al.* 2008). Early evidence suggests that Hyal-4 is restricted to placenta and skeletal muscle (Csóka *et al.* 2001). The enzyme is GPI-linked to the plasma membrane and

appears to have absolute specificity for the GalNAc-GlcA linkages of CS (and possibly DS), with no activity against hyaluronan (Stern 2003).

The PH-20 hyaluronidase, or sperm adhesion molecule 1 (SPAM-1), is found primarily on the plasma membrane of mammalian sperm and is important during the process of fertilisation, where it facilitates sperm penetration of the hyaluronan-rich ECM that surrounds the oocyte (Meyers *et al.* 1997). Although a second PH-20 isoform with activity at acidic pH is also found in the lysosome-derived acrosome of sperm (Cherr *et al.* 2001), it has yet to be determined if this acidic isoform is present in the lysosomes of other cell types where it could be active in the degradation of DS. The commercially available PH-20 preparation from bovine testes ("bovine testicular hyaluronidase") exhibits a bimodal pH-activity curve due to the presence of both isoforms and has a minimum substrate requirement of a hexasaccharide, whereas recombinant human PH-20, which consists of a single enzymatically active protein of 56 kDa, has a slightly acidic pH optimum and a minimum substrate requirement of an octasaccharide (Hofinger *et al.* 2007a and 2008). Both the bovine and the recombinant human PH-20 will degrade hyaluronan down to tetra-, hexa- and octasaccharides as the main reaction products (Hofinger *et al.* 2008), and it is likely that the susceptible regions of DS would be similarly degraded. An exo-endolytic catabolic mechanism has been described for the bovine PH-20, whereby the enzyme sequentially removes disaccharides from the non-reducing end of oligosaccharide substrates (Takagaki *et al.* 1994). In addition to the testes, PH-20 expression has also been detected in the epididymis (Deng *et al.* 2000), breast (Beech *et al.* 2002) and female reproductive tract (Zhang and Martin-DeLeon 2003), suggesting a host of, as yet, undiscovered functions.

In addition to the hyaluronidases, which are endo-β-*N*-acetylhexosaminidases, an acid-active endo-β-glucuronidase enzyme that may cleave GlcA-GalNAc linkages in DS has been found in the liver, kidney, spleen and lung of the rabbit (Takagaki *et al.* 1985 and 1988b). The catalytic mechanisms of this endo-β-glucuronidase have not been characterised, but early

reports using CS as substrate indicate that it will hydrolyse the GlcA-galactose bond of the tetrasaccharide linkage region that connects the GAG to the short peptide intermediates derived from proteolysis of the core protein, and then further degrade the GlcA-GalNAc bonds of these liberated chains to produce oligosaccharides. Although DS was not specifically tested as a substrate, it is predicted that the enzyme would also degrade the GlcA-GalNAc linkages contained within the GlcA-rich domains of DS. The minimum-sized substrate of this endo-β-glucuronidase has not been fully elucidated but is at least the size of an octasaccharide (Takagaki *et al.* 1985 and 1988b).

While the major endoglycosidases predicted to be involved in the intra-cellular degradation of DS (i.e. Hyal-1 and endo-β-glucuronidase) are strictly acid-active (Stern 2003, Takagaki *et al.* 1988b) and thus unlikely to operate outside of the lysosome/late endosome, the precise intra-cellular site of DS endodegradation has yet to be confirmed. Pre-digestion of DS by endoglycosidases appears to facilitate further degradation by generating many intermediate-sized oligosaccharides for simultaneous catabolism by lysosomal exoenzymes (Neufeld and Muenzer 2001). As there are no reported enzymes that will cleave the internal glycosidic linkages of DS that contain IdoA, it is probable that the highly sulphated, IdoA-rich domains of DS are degraded directly by exoenzyme activities without pre-digestion by endoglycosidases.

1.5.2 Exodegradation of dermatan sulphate

Following partial catabolism by endoglycosidases, the final step of DS degradation occurs by the action of highly specific exoenzymes, which reduce the oligosaccharides to monosaccharides and inorganic sulphate (Neufeld and Muenzer 2001). This process occurs in the lysosome and requires the activity of up to seven exoenzymes (up to four sulphatases and up to three exoglycosidases) which, in contrast to the endoglycosidases described in section 1.5.1, can only hydrolyse linkages at the non-reducing termini of DS and must therefore act

sequentially. The step-wise action of these seven exoenzymes is illustrated in Figure 1.3. Hydrolysis of C2 sulphate bonds from non-reducing terminal IdoA residues results from the action of iduronate-2-sulphatase and precedes the removal of the IdoA by α-L-iduronidase. If present, the 4- and/or 6-sulphate esters of the newly-exposed non-reducing terminal GalNAc are hydrolysed by *N*-acetylgalactosamine-4-sulphatase (arylsulphatase B) and *N*-acetylgalactosamine-6-sulphatase, respectively, followed by removal of the GalNAc by one of three β-hexosaminidase isozymes (A, B or S). Glucuronate-2-sulphatase then acts upon the C2 sulphate ester of non-reducing GlcA and, finally, non-reducing terminal GlcA residues are hydrolysed by β-glucuronidase. The monosaccharide and inorganic sulphate products of DS catabolism exit from the lysosome by specific transporters (Mancini *et al.* 1989, Jonas and Jobe 1990) and may subsequently be re-utilised by the cell.

1.6 THE MUCOPOLYSACCHARIDOSES

With the exception of glucuronate-2-sulphatase, where enzyme-deficient patients have not been described, a deficiency in any one of the lysosomal exoenzyme activities required to degrade DS results in the lysosomal accumulation of the partially degraded DS substrates for these exoenzyme activities. Lysosomal storage leads to cell, tissue and organ dysfunction and the urinary secretion of partially degraded GAG, which may in turn lead to clinical symptoms of the mucopolysaccharidoses (MPSs) (Neufeld and Muenzer 2001). As outlined in Table 1.2, five of the eleven reported MPSs result from deficiencies in exoenzymes involved in the degradation of DS and are characterised by the lysosomal accumulation of partially degraded DS: mucopolysaccharidosis (MPS) I, resulting from a deficiency in α-L-iduronidase; MPS II (iduronate-2-sulphatase deficiency); MPS IVA (*N*-acetylgalactosamine-6-sulphatase deficiency); MPS VI (*N*-acetylgalactosamine-4-sulphatase deficiency); and MPS VII (β-glucuronidase deficiency). A modest accumulation of DS also occurs in Sandhoff disease, which results from a deficiency in the major A and B isozymes of β-hexosaminidase,however,

Figure 1.3 Exodegradation of DS

Schematic representation of the exodegradation of DS, which proceeds in a step-wise fashion from the non-reducing end by the sequential action of up to seven exoenzymes: iduronate-2-sulphatase (1); α-L-iduronidase (2); *N*-acetylgalactosamine-4-sulphatase (3); *N*-acetylgalactosamine-6-sulphatase (4); β-hexosaminidase (A, B or S isozyme) (5); glucuronate-2-sulphatase (6); and β-glucuronidase (7). Adapted from Neufeld and Muenzer (2001).

Table 1.2 Classification of MPSs resulting from deficiencies in DS-degrading exoenzymes

NOTE:
This figure is included on page 17 of the print copy of the thesis held in the University of Adelaide Library.

the low residual level of the minor S isozyme is able to prevent a frank MPS phenotype in these patients (Sango *et al.* 1996). All of the exoenzymes that are required for DS degradation are common to the catabolic pathways of other GAGs, and hence storage of other GAG types is a feature of the DS-storing MPSs.

In addition to the MPSs that result from exoenzyme deficiencies, a deficiency in the endoglycosidase, Hyal-1, has also been reported in a patient with lysosomal storage of hyaluronan and designated MPS IX (Natowicz *et al.* 1996). Given that Hyal-1 will degrade the GalNAc-GlcA linkages of CS (and presumably DS) in addition to the *N*-acetylglucosamine-GlcA bonds of hyaluronan, it is predicted that some lysosomal storage of DS and CS would also occur in this MPS.

The MPS disorders are chronic and progressive, and display a broad spectrum of clinical severity both within and between the eleven major types. However, most of the disorders are characterised by multi-system involvement, organomegaly, abnormal facies, dystostosis multiplex (a specific pattern of radiologic changes caused by defective bone formation) and impairments in hearing, vision, respiration, cardiovascular function and joint mobility (Muenzer 2004). The clinical presentation for MPS may be influenced by a combination of factors, including genotype, the level of residual enzyme present, the catalytic capacity of the residual enzyme, and the type and amount of GAGs that accumulate. In general, patients with an MPS in which CS, DS or keratan sulphate is stored (MPS IVA, MPS VI) exhibit severe skeletal abnormalities, whereas MPS in which only heparan sulphate is stored (MPS III) exhibit primarily CNS pathologies. Deficiency in common enzymes required for both DS and heparan sulphate degradation (MPS I, MPS II, MPS VII) may result in both skeletal and CNS pathology (e.g. MPS IH, rapid progressing MPS II). The hyaluronidase-deficient MPS IX patient had a mild clinical phenotype, including periarticular soft tissue masses, mild short stature, an absence of neurological or visceral involvement, and histological and ultrastructural evidence of an MPS (Natowicz *et al.* 1996).

A number of mutations in the genes encoding the DS-degrading exoenzymes that may result in enzyme deficiency have been identified. Most are point mutations or small changes in the gene, but some major DNA re-arrangements and large deletions have been observed in the iduronate-2-sulphatase gene in MPS II (Neufeld and Muenzer 2001). As the clinical severity of the MPSs is thought to relate in part to the residual level of functional enzyme that is able to partially catabolise DS and other GAGs, it is expected that those mutations that result in a complete ablation of enzyme activity would be associated with the severe forms of disease, and genotype-phenotype correlation is possible in some cases. For instance, the null alleles W402X and Q70X, which together account for the majority of the MPS I alleles in the European population (Bunge *et al.* 1994), result in no enzyme activity whatsoever and are associated with the severe form of α-L-iduronidase deficiency, MPS IH (Scott *et al.* 1992a and b), while a frameshift mutation that allows the synthesis of some normal α-L-iduronidase has been linked to the attenuated phenotype, MPS IS (Moskowitz *et al.* 1993, Scott *et al.* 1993a). Interestingly, cultured skin fibroblasts from a patient with this frameshift mutation produce α-L-iduronidase at a level 0.13% of normal, indicating that only a fraction of normal enzyme activity is required to significantly reduce disease severity (Ashton *et al.* 1992). Other genotype-phenotype correlations are not as straight-forward, with the R468W mutation reported in both slow- and rapid-progressing MPS II patients (Crotty *et al.* 1992, Isogai *et al.* 1998). Therefore, it is generally accepted that a patient's overall clinical phenotype will reflect a combination of unique environmental and genetic factors in addition to their specific mutation, such as the presence of gene polymorphisms that may modify expression and affect enzyme function (Scott *et al.* 1993b).

Although a number of important biological functions have been ascribed to DS, the precise association between the particular DS oligosaccharides that accumulate in the DS-storing MPSs and disease pathogenesis is not clear. There have been a number of studies to characterise DS in the MPSs. DS oligosaccharides have been purified from the urine of MPS I

and II patients using a combination of anion exchange and size-exclusion chromatography, characterised using electrospray ionisation-tandem mass spectrometry (ESI-MS/MS) and partially sequenced with recombinant exoenzymes (Fuller *et al.* 2004a and 2006). Oligosaccharides ranging in size from di- to hexadecasaccharides and with varying degrees of sulphation were identified. The presence of DS oligosaccharides containing both GalNAc and UA at the reducing terminus confirmed that both the endo-β-*N*-acetylhexosaminidase and endohexuronidase activities participate in the intra-cellular endodegradation of DS by cleaving the polysaccharide at internal GalNAc-UA and UA-GalNAc glycosidic linkages, respectively. The relatively small sizes of the oligosaccharides terminating in UA (tri- to heptasaccharide) possibly reflects endohexuronidase substrate specificity for terminal regions of DS chains. As the DS oligosaccharides identified contained, on average, only one sulphate per disaccharide, it was inferred that cleavage of DS by both the endo-β-*N*-acetylhexosaminidase and endohexuronidase activities had occurred in the GlcA-rich domains, which are low in sulphation, and hence that these activities represent the acid-active Hyal-1 and endo-β-glucuronidase enzymes described in section 1.5.1. Similarly, Hochuli *et al.* (2003) analysed urinary DS of MPS I, II and VI patients using nuclear magnetic resonance and determined that the major repeating disaccharide unit in excreted DS is composed of unsulphated IdoA and GalNAc(4S) residues.

Some insight into the mechanisms by which the stored DS in the MPSs may influence disease pathology has been provided by studies into the underlying causes of degenerative joint disease in the MPSs, which show that articular chondrocytes cultured from MPS VI animals undergo apoptosis at a higher rate than normal cells, and indicate that this lysis may be induced *in vivo* by DS accumulation in the ECM (Simonaro *et al.* 2001). Based upon these findings, the authors proposed that the age-progressive accumulation of DS fragments in articular chondrocytes in MPS VI patients enhances the propensity for cell death, whereupon the release of bioactive GAG fragments from lysosomes into the extra-cellular environment

perturbs the normal cartilage matrix homeostasis, leading to pathology. By this theory, the varying degree of skeletal involvement observed in the various MPSs may depend, in part, upon individual differences in the quantities and structures of the DS fragments that are accumulating and being released into the surrounding matrix upon cell death. Such a theory, if correct, need not be limited to chondrocytes and may be evoked on a broader scale as one possible explanation for the diversity of clinical symptoms observed in the MPSs. To date, there are no reports of similar studies using other cell types. Accumulation of hyaluronan within the articular cartilage has recently been shown to result in osteoarthritis in a murine model of MPS IX (Martin *et al.* 2008), but it has not yet been established whether the deficiency in Hyal-1 also results in concomitant accumulation of DS at levels sufficient to influence pathology.

1.7 MASS SPECTROMETRY OF DERMATAN SULPHATE OLIGOSACCHARIDES

The importance of DS structure in the mediation of biological activities has given rise to a number of techniques being developed for the analysis of DS and DS-derived oligosaccharides. High-molecular-weight DS has been analysed by cellulose acetate, nitrocellulose, agarose gel and polyacrylamide gel electrophoresis to yield information about physical properties of the chains, such as charge polydispersity and molecular size (Volpi and Maccari 2006). DS oligosaccharides can be measured as fluorescent derivatives following separation by methods such as high-performance liquid chromatography, size-exclusion chromatography or capillary electrophoresis (Kitagawa *et al.* 1995, Volpi 2000, Koketsu and Linhardt 2000). Furthermore, unsaturated oligosaccharides resulting from depolymerisation of DS by the bacterial chondroitinases can be monitored by UV absorbance at a wavelength of 232 nm (Karamanos *et al.* 1994). Byers and co-workers (1998) described the application of gradient polyacrylamide gel electrophoresis for the analysis of GAGs from MPS urine and

tissues, which enabled the identification of DS oligosaccharides ranging in size from high-molecular-weight structures down to small tetra- and hexasaccharides.

More recently, ESI-MS/MS has proven a useful tool for the analysis of oligosaccharides, offering high sensitivity, a soft ionisation approach amenable to maintaining oligosaccharide structure, and compatibility with up-front, in-line liquid chromatography systems (Zaia 2004). Using ESI-MS/MS, ionised oligosaccharides can be identified on the basis of mass-to-charge ratios and their composition further elucidated by collision-induced dissociation, which produces characteristic fragmentation ions derived from the cleavage of specific bonds within the oligosaccharide. There have been several reports on the use of ESI-MS/MS for the identification and characterisation of DS oligosaccharides. Fuller *et al.* (2004a and 2006) employed ESI-MS/MS for the structural characterisation of DS oligosaccharides purified from the urine of MPS patients. In these studies, ESI-MS/MS enabled the identification of di- to hexadecasaccharides containing even and odd numbers of saccharide residues and various degrees of sulphation, and could confirm the identity of the reducing end terminal sugar residue of these oligosaccharides as either GalNAc or UA. ESI-MS/MS has also been used in conjunction with capillary electrophoresis for the study of over-sulphated DS oligosaccharides derived from the DSPG decorin, enabling the identification and characterisation of structures ranging in size from hexa- to eicosasaccharides (Zamfir *et al.* 2003 and 2004).

In addition to providing structural information, ESI-MS/MS may be used in the multiple reaction monitoring (MRM) mode for the quantification of oligosaccharides. MRM enables specific oligosaccharides to be measured by selectively monitoring the signal intensity produced by their unique parent ion/fragmentation ion transitions. The signal intensities produced by the oligosaccharide MRM transitions are related to that produced by a suitable internal standard. ESI-MS/MS is now commonly employed for determination of the variously sulphated disaccharides that result from enzymatic digestion of DS (Oguma *et al.*

2007, Miller *et al.* 2006, Barroso *et al.* 2005), and has been used to measure DS-derived oligosaccharides in biological samples (urine, plasma, blood spots and skin fibroblasts) (Ramsay *et al.* 2003, Fuller *et al.* 2004a and b). A distinct advantage of using ESI-MS/MS for oligosaccharide quantification is that multiple structures differing by as little as one sulphate group can be determined simultaneously from complex mixtures without the prior chromatography step required for measurement by UV or fluorescence, making ESI-MS/MS an attractive candidate for use in situations requiring high-throughput sample analysis.

1.8 RESEARCH AIMS, HYPOTHESES AND SIGNIFICANCE

The degradation of DS is a complex process involving the concerted action of a number of endo- and exoglycosidase activities. Both Hyal-1 and endo-β-glucuronidase activities towards DS have been proposed, however, as outlined in section 1.5.1, the specific roles of these endoglycosidases in the intra-cellular degradation of DS remain unclear. This is largely due to a lack of convenient methods to assess the substrate specificities of these enzymes, which has traditionally entailed chromatographic separation of the oligosaccharide products of their action upon structurally defined substrates, followed by quantification using methods such as UV or fluorescence. Because of its ability to simultaneously measure multiple oligosaccharide structures without the need for time-consuming chromatography, the overall aim of this project was to develop rapid ESI-MS/MS methods for the study of endoglycosidase activities towards DS.

Hypothesis: Endoglycosidase activities towards DS have specific substrate requirements, and such activities are altered when there is an exoenzyme deficiency.

The specific aims of the project were to:

1) synthesise and characterise a series of oligosaccharide substrates containing structural aspects of the physiological DS substrate;
2) develop a method to measure endoglycosidase activities and determine their substrate specificities by quantifying specific oligosaccharide products using ESI-MS/MS;
3) determine the substrate specificities of the DS-degrading endoglycosidases;
4) investigate the functional properties of the DS-degrading endoglycosidases (e.g. pH and anion optima) and the effects of salts and inhibitors upon enzyme activity;
5) determine the sub-cellular location of the endoglycosidase activities; and
6) compare endoglycosidase activities in normal and exoenzyme-deficient (MPS) cells.

Elucidating the substrate specificities and activities of the DS-degrading endoglycosidases will shed light upon the roles of these enzymes in the intra-cellular degradation of DS, and may further provide insight into the mechanisms responsible for the array of stored DS oligosaccharide structures in the MPSs, which may contribute to disease pathology through their unique biological activities. Although the focus of this project is DS, the methodology developed herein will be readily applicable to the study of endoglycosidase activities towards other GAGs of biological relevance, such as heparin/heparan sulphate and hyaluronan.

CHAPTER TWO

MATERIALS AND METHODS

2.1 MATERIALS

2.1.1 General chemicals

Acetic acid, glacial, HPLC grade, >99.5% (v/v)	Ajax Finechem (Seven Hills, NSW, Australia)
Acetic anhydride (d_6)	Sigma-Aldrich (Castle Hill, NSW, Australia)
Acetonitrile, HPLC grade	Ajax Finechem
Ammonia 28% (v/v)	Ajax Finechem
Ammonium acetate	BDH Chemicals (Kilsyth, Victoria, Australia)
Ammonium formate	Ajax Finechem
Apigenin	Sigma-Aldrich
Bovine serum albumin (fraction V)	Sigma-Aldrich
Bovine testicular hyaluronidase (EC 3.2.1.35)	Sigma-Aldrich
Calcium chloride	Merck (Kilsyth, Victoria, Australia)
Chloroform (1% ethanol), analytical grade	Merck
Chondroitinase ABC from *Proteus Vulgaris* (EC 4.2.2.4)	Sigma-Aldrich
Chondroitin sulphate A (sodium salt) from bovine trachea	Sigma-Aldrich
Citric acid monohydrate	Ajax Finechem
Cobalt chloride	BDH Chemicals
Complete Mini protease inhibitor cocktail tablets	Roche Diagnostics (Castle Hill, NSW, Australia)
Cupric sulphate	Ajax Finechem
4-deoxy-L-threo-hex-4-enopyranosyluronic (1,3) *N*-acetylgalactosamine-6-sulphate (ΔUA-GalNAc(6S))	Sigma-Aldrich

4-deoxy-L-threo-hex-4-enopyranosyluronic (1,4) glucosamine-6-sulphate (ΔUA-GlcN(6S))	Sigma-Aldrich
Dermatan sulphate (sodium salt) from porcine intestinal mucosa	Sigma-Aldrich
Dimethylformamide, >99.5% (v/v)	Sigma-Aldrich
3,3-Dimethylglutaric acid	Sigma-Aldrich
Dimethylsulphoxide (DMSO)	Sigma-Aldrich
Disodium hydrogen phosphate	Ajax Finechem
EDTA	Ajax Finechem
Folin-Ciocoulteau's reagent	Merck
Formic acid, 90% (v/v), analytical grade	Ajax Finechem
Glucosamine-6-sulphate (GlcN(6S))	Sigma-Aldrich
β-glucuronidase from bovine liver (EC 3.2.1.31)	Sigma-Aldrich
D-glucuronolactone	Paton Scientific (Stepney, SA, Australia)
Glycine	Merck
HEPES	Sigma-Aldrich
Hydrochloric acid, 37.5% (v/v), anal. grade	Merck
Leupeptin	Sigma-Aldrich
Lithium chloride	BDH Chemicals
Magnesium chloride	Ajax Finechem
Manganese chloride	Ajax Finechem
Methanol, HPLC grade	Merck
4-methylumbelliferone	Sigma-Aldrich
4-methylumbelliferyl-*N*-acetyl-β-D-glucosaminide	Sigma-Aldrich

4-methylumbelliferyl-phosphate	Sigma-Aldrich
Nitric acid, 70% (v/v)	Ajax Finechem
Nonidet P40	Fluka Biochemika (Buchs, Switzerland)
Pepstatin	Sigma-Aldrich
Percoll	Amersham (Uppsala, Sweden)
Phenylmethanesulphonylfluoride (PMSF), >98.5% (v/v)	Sigma-Aldrich
1-phenyl-3-methyl-5-pyrazolone (PMP)	Tokyo Kasei Kogyo (Tokyo, Japan)
3-phenylphenol	Sigma-Aldrich
Protein standard solution (80 g/L) (human serum albumin)	Sigma-Aldrich
Pyridine, >99% (v/v)	Sigma-Aldrich
Sodium acetate	BDH Chemicals
Sodium carbonate	BDH Chemicals
Sodium chloride	Ajax Finechem
Sodium formate	Ajax Finechem
Sodium hydroxide	Ajax Finechem
Sodium sulphate	Ajax Finechem
Sodium tetraborate	Ajax Finechem
Sucrose	Ajax Finechem
Sulphuric acid, 98% (v/v)	BDH Chemicals
Tributylamine, >98.5% (v/v)	Sigma-Aldrich
Tris base	Roche Diagnostics
Trisodium citrate dihydrate	Ajax Finechem
Triton X-100	Sigma-Aldrich

2.1.2 Cell culture materials

Basal Eagle's medium	Sigma-Aldrich
Culture flasks	Greiner Bio-one (Frickenhausen, Germany)
Foetal calf serum	JRH Biosciences (Lenexa, USA)
Ham's F12 medium	Sigma-Aldrich
Phosphate-buffered saline	JRH Biosciences
Trypsin, 0.12% (v/v)	JRH Biosciences

2.1.3 Chromatography materials

Alltima C18-LL 3 μm HPLC column (50 x 2.1 mm)	Alltech Associates (Deerfield, IL, USA)
Bio-Gel P6 (fine)	Bio-Rad (Hercules, CA, USA)
EXSIL ODS 5 μm guard column (2 mm)	SGE (Austin, TX, USA)
Glass chromatography columns	Bio-Rad
Solid phase co-polymeric (C18 and aminopropyl) extraction columns (50 mg/1 mL)	United Chemical Technologies (Bristol, PA, USA)
Solid phase quaternary amine extraction columns (200 mg/3 mL)	United Chemical Technologies

2.1.4 Mouse tissues

Pieces of skin, liver, kidney, ovaries, brain and lung from a congenic C57BL/6J normal female mouse were kindly provided by Dr Kim Hemsley (Lysosomal Diseases Research Unit, Department of Genetic Medicine; Children, Youth and Women's Health Service) and were stored at -20 ^{o}C until required. Mice were bred, housed and maintained in the CYWHS

Animal House, with all breeding and experimental procedures undertaken with the approval of the CYWHS Animal Ethics Committee.

2.1.5 Reagents and solutions

All reagents and solutions were prepared using milli-Q water

Acid phosphatase substrate solution	10 mM 4-methylumbelliferyl-phosphate in 200 mM CH_3COONa, pH 4.5
Carrying solvent	50% (v/v) CH_3CN/0.025% (v/v) HCOOH in H_2O
Chloride diluent	0.16 N HNO_3, 16% CH_3COOH in H_2O (Department of Genetic Medicine, CYWHS)
Chloride standard solution	100 mM NaCl in H_2O (Department of Genetic Medicine, CYWHS)
Citrate-phosphate buffer	50 mM $C_6H_8O_7 \cdot H_2O$, 100 mM Na_2HPO_4, pH 4.8
Diluted Folin-Ciocoulteau's reagent	25% (v/v) Folin-Ciocoulteau's reagent in H_2O
Enzyme buffer A	50 mM Tris-HCl/60 mM CH_3COONa/0.02% (w/v) BSA, pH 8.0
Enzyme buffer B	100 mM CH_3COONa/50 mM NaCl/50 mM Na_2SO_4, pH 5.0
Enzyme buffer C	50 mM CH_3COONa/0.01% (w/v) BSA, pH 5.0
Gelatin reagent	1.24 g dry gelatin in 200 mL H_2O (Department of Genetic Medicine, CYWHS)
D-glucuronolactone solution	0.005% (w/v) D-glucuronolactone in H_2O
Glycine buffer	156 mM Na_2CO_3, 183 mM NaOH, 200 mM $C_2H_5NO_2$, pH 10.7

β-hexosaminidase substrate solution	1.24 mM 4-methylumbelliferyl-*N*-acetyl-β-D-glucosaminide in citrate-phosphate buffer
Internal standard #1 for mass spectrometry (GlcNAc(6S)(d_3))	Prepared by Dr Peter Clements (Department of Genetic Medicine, CYWHS) as per Ramsay *et al.* (2003) (final concentration 3.3 mM)
Internal standard #2 for mass spectrometry (ΔUA-GalNAc(6S))	2 mM ΔUA-GalNAc(6S) in H_2O
Meta-hydroxydiphenyl solution	0.15% (w/v) 3-phenylphenol in H_2O
4-methylumbelliferone standard	0.142 mM 4-methylumbelliferone in H_2O
Mobile phase A	1% (v/v) CH_3CN, 0.1% (v/v) HCOOH in H_2O
Mobile phase B	0.1% (v/v) HCOOH in CH_3CN
PMP derivatising solution A	250 mM PMP, 400 mM NH_4OH, pH 9.1
PMP derivatising solution B	250 mM PMP, 210 mM NaOH in 50% (v/v) MeOH in H_2O, pH 9.1
Protein reagent A	2% (w/v) Na_2CO_3, 0.4% (w/v) NaOH in H_2O
Protein reagent B	1.7% (w/v) $C_6H_5O_7Na_3 \cdot 2H_2O$ in H_2O
Protein reagent C	1% (w/v) $CuSO_4 \cdot 5H_2O$ in H_2O
Protein reagent D	1% (v/v) protein reagent B, 1% (v/v) protein reagent C in protein reagent A
Protein standards	Protein standard solution diluted in 0.9% (v/v) NaCl to give final concentrations of 4, 8, 16 and 32 μg/100 μL
Solvent A	1% (v/v) CH_3CN, 16 mM CH_3COONH_4, 24 mM CH_3COOH, 0.12% (v/v) tributylamine in H_2O

Solvent B	80% (v/v) CH_3CN, 16 mM CH_3COONH_4, 24mM CH_3COOH, 0.12% (v/v) tributylamine in H_2O
Sucrose solution	250 mM sucrose, 1 mM EDTA, 1 μM pepstatin, 1 μM leupeptin, 200 μM PMSF, 10 mM HEPES, pH 7.0
Sulphuric acid/tetraborate solution	12.5 mM $Na_2B_4O_7 \cdot 10H_2O$ in H_2SO_4
Support electrolyte solution	4 drops of gelatin reagent in 3 mL of chloride diluent
Trypsin, 0.012% (v/v)	0.12% trypsin diluted 1:10 in phosphate-buffered saline

2.1.6 Equipment and software

Agilent 1100 binary HPLC pump	Agilent (Santa Clara, CA, USA)
Amicon Ultra centrifugal filtration device (30,000 nominal molecular weight limit)	Millipore (Bedford, MA, USA)
Analyst software (Vers. 1.4.1 and 1.4.2)	Perkin Elmer Sciex (Foster City, CA, USA)
API-3000 mass spectrometer	Perkin Elmer Sciex
API-4000 Q-trap mass spectrometer	Perkin Elmer Sciex
Beckman-Coulter Optima L-100K ultracentrifuge	Beckman-Coulter (Fullerton, CA, USA)
Biofuge fresco benchtop centrifuge	Heraeus (Hanau, Germany)
CERES 900 HDI plate reader	BioTek Instruments (Winooksi, VT, USA)
Chemoview (Version 1.4)	Perkin Elmer Sciex
Fraction collector	Amersham
Gilson 233 autosampler	Gilson (Middleton, WI, USA)

Glass syringes	SGE Analytical Sciences (Austin, TX, USA)
Heraeus Megafuge 1.0R	Heraeus
Hybaid mini-oven	Hybaid equipment (Hybaid, Middlesex, UK)
Labconco chloride titrator	Labconco (Kansas City, Missouri, USA)
LS-50B luminescence spectrometer with A-91 autosampler	Perkin-Elmer
Peristaltic pump	Amersham
Polypropylene microplate (96 well)	Greiner Bio-one
Probe sonicator	Paton Scientific
Shimadzu LC-20AD HPLC pumps	Shimadzu (Kyoto, Japan)
Shimadzu SIL-20AC autosampler	Shimadzu
Supelco Visiprep vacuum manifold	Sigma-Aldrich
Switching valve	Valco (Houston, TX, USA)
Syringe pump	Harvard Apparatus (Holliston, MA, USA)
Ultra-Turrax T25 homogeniser	Janke and Kunkel IKA-Labortechnik (Staufen, Germany)
Ultrospec II Spectrophotometer	LKB Biochrom (Cambridge, England)

2.2 METHODS

2.2.1 Preparation of internal standard (ISTD) #3 for mass spectrometry (ΔUA-GlcNAc(6S)(d_3))

The ISTD #3, ΔUA-GlcNAc(6S)(d_3), was prepared by *N*-acetylation of ΔUA-GlcN(6S) with deuterated acetic anhydride according to the method of Ramsay *et al.* (2003). Three mg of ΔUA-GlcN(6S) was dissolved in 76 μL of a solution containing pyridine (90 μL), dimethylformamide (900 μL), MeOH (64 μL) and acetic anhydride (d_6) (12 μL), and the mixture stirred for 2 hr at 4 ^{o}C. The reaction was quenched with 1 mL of H_2O, lyophilised to

remove solvents and then reconstituted in H_2O to give a concentration of 2 mM. Aliquots were stored at -20 ^oC.

2.2.2 Cell culture

Cell culture was performed under sterile conditions in a Gelman Sciences biohazard hood in a designated cell culture laboratory within a PC2 facility. Cells were maintained at 37 ^oC in a humidified atmosphere containing 5% CO_2 in 75 cm^2 culture flasks that were incubated with loosened lids to facilitate gas exchange. Chinese hamster ovary (CHO)-K1 cells were obtained from the American Type Culture Collection and were cultured in Ham's F 12 medium supplemented with 10% (v/v) foetal calf serum (FCS). Media was changed every second day by aspirating old media and adding 14 mL of fresh, pre-warmed media. Upon reaching confluence, cells were sub-cultured by aspirating media and washing the cells twice with 8 mL of phosphate-buffered saline (PBS). Three mL of trypsin (0.012% (v/v)) was added to the cell monolayer to dislodge the cells, and the trypsin-cell suspension was then divided equally into 10 new flasks containing fresh, pre-warmed media.

Human skin fibroblast cultures were established from primary skin biopsies submitted to this department for diagnosis (Hopwood *et al.* 1982) and were cultured in basal modified Eagle's medium (BME) containing 10% (v/v) FCS. Media was changed once per week by aspirating old media and adding 14 mL of fresh, pre-warmed media. Cells were sub-cultured by aspirating media and washing the cells twice with 8 mL of PBS. Three mL of trypsin (0.12% (v/v)) was added to the cell monolayer to dislodge the cells, and the trypsin-cell suspension was then divided equally into 3 new flasks containing fresh, pre-warmed media.

CHO-K1 cells and skin fibroblasts were harvested by aspirating media and then washing and trypsinising the cells as described above. The trypsin-cell suspension was transferred to a tube containing 1 mL of PBS (1% (v/v) FCS) and centrifuged for 5 min at

1000 x *g* to pellet cells. The supernatant was discarded and the cell pellet washed twice with PBS and stored at -20 ^{o}C.

2.2.3 Sub-cellular fractionation

To perform sub-cellular fractionation on skin fibroblasts and CHO-K1 cells, three 75 cm^2 culture flasks were harvested as described in section 2.2.2, except that following the second PBS wash, the cell pellets were pooled and resuspended in 1.5 mL of sucrose solution. The cell suspension was drawn into a 5 mL syringe using a 23-gauge needle, subjected to three hypobaric shocks and then centrifuged at 170 x *g* for 5 min at 4 ^{o}C to remove cellular debris. The supernatant was diluted to 3 mL with sucrose solution, loaded onto 17 mL of 18% (v/v) Percoll in sucrose solution and then centrifuged at 29,400 x *g* for 1 hr at 4 ^{o}C. Following centrifugation, 20 x 1 mL fractions were collected from the top of the gradient and stored at -20 ^{o}C.

2.2.4 Preparation of oligosaccharide substrates

2.2.4.1 *Glycosaminoglycan digestion*

Oligosaccharides were prepared from CS-A and DS by enzymatic degradation of the polysaccharides with chondroitinase ABC and bovine testicular hyaluronidase (BTH). For chondroitinase ABC digestion, DS (100 mg) and CS-A (300 mg) were individually dissolved in 20 mL of enzyme buffer A and digested with chondroitinase ABC (0.75 U and 1.5 U, respectively) at 37 ^{o}C for 50 min. For BTH digestion, 100 mg of CS-A was dissolved in 4 mL of enzyme buffer B and digested with 2, 200 U BTH at 37 ^{o}C for 24 hr. Digests were terminated by heating in a 100 ^{o}C water bath for 15 min and then lyophilised and resuspended in 4 mL of 0.5 M $HCOONH_4$.

2.2.4.2 *Size fractionation of oligosaccharides*

2.2.4.2.1 Preparation of Bio-Gel P6 column

A Bio-Gel P6 column was prepared according to the manufacturer's instructions. Briefly, 50g of P6 resin was added to 650 mL of 0.5 M $HCOONH_4$ and allowed to hydrate overnight at room temperature. Following hydration, half the supernatant was decanted, the hydrated resin solution was degassed for 10 min, and then a further 800 mL of degassed 0.5 M $HCOONH_4$ was added and the gel allowed to settle. The supernatant was decanted to remove fines and the gel resuspended in 800 mL of the same buffer. De-fining was repeated twice further, and the slurry then poured into a glass chromatography column (170 x 1.5 cm) that was one-fifth filled with 0.5 M $HCOONH_4$, and allowed to settle under gravity overnight. Four mL of 0.5 M $HCOONH_4$ was added to the top of the gel bed, and the column was then attached to a reservoir of 0.5 M $HCOONH_4$ *via* a peristaltic pump. The column outlet was opened and the operating flow rate was calibrated to 8 mL/hr, following which the column was equilibrated with two column volumes (600 mL) of 0.5 M $HCOONH_4$.

2.2.4.2.2 Calibration of Bio-Gel P6 column

The total volume (V_t) and the void volume (V_0) of the Bio-Gel P6 column were determined from the elution position of NaCl and undigested CS-A, respectively. Seven mg of CS-A and 0.9 mg of NaCl were dissolved in 4 mL of 0.5 M $HCOONH_4$, and the mixture was applied to the column as described below (section 2.2.4.2.3).

2.2.4.2.3 Size-exclusion chromatography on Bio-Gel P6 column

Prior to loading samples onto the column, the peristaltic pump was detached, the buffer head was carefully removed from the top of the gel bed, and the 4 mL sample (sections 2.2.4.1 and 2.2.4.2.2) was then applied and allowed to enter the bed completely. This was followed with 4 mL of 0.5 M $HCOONH_4$ to wash the sample into the bed, and then 4 mL of 0.5 M

$HCOONH_4$ was added to the top of the bed, the pump was re-attached, and the column was run in 0.5 M $HCOONH_4$ at the operating flow rate (8 mL/hr). Seventy fractions of 4 mL were collected and assayed for UA equivalents (section 2.2.8). The 70 fractions collected following application of the CS-A/NaCl calibration mixture to the column (section 2.2.4.2.2) were additionally assayed for the presence of chloride (section 2.2.10). The fractions from the Bio-Gel P6 column were lyophilised, and the oligosaccharides in these fractions reconstituted in H_2O to give a final concentration of 20 to 40 mM as determined by UA content (section 2.2.8). Oligosaccharides were stored at -20 ^oC.

2.2.4.3 *β-glucuronidase digestion of oligosaccharides*

Seventy nmol of selected oligosaccharides (section 2.2.4.2.3) was lyophilised, reconstituted in 100 μL of enzyme buffer C and digested with β-glucuronidase (0.1 mU-10, 000 U) at 37 ^oC for 16 hr, and then lyophilised.

2.2.5 Preparation of samples for endoglycosidase product assay

To prepare skin fibroblast and CHO-K1 homogenates for the endoglycosidase product assay, frozen cell pellets (section 2.2.2) were resuspended in 100 μL of 100 mM HCOONa, pH 3.5, and sonicated for 20 s at 4 ^oC. To prepare mouse tissue homogenates, frozen tissue pieces (skin, liver, kidney, ovaries, brain and lung) were thawed on ice, then 1 mL of cold 100 mM HCOONa (containing one Complete Mini protease inhibitor cocktail tablet/10 mL plus 1 μM pepstatin), pH 3.5, was added and the tissues homogenised at 4 ^oC with an Ultra-Turrax T25 probe homogeniser until an even suspension was attained. The tissue homogenates were then sonicated for 20 s at 4 ^oC.

Percoll density gradient fractions containing microsomes, lysosomes and endosomes (prepared as described in section 2.2.3) were pooled, and an equal volume of 0.5 M NaCl/0.2% (v/v) Nonidet P40 was added to each pooled fraction. The pooled fractions were

then subjected to seven freeze/thaw cycles and centrifuged at 100,000 x *g* for 1 hr at 4 °C to remove Percoll. The microsomal, endosomal and lysosomal fractions were then concentrated to 0.2 mL in an Amicon Ultra centrifugal filtration device and dialysed overnight against 1 L of 100 mM HCOONa, pH 3.5, at 4 °C to remove residual sucrose solution.

2.2.6 Endoglycosidase product assay

The endoglycosidase product assay was performed by adding 50 nmol of oligosaccharide substrate (section 2.2.4.2.3) to 100 µL of sample (skin fibroblast, CHO-K1 and mouse tissue homogenates and concentrated microsomal, endosomal and lysosomal fractions (section 2.2.5)), and incubating the mixture at 37 °C for 24 hr. Negative controls, in which substrate was added to the samples after the 24 hr incubation period, were included in each assay run to correct for background interference. Following the 24 hr incubation period, samples were lyophilised and then resuspended in 1.5 mL of 100 mM CH_3COONH_4, pH 5.0, containing 2 nmol of ISTD #3 (prepared as described in section 2.2.1), and passed over solid phase quaternary amine extraction columns to extract oligosaccharides. The columns were primed with 3 mL each of MeOH, H_2O and 100 mM CH_3COONH_4, pH 5.0, after which the 1.5 mL sample was applied and allowed to enter the solid phase completely. Columns were washed with 2 x 3 mL of 100 mM CH_3COONH_4, pH 5.0, and dried thoroughly on a vacuum manifold. Oligosaccharides were then eluted from the columns with 500 µL of 1.2 M LiCl/100 mM CH_3COONH_4, pH 5.0, and lyophilised.

2.2.7 Protein determination

The protein content of the skin fibroblast, CHO-K1 and mouse tissue homogenates prepared for the endoglycosidase product assay (section 2.2.5) and the fibroblast homogenates prepared for mass spectrometry (section 2.2.11.4) was determined by the method of Lowry *et al.* (1951). Briefly, duplicate 2 µL aliquots of the homogenates were diluted to 100 µL with 0.9%

(w/v) NaCl, and 1 mL of freshly-prepared protein reagent D was added. The samples were then vortexed and allowed to stand at room temperature for 1 min. Next, 100 μL of diluted Folin-Ciocoulteau's reagent was added and the samples then vortexed immediately and left at room temperature for a further 30 min. Absorbance was read at 750 nm on an Ultrospec II spectrophotometer and protein in the samples was calculated from a five-point standard curve constructed using 0, 4, 8, 16 and 32 μg protein standards.

2.2.8 UA determination

The UA content of the fractions from the Bio-Gel P 6 column (section 2.2.4.2.3) was determined by the method of Blumenkrantz and Asboe-Hansen (1973). Duplicate 50 μL aliquots of each fraction were diluted to 200 μL with H_2O, followed by the addition of 1.2 mL of sulphuric acid/tetraborate solution and vortexed. Samples were heated for 5 min in a 100 ^{o}C water bath and then allowed to cool to room temperature, followed by the addition of 20 μL of meta-hydroxydiphenyl solution and vortexed. After standing for 5 min at room temperature, a 200 μL aliquot of each sample was transferred to a clear, flat-bottomed 96-well polypropylene microplate. Absorbance was read at 520 nm on a CERES 900 HDI plate reader and UA content calculated against a standard curve constructed from 1, 2, 5 and 10 μg UA equivalent aliquots of D-glucuronolactone solution.

2.2.9 β-hexosaminidase and acid phosphatase activity determination

β-hexosaminidase and acid phosphatase activities in fractions collected from Percoll density gradients (section 2.2.3) were measured by the method of Leaback and Walker (1961) and Kolodny and Mumford (1976), respectively. One hundred μL of β-hexosaminidase substrate solution or 50 μL of acid phosphatase substrate solution was added to a 10 μL aliquot of each gradient fraction, and the mixtures incubated at 37 ^{o}C for 30 min. Substrate blanks (100 μL of

β-hexosaminidase substrate solution only and 50 µL of acid phosphatase substrate solution only) were included in each assay. The reaction was stopped by the addition of 1.6 mL of glycine buffer and fluorescence was read on an LS-50B luminescence spectrometer. The fluorescence value of the substrate blank was subtracted from that of the samples and enzyme activity in the fractions was calculated by relating the fluorescence of the samples to that of the 2.84 nmol of 4-methylumbelliferone standard.

2.2.10 Chloride determination

The concentration of chloride in fractions from the Bio-Gel P6 column (section 2.2.4.2.3) was determined by coulimetric titration. Aliquots of column fractions were diluted 1:10 in H_2O, and 10 µL of each diluted sample was added to 3 mL of support electrolyte solution and read on a Labconco chloride titrator that was previously calibrated using a 10 µL aliquot of 100 mM chloride standard solution. Chloride levels in the samples from the Bio-Gel P6 column were corrected for the chloride level detected in the support electrolyte solution blank.

2.2.11 Sample preparation for mass spectrometry

2.2.11.1 *Preparation of samples from Bio-Gel P6 column*

Ten µg UA equivalent aliquots of fractions from the Bio-Gel P6 column (section 2.2.4.2.3) were lyophilised and resuspended in 100 µL of PMP derivatising solution A, and the oligosaccharides in these samples were derivatised at 70 ^{o}C for 90 min. Samples were acidified with 100 µL of 0.8 M HCOOH, made up to 500 µL with H_2O and then extracted with an equal volume of $CHCl_3$ to remove excess PMP. The lower $CHCl_3$ layer was removed and discarded. Chloroform extraction was repeated twice and the aqueous layer lyophilised, resuspended in carrying solvent and stored at -20 ^{o}C.

2.2.11.2 *Preparation of samples from endoglycosidase product assay*

Samples from the endoglycosidase product assay (section 2.2.6) were PMP-derivatised using the method described in section 2.2.11.1 above, except that following lyophilisation the aqueous layer from the third $CHCl_3$ extraction was resuspended in 100 µL of 2.4% (v/v) tributylamine in H_2O and desalted using an HPLC column. Solvents were delivered at 0.25 mL/min using an Agilent 1100 binary HPLC pump. Samples (20 µL) were injected into a stream of 100% solvent A with a Gilson 233 autosampler and loaded onto the HPLC column. The column was then stripped with 100% solvent B from 1.0 to 5.0 min and re-equilibrated with solvent A from 5.1 to 8.0 min. The elution profiles of the PMP-oligosaccharides from the HPLC column were monitored by mass spectrometry; di- to octasaccharides co-eluted from the column and were detected at 4.0 min. Salts eluting from the column from 0 to 2.5 min were diverted to waste *via* a switching valve.

2.2.11.3 *Preparation of samples from β-glucuronidase digests*

Oligosaccharides from the *β*-glucuronidase digests (section 2.2.4.3) were PMP-derivatised using the method described in section 2.2.11.1 above, except that the derivatising solution contained 1 nmol of ISTD #1, and that the aqueous layer from the first $CHCl_3$ extraction was removed and applied to a solid phase co-polymeric extraction cartridge that was previously primed with 2 x 1 mL each of MeOH, H_2O and H_2O (pH 11.5 with NH_4OH). Following application to the column, the aqueous layer was allowed to enter the solid phase and the column was then washed with 3 x 1 mL H_2O washes and dried on a vacuum manifold. Remaining PMP was removed with 2 x 1 mL $CHCl_3$ washes, the column was again dried thoroughly, and PMP-oligosaccharides were eluted with 3 x 200 µL of an aqueous solution of 50% (v/v) CH_3CN (pH 11.5 with NH_4OH) and lyophilised. PMP-oligosaccharides were resuspended in carrying solvent and stored at -20 ^{o}C.

2.2.11.4 *Preparation of density gradient fractions and skin fibroblasts*

To prepare fractions from the Percoll density gradients (section 2.2.3) for mass spectrometric analysis, 250 pmol of ISTD #2 was added to a 250 µL aliquot of each gradient fraction and the samples then lyophilised. Samples were resuspended in 100 µL of PMP derivatising solution B, heated at 70 ^{o}C for 45 min, vortexed briefly and then centrifuged at 13,000 x *g* for 1 min. Next, 100 µL of CH_3CN was added and the samples cooled at -20 ^{o}C for 10 min to precipitate protein, which was subsequently removed by centrifugation at 13,000 x *g* for 10 min. The protein-free supernatant was transferred to a new tube, acidified with 100 µL of 0.8 M HCOOH, made up to 600 µL with H_2O, extracted with 750 µL of $CHCl_3$ to remove excess PMP, and then centrifuged at 13,000 x *g* for 5 min. Following centrifugation, the upper aqueous phase was removed and extracted twice further with 500 µL of $CHCl_3$. PMP-oligosaccharides in the aqueous phase were then separated by reversed-phase HPLC. Mobile phases were delivered at 0.2 mL/min using Shimadzu LC-20AD HPLC pumps. Twenty µL of each sample was injected into a stream of mobile phase A with a Shimadzu SIL-20AC autosampler and loaded onto the HPLC column. A linear elution gradient of up to 65% mobile phase B was established from 0.5 to 6.5 min, and the column then stripped with 100% mobile phase B from 6.6 to 7.0 min and re-equilibrated with mobile phase A from 7.1 to 10.5 min. The elution profiles of the PMP-oligosaccharides in the HPLC separations were monitored by mass spectrometry. Salts eluting from the column from 0 to 4.0 min were diverted to waste *via* a switching valve.

Skin fibroblast homogenates were prepared for mass spectrometry by resuspending one frozen cell pellet (section 2.2.2) in 200 µL of 20 mM Tris-HCl/0.5 M NaCl, pH 7.2, and sonicating the preparations for 20 s at 4 ^{o}C. Two hundred and fifty pmol of ISTD #2 was added to aliquots of the fibroblast homogenates, and the samples were then lyophilised, PMP-derivatised and analysed by reversed-phase HPLC as described above. Remaining fibroblast homogenates were stored at -20 ^{o}C.

2.2.12 Mass spectrometry of oligosaccharides

Mass spectrometric analysis of oligosaccharides was performed by ESI-MS/MS in the negative ion mode using a PE Sciex API 3000 triple-quadrupole mass spectrometer or an MDS Sciex 4000 Q-trap triple-quadrupole mass spectrometer, each equipped with Analyst software (Versions 1.4.1 and 1.4.2, respectively) and a turbo-ionspray source. Nitrogen was used as nebuliser (NEB), curtain (CUR), auxiliary (AUX) and collision (CAD) gas.

2.2.12.1 *Identification of oligosaccharides*

PMP-oligosaccharides from the Bio-Gel P6 column (section 2.2.11.1) were directly infused into the ion source of the API 3000 instrument at 10 µL/min in a glass syringe using a syringe pump, with NEB and CUR gas flows set at 10 and 6, respectively, ion spray voltage (IS) set at -4500 V and temperature (TEM) set at 200 ^{o}C. Oligosaccharides were identified on the basis of mass-to-charge ratios (*m/z*) by ESI-MS scans (300 to 1000 amu in 1 s) and then further characterised by ESI-MS/MS to confirm the structural assignments made by ESI-MS and, for selected oligosaccharides, to also identify a suitable product ion for MRM. For ESI-MS/MS (product ion) analysis, the collision energy was ramped from -130 to -4 in 4 V increments with the collision cell exit potential set at -15 V, while Q3 was scanned from 0 to 1500 amu in 3 s.

2.2.12.2 *Quantification of oligosaccharides*

Relative quantification of PMP-oligosaccharides was performed using the MRM mode. An overview of the MRM transitions used for each of the four acquisition methods employed (oligosaccharide scans #1-4) is compiled in Tables 2.1 to 2.4. Samples from the endoglycosidase product assay (section 2.2.11.2) were analysed on the API 3000 instrument using scan #1, with NEB, CUR and CAD set at 12, 6 and 4, respectively, IS set at -4000 V and TEM set at 400 ^{o}C; each MRM pair was monitored for 100 msec. Samples from the β-

glucuronidase digests (section 2.2.11.3) were loaded into a glass syringe, manually injected (20 µL) into the ion source of the API 3000 instrument at 80 µL/min using a stream of carrying solvent, and analysed using scans #2 and #3, with NEB, CUR and CAD set at 10, 6 and 4, respectively, IS set at -4500 V and TEM set at 200 ^{o}C; each MRM pair was monitored for 200 m sec. Skin fibroblast homogenates and fractions from the Percoll density gradients (section 2.2.11.4) were analysed on the 4000 Q-trap instrument using scan #4, with NEB, CUR and AUX set at 30, 15 and 50, respectively, CAD set to medium, interface heater set to ON, IS set at -4500 V and TEM set at 400 ^{o}C; each MRM pair was monitored for 100 msec. In each of the oligosaccharide scans, the MRM pairs were monitored at unit resolution; for each measurement, consecutive scans over the injection period were averaged. The minimum acceptable MRM peak height was defined as 3-fold the average background level. Relative oligosaccharide levels were determined by relating the peak heights of the PMP-oligosaccharides to the peak height of the ISTD (API 3000 instrument), or the peak areas of the PMP-oligosaccharides to the peak area of the ISTD (4000 Q-trap instrument). PMP-oligosaccharides falling below the minimum acceptable MRM peak height were assigned a relative level of zero.

Table 2.1 ESI-MS/MS parameters for oligosaccharide scan #1[a]

Oligosaccharide	Precursor Ion (*m/z*)	DP (V)	FP (V)	EP (V)	Product Ion (*m/z*)	CE (V)	CXP (V)
ΔUA-HNAc(d_3) (+S) (ISTD)	791.4	-76	-224	-9	259.0	-78	-15
ΔUA-HNAc (+S)	788.2	-66	-219	-9	534.3	-35	-6
ΔUA-HNAc-UA (+S)	964.3	-158	-164	-5	331.1	-50	-20
ΔUA-HNAc-UA-HNAc (+2S)	623.2	-50	-155	-10	496.1	-25	-6
ΔUA-[HNAc-UA]$_2$ (+2S)	711.3	-65	-184	-10	624.3	-26	-8
ΔUA-HNAc-[UA-HNAc]$_2$ (+2S)	813.0	-84	-240	-10	506.1	-36	-6
ΔUA-HNAc-[UA-HNAc]$_2$ (+3S)	568.3	-45	-156	-8	546.2	-25	-3
ΔUA-[HNAc-UA]$_3$ (+3S)	627.0	-46	-131	-10	648.0	-25	-7
ΔUA-HNAc-[UA-HNAc]$_3$ (+3S)	694.8	-66	-182	-12	610.3	-27	-6
ΔUA-HNAc-[UA-HNAc]$_3$ (+4S)	540.8	-46	-149	-7	516.8	-22	-13

[a]DP, declustering potential; FP, focussing potential; EP, entrance potential; CE, collision energy; CXP, exit potential; ΔUA, unsaturated uronic acid; UA, uronic acid; HNAc, *N*-acetylhexosamine; S, sulphate

Table 2.2 ESI-MS/MS parameters for oligosaccharide scan #2[a]

Oligosaccharide	Precursor Ion (*m/z*)	DP (V)	FP (V)	EP (V)	Product Ion (*m/z*)	CE (V)	CXP (V)
HNAc(d_3) (+S) (ISTD)	633.4	-41	-200	-10	259.1	-42	-15
UA-HNAc-UA (+S)	982.3	-127	-93	-14	331.1	-52	-17
[2 x UA] [2 x HNAc] (+S)	592.3	-32	-159	-10	505.1	-18	-7
[2 x UA] [2 x HNAc] (+2S)	632.3	-41	-235	-12	505.1	-25	-7
UA-[HNAc-UA]$_2$ (+2S)	720.2	-67	-289	-10	331.5	-36	-5
[3 x UA] [3 x HNAc] (+2S)	547.5	-14	-80	-10	489.0	-17	-5
[3 x UA] [3 x HNAc] (+3S)	574.5	-40	-195	-6	489.9	-22	-6
UA-[HNAc-UA]$_3$ (+3S)	633.0	-37	-134	-12	331.1	-30	-4
[4 x UA] [4 x HNAc] (+3S)	700.5	-67	-250	-10	615.8	-27	-8
[4 x UA] [4 x HNAc] (+4S)	545.3	-44	-118	-10	523.0	-22	-6
UA-[HNAc-UA]$_4$ (+3S)	568.8	-80	-188	-10	528.8	-25	-7
UA-[HNAc-UA]$_4$ (+4S)	589.3	-44	-134	-9	546.0	-18	-6
[5 x UA] [5 x HNAc] (+4S)	640.0	-56	-172	-7	576.7	-23	-7
[5 x UA] [5 x HNAc] (+5S)	528.2	-28	-109	-6	576.5	-20	-7
UA-[HNAc-UA]$_5$ (+4S)	684.2	-69	-211	-7	717.5	-25	-9
[6 x UA] [6 x HNAc] (+5S)	603.8	-53	-213	-14	553.0	-21	-8
[6 x UA] [6 x HNAc] (+6S)	516.5	-36	-133	-5	172.9	-24	-10
UA-[HNAc-UA]$_6$ (+5S)	562.3	-54	-160	-5	613.8	-18	-6

[a]DP, d eclustering p otential; FP, f ocussing p otential; E P, entrance p otential; CE, c ollision e nergy; C XP, e xit potential; UA, uronic acid; HNAc, *N*-acetylhexosamine; S, sulphate

Table 2.3 ESI-MS/MS parameters for oligosaccharide scan #3[a]

Oligosaccharide	Precursor Ion (*m/z*)	DP (V)	FP (V)	EP (V)	Product Ion (*m/z*)	CE (V)	CXP (V)
HNAc(d_3) (+S) (ISTD)	633.4	-41	-200	-10	259.1	-42	-15
ΔUA-HNAc (+S)	788.2	-66	-219	-9	534.3	-35	-6
ΔUA-HNAc-UA (+S)	964.3	-130	-224	-5	331.1	-50	-20
ΔUA-HNAc-UA-HNAc (+2S)	623.2	-50	-155	-10	496.1	-25	-6
ΔUA-[HNAc-UA]$_2$ (+2S)	711.3	-65	-184	-10	624.3	-26	-8
ΔUA-HNAc-[UA-HNAc]$_2$ (+2S)	813.0	-84	-240	-10	506.1	-36	-6
ΔUA-HNAc-[UA-HNAc]$_2$ (+3S)	568.3	-45	-156	-8	546.2	-25	-3
ΔUA-[HNAc-UA]$_3$ (+3S)	627.0	-46	-131	-10	648.0	-25	-7
ΔUA-HNAc-[UA-HNAc]$_3$ (+3S)	694.8	-66	-182	-12	610.3	-27	-6
ΔUA-HNAc-[UA-HNAc]$_3$ (+4S)	540.8	-46	-149	-7	516.8	-22	-13
ΔUA-[HNAc-UA]$_4$ (+4S)	585.0	-55	-140	-9	172.9	-42	-10
ΔUA-[HNAc-UA]$_4$ (+4S)	585.0	-55	-140	-9	269.1	-33	-13
ΔUA-HNAc-[UA-HNAc]$_4$ (+4S)	635.8	-62	-184	-11	643.2	-26	-8
ΔUA-HNAc-[UA-HNAc]$_4$ (+5S)	524.5	-49	-168	-6	572.3	-20	-6
ΔUA-HNAc-[UA-HNAc]$_5$ (+5S)	600.3	-57	-180	-4	597.3	-24	-7
ΔUA-HNAc-[UA-HNAc]$_5$ (+6S)	513.3	-43	-155	-7	549.5	-20	-5
ΔUA-HNAc-[UA-HNAc]$_6$ (+6S)	576.7	-56	-164	-5	625.2	-22	-7
ΔUA-HNAc-[UA-HNAc]$_7$ (+7S)	559.8	-56	-180	-5	597.5	-20	-7

[a]DP, declustering potential; FP, focussing potential; EP, entrance potential; CE, collision energy; CXP, exit potential; ΔUA, unsaturated uronic acid; UA, uronic acid; HNAc, *N*-acetylhexosamine; S, sulphate

Table 2.4 ESI-MS/MS parameters for oligosaccharide scan #4[a]

Oligosaccharide	Precursor Ion (*m/z*)	DP (V)	EP (V)	Product Ion (*m/z*)	CE (V)	CXP (V)
ΔUA-HNAc (+S) (ISTD)	788.1	-90	-10	534.1	-34	-15
HNAc (+S)	630.4	-42	-10	256.1	-42	-15
HNAc (+2S)	710.0	-36	-10	256.0	-58	-17
[1 x UA] [1 x HNAc] (+S)	806.0	-76	-10	295.0	-48	-7
UA-HNAc-UA (+S)	982.3	-81	-10	330.9	-48	-23
[2 x UA] [2 x HNAc] (+2S)	632.4	-56	-10	505.0	-26	-5
UA-[HNAc-UA]$_2$ (+2S)	720.4	-66	-10	269.0	-48	-17
[3 x UA] [3 x HNAc] (+2S)	822.0	-81	-10	515.1	-38	-13
[3 x UA] [3 x HNAc] (+3S)	862.0	-66	-10	821.9	-22	-13

[a]DP, declustering potential; EP, entrance potential; CE, collision energy; CXP, exit potential; ΔUA, unsaturated uronic acid; UA, uronic acid; HNAc, *N*-acetylhexosamine; S, sulphate

CHAPTER THREE

PREPARATION AND CHARACTERISATION OF OLIGOSACCHARIDE SUBSTRATES

3.1 INTRODUCTION

In order to investigate the substrate specificities of the DS-degrading endoglycosidases, a series of defined oligosaccharides containing structural features of the physiological substrate was required. Based on the domain structure of DS (section 1.2), it is likely that two distinct types of oligosaccharides are generated as intermediates during the turnover of a typical DS polysaccharide strand, and that these are the predominant substrate structures encountered by the DS-degrading endoglycosidases. The first of these oligosaccharide types is derived from the GlcA-rich domains of the polysaccharide and is composed of repeating GlcA-GalNAc disaccharide subunits, and the second is derived from the IdoA-rich domains and comprises IdoA-GalNAc disaccharides. Such structures can be generated by enzymatically degrading CS-A from bovine trachea and DS from porcine intestinal mucosa using the bacterial endoenzyme, chondroitinase ABC. This enzyme breaks the GalNAc-UA linkages in GAGs by an eliminative mechanism to generate products containing Δ4,5-unsaturated UA (ΔUA) and GalNAc residues at the newly-formed non-reducing and reducing ends, respectively (Yamagata *et al.* 1968) (Figure 3.1). The oligosaccharide products of CS-A digestion will contain predominantly GlcA-GalNAc(4S) disaccharides, with some GlcA-GalNAc(6S) disaccharides also present (Muthusamy *et al.* 2004), and thus reflect the GlcA-rich domains of DS. Those from the digestion of porcine intestinal mucosa DS, which contains an atypically high IdoA content (more than 90% of total UA), will comprise mainly IdoA-GalNAc(4S) disaccharides (Sudo *et al.* 2001) and therefore represent the IdoA-rich domains.

Yang *et al.* (2000) have reported the preparation of di- to dodecasaccharides of the IdoA-GalNAc(4S) variety, using an approach that involves degrading DS from porcine intestinal mucosa with chondroitinase ABC, purifying the oligosaccharide products by size-exclusion chromatography and then identifying the individual sugar species by ESI-MS/MS. In this chapter, a similar approach was adopted to prepare oligosaccharides from CS-A and DS that reflect the putative physiological substrates derived from the GlcA-rich and the IdoA-

rich domains of DS polysaccharide, respectively. A second series of oligosaccharide substrates representing the GlcA-rich domains of DS was prepared by digesting CS-A with bovine testicular hyaluronidase (BTH) (also known as PH-20), an endo-β-*N*-acetylhexosaminidase that will hydrolyse the GalNAc-GlcA linkages to reduce the polymer to tetra- and hexasaccharides (Hofinger *et al.* 2008) (see section 1.5.1).

A

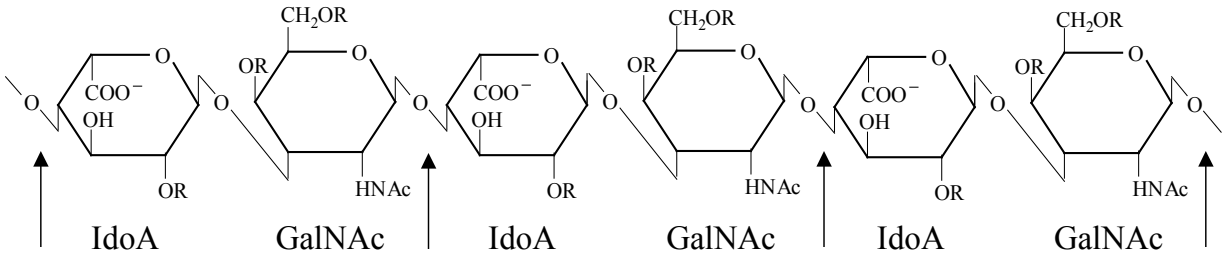

B

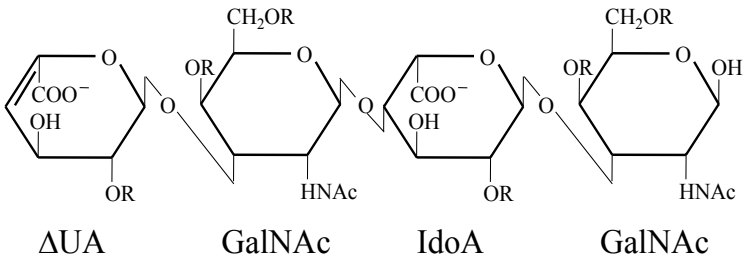

Figure 3.1 Degradation of DS by chondroitinase ABC

Chondroitinase ABC will cleave between GalNAc and UA residues in CS-A and DS by an eliminative mechanism to generate products containing Δ4,5-unsaturated UA at the non-reducing end. Panel A illustrates the glycosidic linkages in DS that are susceptible to cleavage by chondroitinase ABC (indicated with arrows). Panel B shows a representative oligosaccharide product of limited chondroitinase ABC digestion of DS. IdoA, iduronic acid; GalNAc, *N*-acetylgalactosamine; ΔUA, Δ4,5-unsaturated UA; R=H or SO_3^-.

3.2 RESULTS

3.2.1 Preparation and purification of oligosaccharides

CS-A from bovine trachea and DS from porcine intestinal mucosa were digested with BTH and chondroitinase ABC as described in section 2.2.4.1 and the resulting oligosaccharides were purified on a Bio-Gel P6 size-exclusion column (section 2.2.4.2). The total volume (V_t) (248 mL; fraction 62) and the void volume (V_0) (96 mL; fraction 24) of the column were previously determined from the elution positions of NaCl and undigested CS-A, respectively (section 2.2.4.2.2). Figure 3.2 shows the chromatograms of the oligosaccharides, which each displayed a series of partially separated peaks reflecting an incomplete purification of oligosaccharides of various sizes. Of the total UA-positive material from the BTH digest of CS-A, 96% eluted within the fractionation range of the column (112-244 mL; fractions 28-61), with a partial separation of hexadeca- to trisaccharides between 128- and 196 mL (fractions 32-49) (Figure 3.2A). Seventy-five percent of the total UA-positive material from the chondroitinase ABC digest of CS-A eluted within this fractionation range, with a partial separation of tetradeca- to disaccharides between 124- and 204 mL (fractions 31-51) (Figure 3.2B). Likewise, 75% of the total UA-positive material from the chondroitinase ABC digest of DS eluted within the column fractionation range, with a partial separation of tetradeca- to disaccharides between 124- and 204 mL (fractions 31-51) (Figure 3.2C). From each peak in the three chromatograms that eluted within the column fractionation range, the fraction containing the highest concentration of UA was selected, and the oligosaccharides in these selected fractions (denoted with asterisks in Figures 3.2A-C) were analysed by MS.

3.2.2 MS of oligosaccharides

Oligosaccharides from the BTH and chondroitinase ABC digests of CS-A and DS that eluted from the Bio-Gel P6 column in the fractions selected in section 3.2.1 were PMP-derivatised (section 2.2.11.1) and identified based on mass-to-charge ratio (*m/z*) by ESI-

Figure 3.2 Purification of oligosaccharides from BTH and chondroitinase ABC digests of CS-A and DS

CS-A and DS were subjected to limited digestion with BTH and chondroitinase ABC. The digests were size-fractionated on a Bio-Gel P6 column (170 x 1.5 cm) and the fractions were assayed for UA. The chromatograms of the oligosaccharides from the BTH digest of CS-A (panel A) and of the oligosaccharides from the chondroitinase ABC digests of CS-A (panel B) and DS (panel C) are shown. The V_t (248 mL; fraction 62) and the V_0 (96 mL; fraction 24) of the column were determined from the elution positions of NaCl and undigested CS-A, respectively. The asterisks denote the fractions selected for MS analysis.

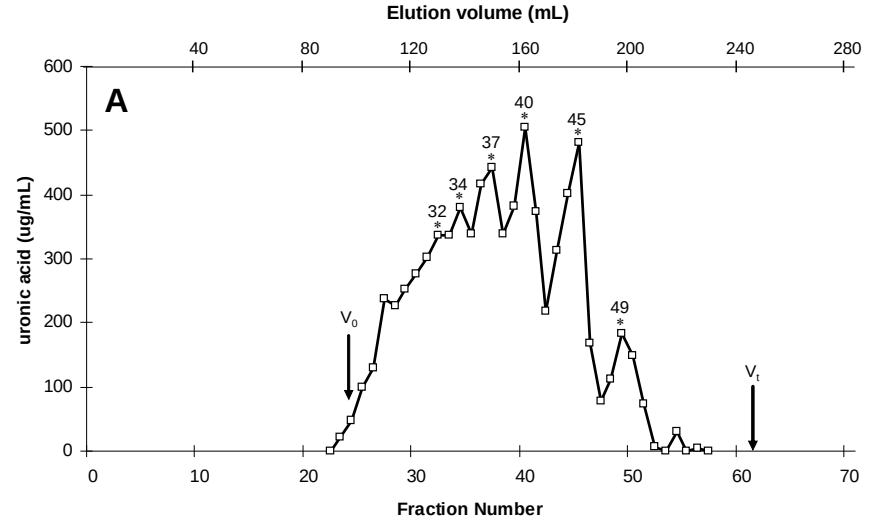
A
Elution volume (mL)
uronic acid (ug/mL)
Fraction Number
V0
Vt
32
34
37
40
45
49

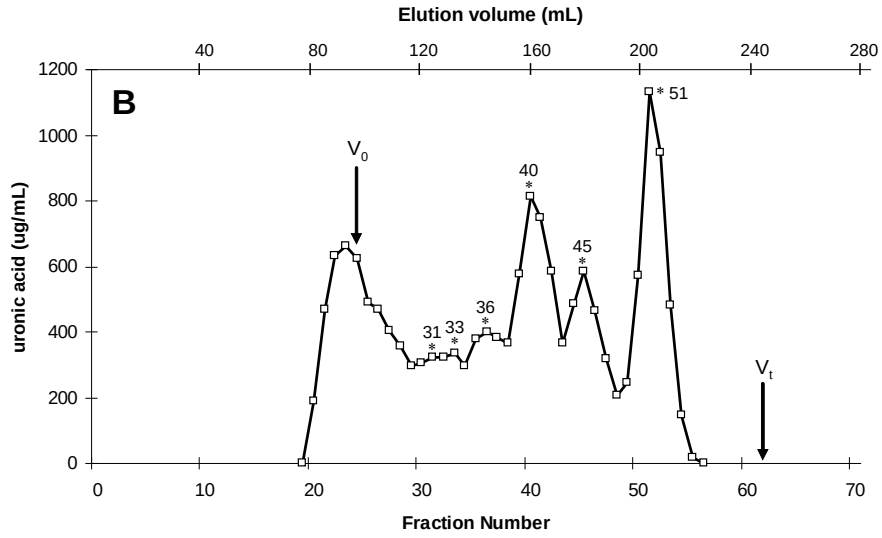
B
Elution volume (mL)
uronic acid (ug/mL)
Fraction Number
V0
Vt
31
33
36
40
45
51

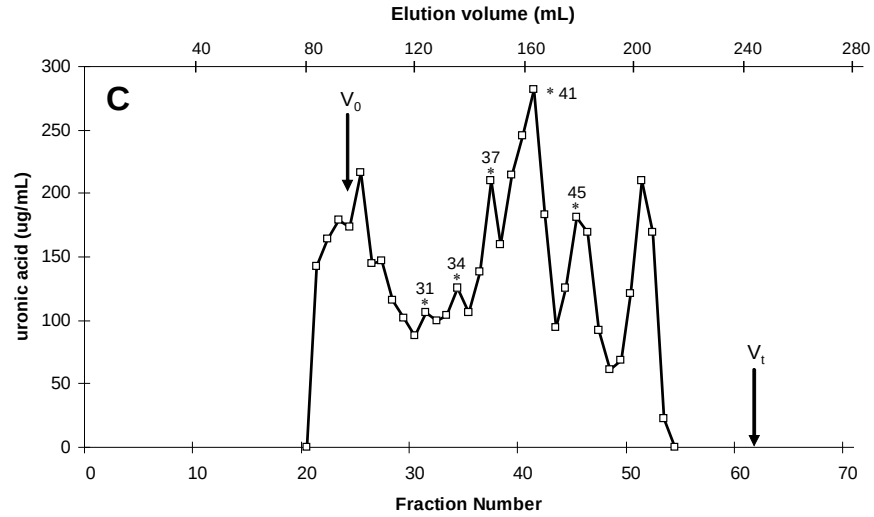
C
Elution volume (mL)
uronic acid (ug/mL)
Fraction Number
V0
Vt
31
34
37
41
45

MS (section 2.2.12.1). Figures 3.3 to 3.5 show the mass spectra of the oligosaccharides from each digest that eluted from the column in successive fractions between the V_0 and the V_t. These spectra illustrate that each fraction contained a mixture of different-sized oligosaccharides, reflecting the incomplete separation of the oligosaccharides achieved on Bio-Gel P6 (Figure 3.2). Based upon the relative intensities of the *m/z* produced by each oligosaccharide, it was deduced that the first fraction from the BTH digestion of CS-A (fraction 32, eluting at 128 mL) contained principally tetradecasaccharide, with some dodeca-, trideca- and hexadecasaccharide also present in smaller amounts (Figure 3.3A), whereas the following fraction (fraction 34; 136 mL) contained mainly dodecasaccharide, in addition to some undeca- and tetradecasaccharide (Figure 3.3B). The subsequent fractions, i.e. numbers 37 (148 mL), 40 (160 mL), 45 (180 mL) and 49 (196 mL), contained nona- and decasaccharide, hepta- and octasaccharide, penta- and hexasaccharide, and tri- and tetrasaccharide, respectively (Figures 3.3C-F). In each of these fractions, the oligosaccharide containing an even number of saccharide residues was predominant over that containing an odd number of residues.

ESI-MS analysis of the fractions from the chondroitinase ABC digestion of CS-A indicated that the first fraction (fraction 31; 124 mL) contained primarily dodecasaccharide, with some deca- and undecasaccharide (Figure 3.4A), while the next (fraction 33; 132 mL) had principally decasaccharide, with some octa- and nonasaccharide (Figure 3.4B). Fractions 36 (144 mL), 40 (160 mL) and 45 (180 mL) contained hepta- and octasaccharide, penta- and hexasaccharide, and tri- and tetrasaccharide, respectively, with the even oligosaccharide again the more abundant in each case (Figures 3.4C-E). Fraction 51 (204 mL) from this digest contained the disaccharide, which was the only oligosaccharide purified to homogeneity from each of the three digests performed (Figure 3.4F).

From the chondroitinase ABC digestion of DS, a preponderance of dodecasaccharide was detected in the first fraction (fraction 31; 124 mL), with smaller quantities of deca- and

tetradecasaccharide also observed (Figure 3.5A). The ensuing fractions, i.e. numbers 34 (136 mL), 37 (148 mL), 41 (164 mL) and 45 (180 mL), had nona- and decasaccharide, hepta- and octasaccharide, penta- and hexasaccharide, and tri- and tetrasaccharide, respectively, with the even-numbered oligosaccharide again the more abundant in each fraction (Figures 3.5B-E).

For most of the oligosaccharides identified in the fractions from the Bio-Gel P6 column, multiple sulphated species were identified, which also co-eluted (Figures 3.3-3.5). The number of sulphates per oligosaccharide increased with the size of each oligosaccharide, up to the equivalent of one sulphate per disaccharide. The oligosaccharides displayed multiply-charged ions and as such were identified from $[M-H]^{-1}$ for the di- and trisaccharides through to $[M-7H]^{-7}$ for the hexadecasaccharide, where M represents the mass of the oligosaccharide, -(x)H represents the number of hydrogen atoms lost during ionisation, and $^{-(x)}$ indicates the overall charge state of the oligosaccharide ion. In general, the most abundant charge state for the oligosaccharide ions corresponded to one charge per sulphate group (Figures 3.3-3.5).

As indicated above, the mass spectra of the oligosaccharides identified in the fractions from the Bio-Gel P6 column were dominated by *m/z* peaks corresponding to even oligosaccharide structures containing non-reducing end UA and reducing end GalNAc residues (di-, tetra-, hexa-, octasaccharide etc.). Peaks corresponding to odd oligosaccharides with UA at both termini (tri-, penta-, heptasaccharide etc.) were also seen in each spectrum (Figures 3.3-3.5), but were considerably fewer in number and generally of lower intensity than those representing the even oligosaccharides, indicating that the odd oligosaccharides were present in very low quantities. The relatively low abundance of the odd oligosaccharides in comparison to the even oligosaccharides is exemplified in Figure 3.3D, where the octasaccharide from the BTH digest of CS-A ($[GlcA-GalNAc]_4$) is represented by four high-intensity (> 50%) *m/z* peaks (545, 642, 700 and 727) and three lower-intensity *m/z* peaks (502, 525 and 616), while the co-eluting heptasaccharide ($GlcA-[GalNAc-GlcA]_3$) shows only one

high- and one low-intensity *m/z* peak (633 and 575, respectively). Similarly, the decasaccharide from the chondroitinase ABC digest of DS (ΔUA-GalNAc-[IdoA-GalNAc]$_4$) (Figure 3.5B) is seen as five high-intensity *m/z* peaks (489, 524, 572, 592 and 636) and one low-intensity *m/z* peak (655), whereas the co-eluting nonasaccharide (ΔUA-[GalNAc-IdoA]$_4$) is indicated by a single peak of low intensity at *m/z* 584.

The odd oligosaccharides from the Bio-Gel P6 column were less variably sulphated and were observed in fewer charge states than the even oligosaccharides of comparable size (i.e. those one monosaccharide residue smaller or larger). Figure 3.3D shows an example of the heptasaccharide from the BTH digest of CS-A (GlcA-[GalNAc-GlcA]$_3$), which is seen only in the trisulphated form as a -3 ion, but the octasaccharide ([GlcA-GalNAc]$_4$) has 2-4 sulphates and is observed as both -3 and -4 ions. Similarly, in Figure 3.5B it can be seen that the nonasaccharide from the chondroitinase ABC digest of DS (ΔUA-[GalNAc-IdoA]$_4$) is present solely with 4 sulphates as a -4 ion, but the decasaccharide (ΔUA-GalNAc-[IdoA-GalNAc]$_4$) contains 3-5 sulphates and is present as -4 and -5 ions. A summary of the oligosaccharide structures from the BTH and chondroitinase ABC digests of CS-A and DS that were identified in the fractions from the Bio-Gel P6 column is presented in Tables 3.1 to 3.3.

Figure 3.3 ESI-MS of oligosaccharides from BTH digestion of CS-A

Oligosaccharides resulting from limited BTH digestion of CS-A were purified by size-exclusion chromatography, derivatised with PMP and analysed by ESI-MS. Panel A shows the mass spectrum of CS-A oligosaccharides eluting from the column in fraction 32 (128 mL), indicating the presence of a dodecasaccharide, $[GlcA\text{-}GalNAc]_6$ (+5S) (*m/z* 604.2 $[M\text{-}5H]^{-5}$); a tridecasaccharide, GlcA-$[GalNAc\text{-}GlcA]_6$ (+5S) (*m/z* 639.3 $[M\text{-}5H]^{-5}$); a tetradecasaccharide, $[GlcA\text{-}GalNAc]_7$ (+5-7S) (*m/z* 537.3, 550.7 and 645.0 $[M\text{-}PMP\text{-}(5\text{-}6)H]^{-(5\text{-}6)}$ and *m/z* 508.1, 579.8, 679.8, 696.0 and 712.0 $[M\text{-}(5\text{-}7)H]^{-(5\text{-}7)}$); and a hexadecasaccharide, $[GlcA\text{-}GalNAc]_8$ (+6-7S) (*m/z* 613.7 $[M\text{-}PMP\text{-}6H]^{-6}$ and *m/z* 562.5 and 642.8 $[M\text{-}(6\text{-}7)H]^{-(6\text{-}7)}$). Panel B shows the mass spectrum of CS-A oligosaccharides eluting from the column in fraction 34 (136 mL), indicating the presence of an undecasaccharide, GlcA-$[GalNAc\text{-}GlcA]_5$ (+4S) (*m/z* 640.8 $[M\text{-}PMP\text{-}4H]^{-4}$ and *m/z* 684.3 $[M\text{-}4H]^{-4}$); a dodecasaccharide, $[GlcA\text{-}GalNAc]_6$ (+4-6S) (*m/z* 553.5, 569.0 and 691.8 $[M\text{-}PMP\text{-}(4\text{-}5)H]^{-(4\text{-}5)}$ and *m/z* 516.5, 588.0, 604.2, 620.0, 735.2, 755.3 and 775.2 $[M\text{-}(4\text{-}6)H]^{-(4\text{-}6)}$); and a tetradecasaccharide, $[GlcA\text{-}GalNAc]_7$ (+6S) (*m/z* 550.7 $[M\text{-}PMP\text{-}6H]^{-6}$ and *m/z* 579.8 $[M\text{-}6H]^{-6}$). Panel C shows the mass spectrum of CS-A oligosaccharides eluting from the column in fraction 37 (148 mL), indicating the presence of a nonasaccharide, GlcA-$[GalNAc\text{-}GlcA]_4$ (+3-4S) (*m/z* 546.0 and 701.3 $[M\text{-}PMP\text{-}(3\text{-}4)H]^{-(3\text{-}4)}$ and *m/z* 569.0, 589.5, 759.5 and 786.0 $[M\text{-}(3\text{-}4)H]^{-(3\text{-}4)}$); and a decasaccharide, $[GlcA\text{-}GalNAc]_5$ (+3-5S) (*m/z* 576.8 and 596.7 $[M\text{-}PMP\text{-}4H]^{-4}$ and *m/z* 528.2, 620.3, 640.3, 660.5, 854.3 and 880.8 $[M\text{-}(3\text{-}5)H]^{-(3\text{-}5)}$). Panel D shows the mass spectrum of CS-A oligosaccharides eluting from the column in fraction 40 (160 mL), indicating the presence of a heptasaccharide, GlcA-$[GalNAc\text{-}GlcA]_3$ (+3S) (*m/z* 575.0 $[M\text{-}PMP\text{-}3H]^{-3}$ and *m/z* 633.3 $[M\text{-}3H]^{-3}$); and an octasaccharide, $[GlcA\text{-}GalNAc]_4$ (+2-4S) (*m/z* 502.0, 616.0 and 642.8 $[M\text{-}PMP\text{-}(3\text{-}4)H]^{-(3\text{-}4)}$ and *m/z* 525.7, 545.5, 700.7 and 727.5 $[M\text{-}(3\text{-}4)H]^{-(3\text{-}4)}$). Panel E shows the mass spectrum of CS-A oligosaccharides eluting from the column in fraction 45 (180 mL), indicating the presence of a pentasaccharide, GlcA-$[GalNAc\text{-}GlcA]_2$ (+2S) (*m/z* 633.7 $[M\text{-}PMP\text{-}2H]^{-2}$ and *m/z* 720.3 $[M\text{-}2H]^{-2}$); and a hexasaccharide, $[GlcA\text{-}GalNAc]_3$ (+2-3S) (*m/z* 516.3 and 735.0 $[M\text{-}PMP\text{-}(2\text{-}3)H]^{-(2\text{-}3)}$ and *m/z* 547.8, 574.5, 822.3 and 861.8 $[M\text{-}(2\text{-}3)H]^{-(2\text{-}3)}$). Panel F shows the mass spectrum of CS-A oligosaccharides eluting from the column in fraction 49 (196 mL), indicating the presence of a trisaccharide, GlcA-GalNAc-GlcA (+S) (*m/z* 982.5 $[M\text{-}H]^{-1}$); and a tetrasaccharide, $[GlcA\text{-}GalNAc]_2$ (+1-2S) (*m/z* 505.4 and 545.5 $[M\text{-}PMP\text{-}2H]^{-2}$, *m/z* 592.3 and 632.5 $[M\text{-}2H]^{-2}$ and *m/z* 515.8 $[M+Na\text{-}PMP\text{-}2H]^{-2}$).

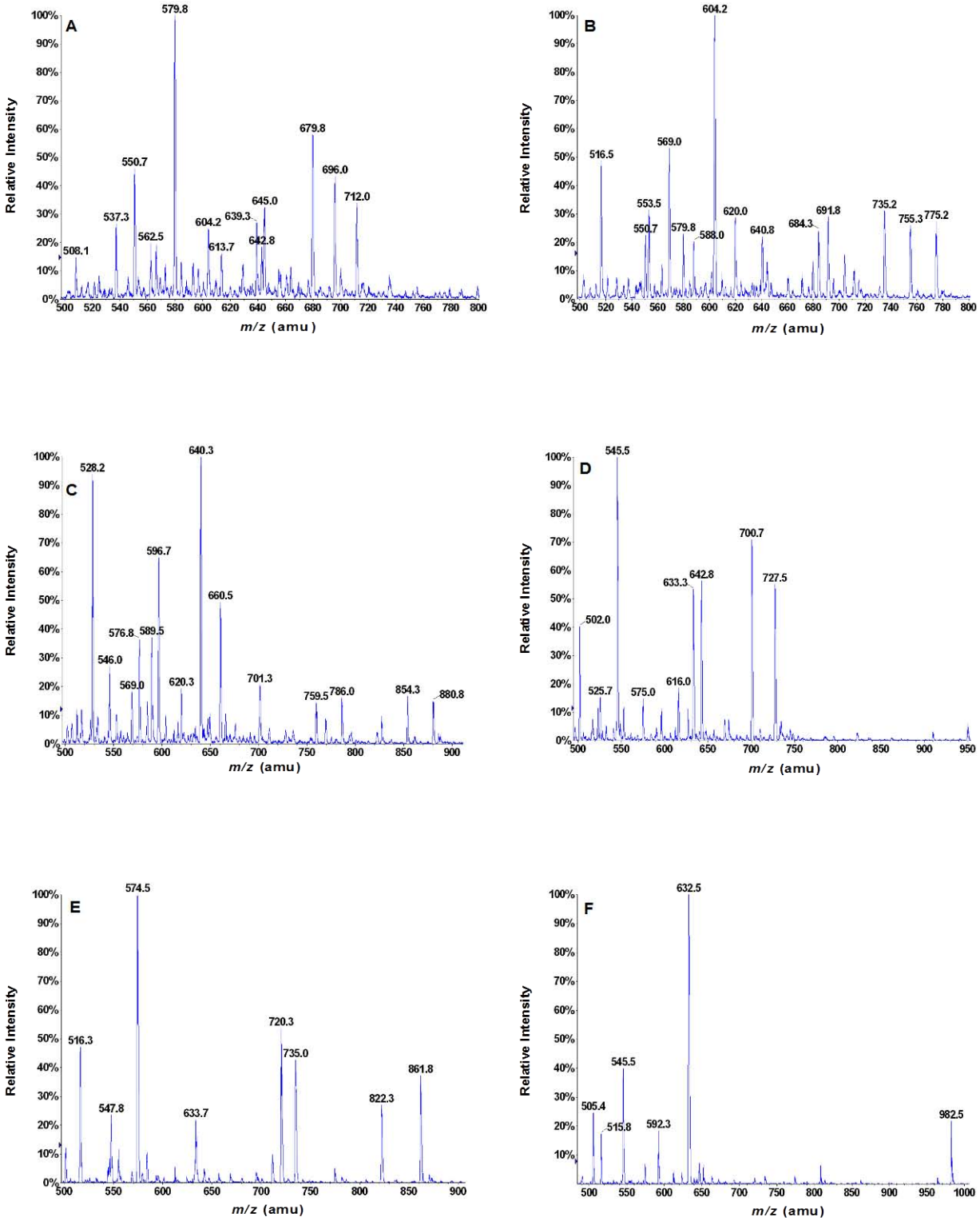
A
579.8
679.8
550.7
696.0
645.0
712.0
537.3
639.3
604.2
562.5
642.8
613.7
508.1
B
604.2
569.0
516.5
553.5
620.0
691.8
735.2
550.7
579.8
588.0
640.8
684.3
755.3
775.2
C
640.3
528.2
596.7
660.5
576.8
589.5
546.0
569.0
620.3
701.3
759.5
786.0
854.3
880.8
D
545.5
700.7
633.3
642.8
727.5
502.0
525.7
575.0
616.0
E
574.5
516.3
720.3
735.0
861.8
547.8
633.7
822.3
F
632.5
545.5
505.4
515.8
592.3
982.5
Relative Intensity
m/z (amu)

Figure 3.4 ESI-MS of oligosaccharides from chondroitinase ABC digestion of CS-A

Oligosaccharides resulting from limited chondroitinase ABC digestion of CS-A were purified by size-exclusion chromatography, derivatised with PMP and analysed by ESI-MS. Panel A shows the mass spectrum of CS-A oligosaccharides eluting from the column in fraction 31 (124 mL), indicating the presence of a decasaccharide, ΔUA-GalNAc-[GlcA-GalNAc]$_4$ (+4S) (*m/z* 636.5 [M-4H]$^{-4}$); an undecasaccharide, ΔUA-[GalNAc-GlcA]$_5$ (+4-5S) (*m/z* 559.8 and 680.0 [M-(4-5)H]$^{-(4-5)}$ and *m/z* 705.3 [M+Na-4H]$^{-4}$); and a dodecasaccharide, ΔUA-GalNAc-[GlcA-GalNAc]$_5$ (+4-6S) (*m/z* 565.3 and 687.3 [M-PMP-(4-5)H]$^{-(4-5)}$ and *m/z* 513.5, 600.3, 616.3 and 730.7 [M-(4-6)H]$^{-(4-6)}$). Panel B shows the mass spectrum of CS-A oligosaccharides eluting from the column in fraction 33 (132 mL), indicating the presence of an octasaccharide, ΔUA-GalNAc-[GlcA-GalNAc]$_3$ (+4S) (*m/z* 541.3 [M-4H]$^{-4}$); a nonasaccharide, ΔUA-[GalNAc-GlcA]$_4$ (+3-4S) (*m/z* 695.3 [M-PMP-3H]$^{-3}$ and *m/z* 584.8 and 753.5 [M-(3-4)H]$^{-(3-4)}$); and a decasaccharide, ΔUA-GalNAc-[GlcA-GalNAc]$_4$ (+3-5S) (*m/z* 572.3 and 592.2 [M-PMP-4H]$^{-4}$, *m/z* 524.5, 616.3, 636.2 and 655.8 [M-(4-5)H]$^{-(4-5)}$ and *m/z* 661.3 [M+Na-4H]$^{-4}$). Panel C shows the mass spectrum of CS-A oligosaccharides eluting from the column in fraction 36 (144 mL), indicating the presence of a heptasaccharide, ΔUA-[GalNAc-GlcA]$_3$ (+3S) (*m/z* 569.0 [M-PMP-3H]$^{-3}$ and *m/z* 627.0 [M-3H]$^{-3}$); and an octasaccharide, ΔUA-GalNAc-[GlcA-GalNAc]$_3$ (+3-4S) (*m/z* 497.5 and 637.0 [M-PMP-(3-4)H]$^{-(3-4)}$, *m/z* 541.0, 694.8 and 721.5 [M-(3-4)H]$^{-(3-4)}$ and *m/z* 728.8 [M+Na-3H]$^{-3}$). Panel D shows the mass spectrum of CS-A oligosaccharides eluting from the column in fraction 40 (160 mL), indicating the presence of a pentasaccharide, ΔUA-[GalNAc-GlcA]$_2$ (+2S) (*m/z* 624.3 [M-PMP-2H]$^{-2}$ and *m/z* 711.5 [M-2H]$^{-2}$); and a hexasaccharide, ΔUA-GalNAc-[GlcA-GalNAc]$_2$ (+2-3S) (*m/z* 510.4 and 726.0 [M-PMP-(2-3)H]$^{-(2-3)}$, *m/z* 568.3, 813.0 and 853.0 [M-(2-3)H]$^{-(2-3)}$ and *m/z* 864.0 [M+Na-2H]$^{-2}$). Panel E shows the mass spectrum of CS-A oligosaccharides eluting from the column in fraction 45 (180 mL), indicating the presence of a trisaccharide, ΔUA-GalNAc-GlcA (+S) (*m/z* 964.3 [M-H]$^{-1}$); and a tetrasaccharide, ΔUA-GalNAc-GlcA-GalNAc (+2S) (*m/z* 536.3 [M-PMP-2H]$^{-2}$, *m/z* 623.0 [M-2H]$^{-2}$ and *m/z* 634.7 [M+Na-2H]$^{-2}$). Panel F shows the mass spectrum of CS-A oligosaccharides eluting from the column in fraction 51 (204 mL), indicating the presence of a disaccharide, ΔUA-GalNAc (+S) (*m/z* 614.5 [M-PMP-H]$^{-1}$, *m/z* 788.3 [M-H]$^{-1}$, *m/z* 636.5 [M+Na-PMP-H]$^{-1}$ and *m/z* 810.3 [M+Na-H]$^{-1}$).

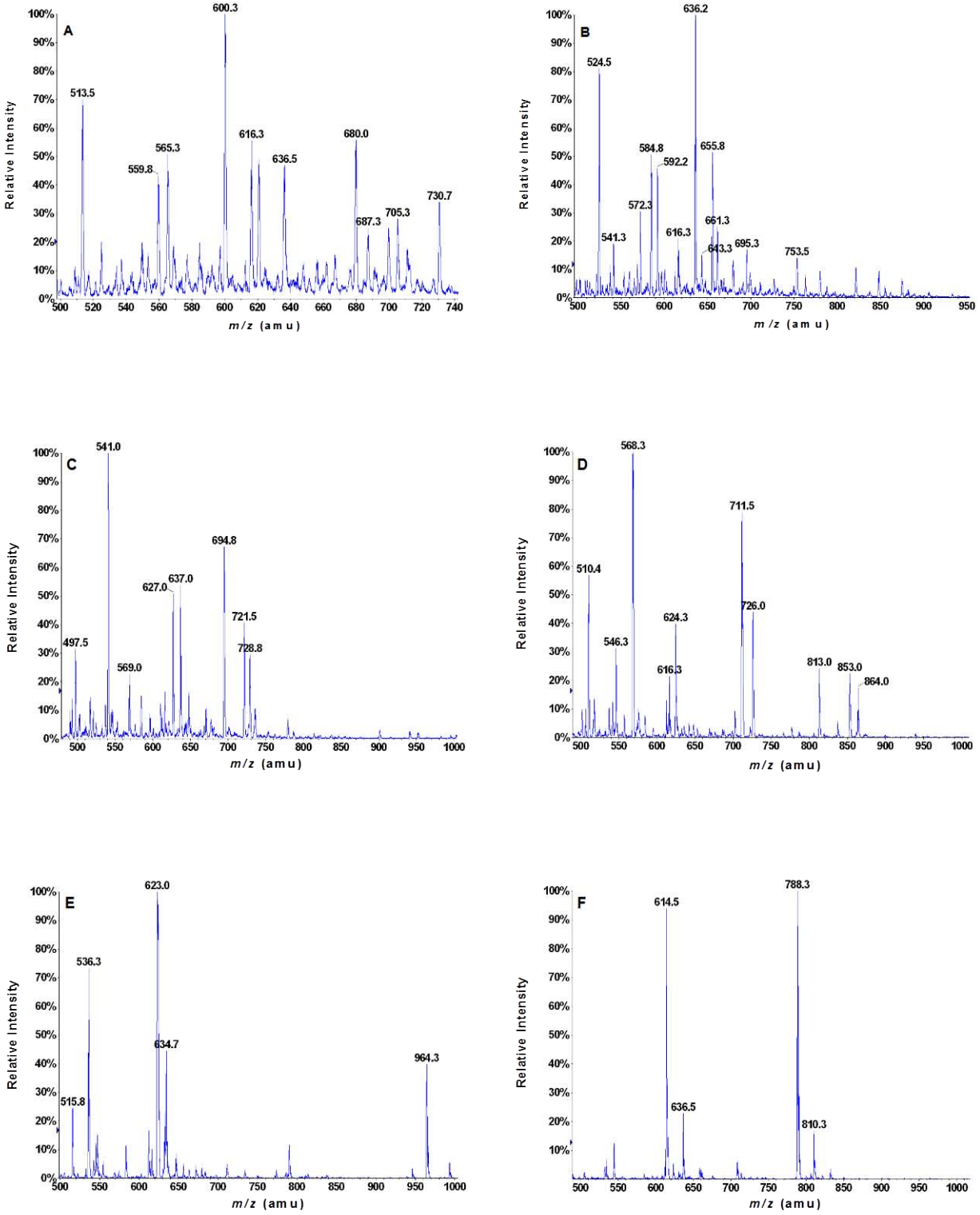
A
600.3
513.5
565.3
559.8
616.3
636.5
680.0
687.3
705.3
730.7
B
636.2
524.5
584.8
592.2
655.8
572.3
661.3
616.3
541.3
643.3
695.3
753.5
C
541.0
694.8
627.0
637.0
721.5
497.5
728.8
569.0
D
568.3
711.5
510.4
726.0
624.3
546.3
813.0
853.0
616.3
864.0
E
623.0
536.3
634.7
964.3
515.8
F
788.3
614.5
636.5
810.3
Relative Intensity
m/z (amu)

Figure 3.5 ESI-MS of oligosaccharides from chondroitinase ABC digestion of DS

Oligosaccharides resulting from limited chondroitinase ABC digestion of DS were purified by size-exclusion chromatography, derivatised with PMP and analysed by ESI-MS. Panel A shows the mass spectrum of DS oligosaccharides eluting from the column in fraction 31 (124 mL), indicating the presence of a decasaccharide, ΔUA-GalNAc-[IdoA-GalNAc]$_4$ (+4S) (*m/z* 636.2 [M-4H]$^{-4}$); a dodecasaccharide, ΔUA-GalNAc-[IdoA-GalNAc]$_5$ (+4-6S) (*m/z* 484.5, 549.5 and 565.5 [M-PMP-(5-6)H]$^{-(5-6)}$ and *m/z* 513.5, 600.5 and 616.3 [M-(5-6)H]$^{-(5-6)}$); and a tetradecasaccharide, ΔUA-GalNAc-[IdoA-GalNAc]$_6$ (+5-6S) (*m/z* 534.3 [M-PMP-6H]$^{-6}$ and *m/z* 576.8 [M-6H]$^{-6}$). Panel B shows the mass spectrum of DS oligosaccharides eluting from the column in fraction 34 (136 mL), indicating the presence of a nonasaccharide, ΔUA-[GalNAc-IdoA]$_4$ (+4S) (*m/z* 584.8 [M-4H]$^{-4}$); and a decasaccharide, ΔUA-GalNAc-[IdoA-GalNAc]$_4$ (+3-5S) (*m/z* 489.6, 572.3 and 592.2 [M-PMP-(4-5)H]$^{-(4-5)}$ and *m/z* 524.8, 636.0 and 655.5 [M-(4-5)H]$^{-(4-5)}$). Panel C shows the mass spectrum of DS oligosaccharides eluting from the column in fraction 37 (148 mL), indicating the presence of a heptasaccharide, ΔUA-[GalNAc-IdoA]$_3$ (+3S) (*m/z* 627.2 [M-3H]$^{-3}$); and an octasaccharide, ΔUA-GalNAc-[IdoA-GalNAc]$_3$ (+3-4S) (*m/z* 497.5 and 636.8 [M-PMP-(3-4)H]$^{-(3-4)}$ and *m/z* 541.0, 694.8 and 721.5 [M-(3-4)H]$^{-(3-4)}$). Panel D shows the mass spectrum of DS oligosaccharides eluting from the column in fraction 41 (164 mL), indicating the presence of a pentasaccharide, ΔUA-[GalNAc-IdoA]$_2$ (+2S) (*m/z* 711.3 [M-2H]$^{-2}$); and a hexasaccharide, ΔUA-GalNAc-[IdoA-GalNAc]$_2$ (+2-3S) (*m/z* 510.3 and 725.8 [M-PMP-(2-3)H]$^{-(2-3)}$ and *m/z* 568.5, 813.0 and 853.0 [M-(2-3)H]$^{-(2-3)}$). Panel E shows the mass spectrum of DS oligosaccharides eluting from the column in fraction 45 (180 mL), indicating the presence of a trisaccharide, ΔUA-GalNAc-IdoA (+S) (*m/z* 964.5 [M-H]$^{-1}$); and a tetrasaccharide, ΔUA-GalNAc-IdoA-GalNAc (+1-2S) (*m/z* 536.3 [M-PMP-2H]$^{-2}$, *m/z* 583.5 and 623.3 [M-2H]$^{-2}$, *m/z* 547.3 [M+Na-PMP-2H]$^{-2}$ and *m/z* 634.7 [M+Na-2H]$^{-2}$).

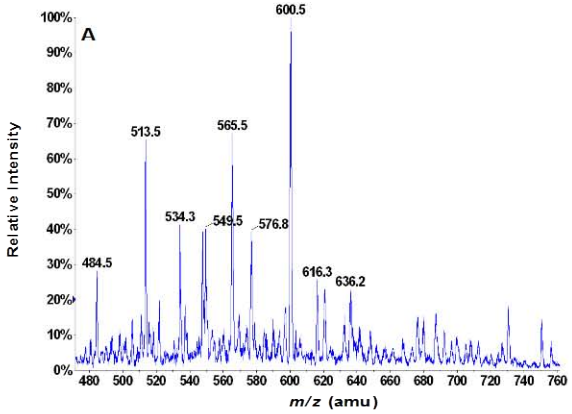
A
600.5
513.5
565.5
534.3
549.5
576.8
484.5
616.3
636.2
Relative Intensity
m/z (amu)

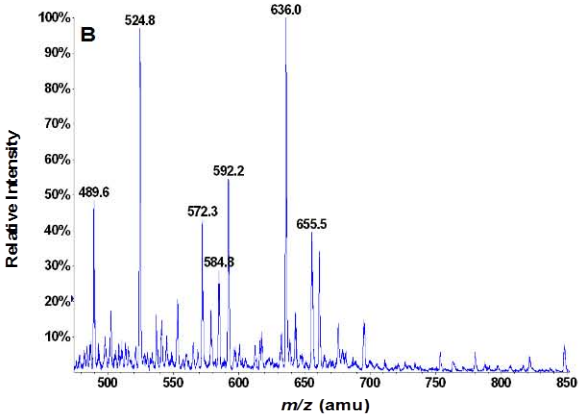
B
636.0
524.8
592.2
489.6
572.3
655.5
584.3
Relative Intensity
m/z (amu)

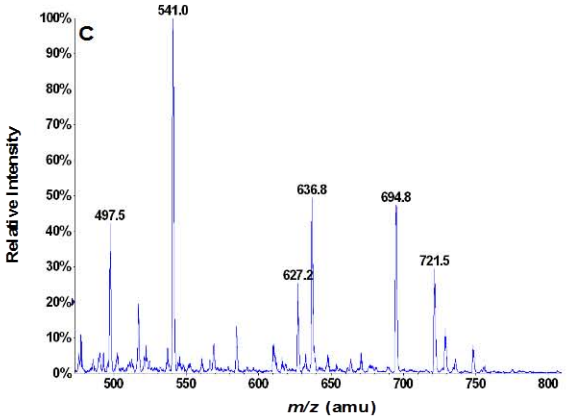
C
541.0
636.8
694.8
497.5
721.5
627.2
Relative Intensity
m/z (amu)

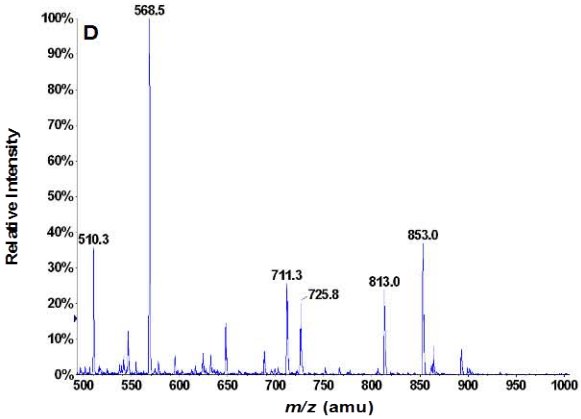
D
568.5
853.0
510.3
711.3
813.0
725.8
Relative Intensity
m/z (amu)

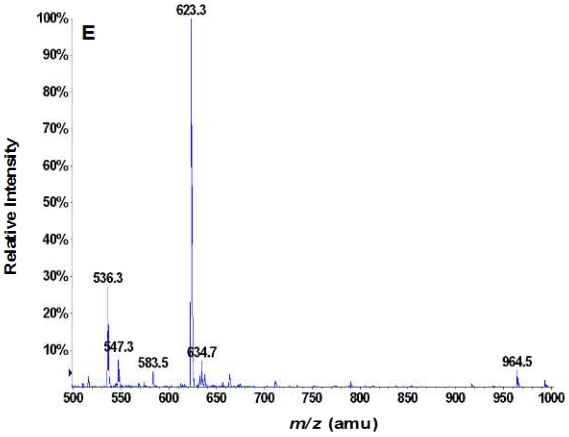
E
623.3
536.3
547.3
583.5
634.7
964.5
Relative Intensity
m/z (amu)

Table 3.1 Proposed structures of oligosaccharides from BTH digestion of CS-A

Proposed Structure[a]	No. sulphate groups	Charge states observed	Elution on fraction no.	Bio-Gel P6[b] mL
GlcA-GalNAc-GlcA	1	-1	49	196
$[GlcA\text{-}GalNAc]_2$	1-2	-2	49	196
$GlcA\text{-}[GalNAc\text{-}GlcA]_2$	2	-2	45	180
$[GlcA\text{-}GalNAc]_3$	2-3	-2,-3	45	180
$GlcA\text{-}[GalNAc\text{-}GlcA]_3$	3	-3	40	160
$[GlcA\text{-}GalNAc]_4$	2-4	-3,-4	40	160
$GlcA\text{-}[GalNAc\text{-}GlcA]_4$	3-4	-3,-4	37	148
$[GlcA\text{-}GalNAc]_5$	3-5	-3,-4,-5	37	148
$GlcA\text{-}[GalNAc\text{-}GlcA]_5$	4	-4	34	136
$[GlcA\text{-}GalNAc]_6$	4-6	-4,-5,-6	32/34	128-136
$GlcA\text{-}[GalNAc\text{-}GlcA]_6$	5	-5	32	128
$[GlcA\text{-}GalNAc]_7$	5-7	-5,-6,-7	32/34	128/136
$[GlcA\text{-}GalNAc]_8$	6-7	-6,-7	32	128

[a]GlcA, glucuronic acid; GalNAc, *N*-acetylgalactosamine

[b]see Figure 3.2A

Table 3.2 Proposed structures of oligosaccharides from chondroitinase ABC digestion of CS-A

Proposed Structure[a]	No. sulphate groups	Charge states observed	Elution on fraction no.	Bio-Gel P6[b] mL
ΔUA-GalNAc	1	-1	51	204
ΔUA-GalNAc-GlcA	1	-1	45	180
ΔUA-GalNAc-GlcA-GalNAc	2	-2	45	180
ΔUA-[GalNAc-GlcA]$_2$	2	-2	40	160
ΔUA-GalNAc-[GlcA-GalNAc]$_2$	2-3	-2,-3	40	160
ΔUA-[GalNAc-GlcA]$_3$	3	-3	36	144
ΔUA-GalNAc-[GlcA-GalNAc]$_3$	3-4	-3,-4	33/36	132/144
ΔUA-[GalNAc-GlcA]$_4$	3-4	-3,-4	33	132
ΔUA-GalNAc-[GlcA-GalNAc]$_4$	3-5	-4,-5	31/33	124/132
ΔUA-[GalNAc-GlcA]$_5$	4-5	-4,-5	31	124
ΔUA-GalNAc-[GlcA-GalNAc]$_5$	4-6	-4,-5,-6	31	124

[a]ΔUA, unsaturated uronic acid; GlcA, glucuronic acid; GalNAc, *N*-acetylgalactosamine

[b]see Figure 3.2B

Table 3.3 Proposed structures of oligosaccharides from chondroitinase ABC digestion of DS

Proposed Structure[a]	No. sulphate groups	Charge states observed	Elution on fraction no.	Bio-Gel P6[b] mL
ΔUA-GalNAc-IdoA	1	-1	45	180
ΔUA-GalNAc-IdoA-GalNAc	1-2	-2	45	180
ΔUA-[GalNAc-IdoA]$_2$	2	-2	41	164
ΔUA-GalNAc-[IdoA-GalNAc]$_2$	2-3	-2,-3	41	164
ΔUA-[GalNAc-IdoA]$_3$	3	-3	37	148
ΔUA-GalNAc-[IdoA-GalNAc]$_3$	3-4	-3,-4	37	148
ΔUA-[GalNAc-IdoA]$_4$	4	-4	34	136
ΔUA-GalNAc-[IdoA-GalNAc]$_4$	3-5	-4,-5	31/34	124/136
ΔUA-GalNAc-[IdoA-GalNAc]$_5$	4-6	-5,-6	31	124
ΔUA-GalNAc-[IdoA-GalNAc]$_6$	5-6	-6	31	124

[a]ΔUA, unsaturated uronic acid; IdoA, iduronic acid; GalNAc, *N*-acetylgalactosamine

[b]see Figure 3.2C

Once identified, the oligosaccharides from the BTH and chondroitinase ABC digests were further characterised by ESI-MS/MS (section 2.2.12.1). Figures 3.6 and 3.7 display representative product ion spectra for the oligosaccharides that were identified in the BTH digest of CS-A, and for the oligosaccharides from the chondroitinase ABC digest of DS, respectively. These spectra show that the oligosaccharides from both digests generated a number of common product ions (e.g. *m/z* 173, 238, 256, 282, 300, 331). Of these, *m/z* 256 and 300 were seen exclusively in the spectra from the oligosaccharides terminating in GalNAc (i.e. the even oligosaccharides), such as the tetra- and hexasaccharides from CS-A (Figures 3.6D and F) and DS (Figures 3.7B and E). The product ion at *m/z* 331 was observed only in the spectra from the oligosaccharides terminating in UA (i.e. the odd oligosaccharides), and this is seen for the CS-A tri- and pentasaccharides in Figures 3.6A and B, and the DS pentasaccharide in Figure 3.7C. It can also be seen that product ions at *m/z* 175 and 193 were generated from the CS-A oligosaccharides, but not from the DS oligosaccharides. For example, both of these product ions are evident in the spectra from the CS-A tetra- and hexasaccharides (Figures 3.6D and F), but neither is observed in the spectra from the DS tetra- and hexasaccharides generated at similar collision energy (CE) (Figures 3.7B and E). The product ion spectra further illustrate that different product ions were generated from high- and low collision energy scans performed on the same oligosaccharide. This is evident when the spectrum from the product ion scan of the CS-A tetrasaccharide performed at CE -24 (Figure 3.6C), which shows product ions at *m/z* 325, 438, 505, 545, 592, 652 and 1011, is compared with that performed at CE -60 (Figure 3.6D), where product ions at *m/z* 172, 175, 193, 238, 255, 282 and 300 are observed. The DS hexasaccharide is a further example of this phenomenon. Product ions were seen at *m/z* 173, 483, 510, 546 and 725 in scans performed on the hexasaccharide at CE -24 (Figure 3.7D), but were detected at *m/z* 173, 175, 238, 256, 281 and 300 in those performed at CE -60 (Figure 3.7E).

Figure 3.6 ESI-MS/MS of selected oligosaccharides from BTH digestion of CS-A

Oligosaccharides resulting from limited BTH digestion of CS-A were purified by size-exclusion chromatography, derivatised with PMP, identified by ESI-MS and then further characterised by ESI-MS/MS. Panel A shows the product ion spectrum at a collision energy (CE) of -44 of the CS-A trisaccharide, GlcA-GalNAc-GlcA (+S), which eluted from the column in fraction 49 (196 mL), with the $[M-H]^{-1}$ ion at *m/z* 982.7. Major product ions were observed at *m/z* 331.3, 458.0, 728.3 and 808.5. Panel B shows the product ion spectrum at CE -28 of the CS-A pentasaccharide, GlcA-$[GalNAc-GlcA]_2$ (+2S), which eluted from the column in fraction 45 (180 mL), with the $[M-2H]^{-2}$ ion at *m/z* 720.2. Major product ions were observed at *m/z* 331.0, 457.9, 593.3, 633.3 and 855.3. Panel C shows the product ion spectrum at CE -24 of the CS-A tetrasaccharide, $[GlcA-GalNAc]_2$ (+2S), which eluted from the column in fraction 49 (196 mL), with the $[M-2H]^{-2}$ ion at *m/z* 632.3. Major product ions were observed at *m/z* 325.9, 438.1, 505.1, 545.3, 592.3, 652.2 and 1011.7. Panel D shows the product ion spectrum of the same CS-A tetrasaccharide, $[GlcA-GalNAc]_2$ (+2S), but at CE -60. Major product ions were observed at *m/z* 172.9, 175.4, 193.1, 238.9, 255.9, 282.0 and 300.3. Panel E shows the product ion spectrum at CE -24 of the CS-A hexasaccharide, $[GlcA-GalNAc]_3$ (+3S), which eluted from the column in fraction 45 (180 mL), with the $[M-3H]^{-3}$ ion at *m/z* 574.3. Major product ions were observed at *m/z* 173.4, 457.4, 489.3, 516.7 and 735.3. Panel F shows the product ion spectrum of the same CS-A hexasaccharide, $[GlcA-GalNAc]_3$ (+3S), but at CE -56. Major product ions were observed at *m/z* 173.1, 175.1, 193.4, 256.0, 282.0 and 396.1.

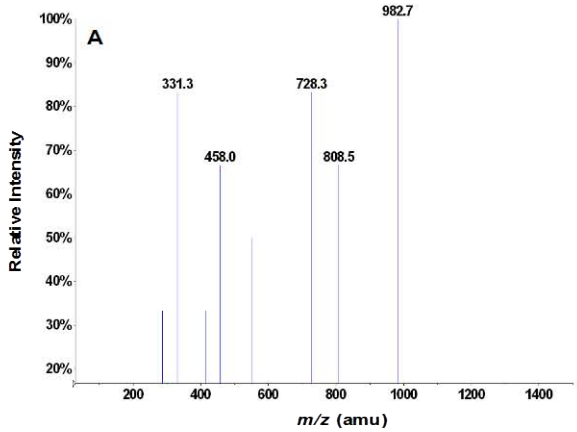
A
982.7
331.3
728.3
458.0
808.5
Relative Intensity
m/z (amu)

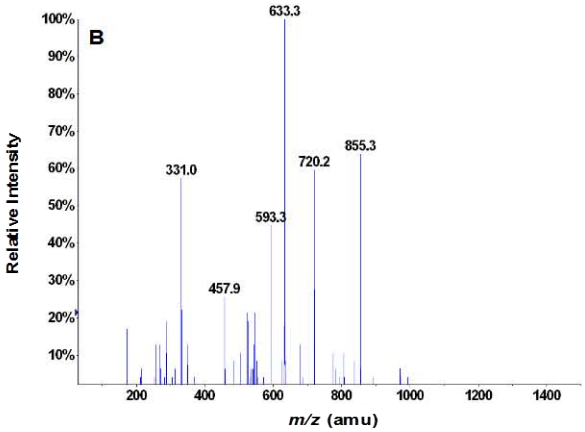
B
633.3
855.3
720.2
331.0
593.3
457.9
Relative Intensity
m/z (amu)

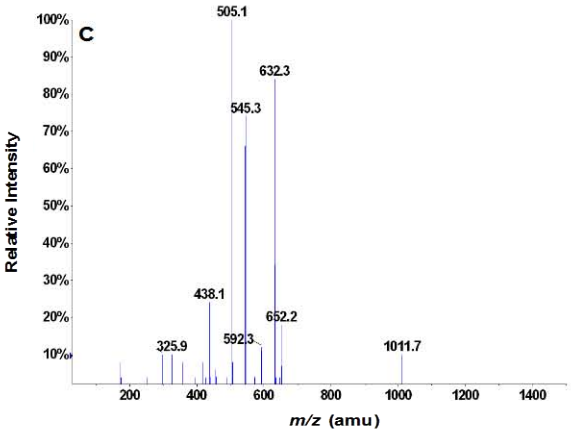
C
505.1
632.3
545.3
438.1
652.2
592.3
325.9
1011.7
Relative Intensity
m/z (amu)

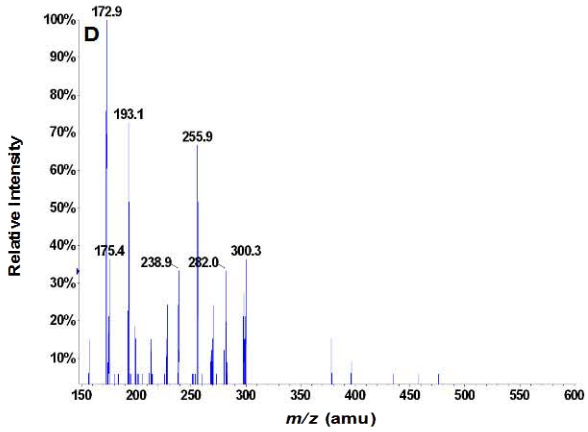
D
172.9
193.1
255.9
175.4
238.9
282.0
300.3
Relative Intensity
m/z (amu)

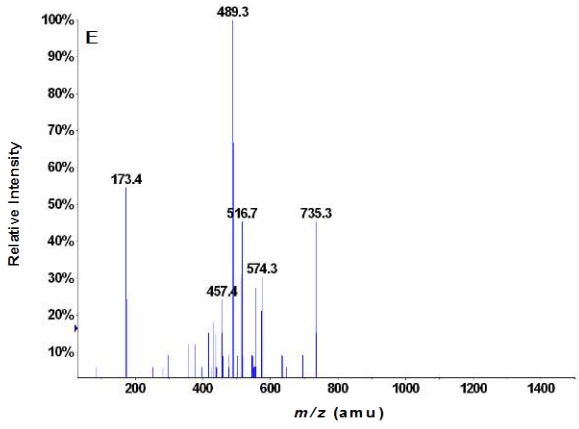
E
489.3
173.4
516.7
735.3
574.3
457.4
Relative Intensity
m/z (amu)

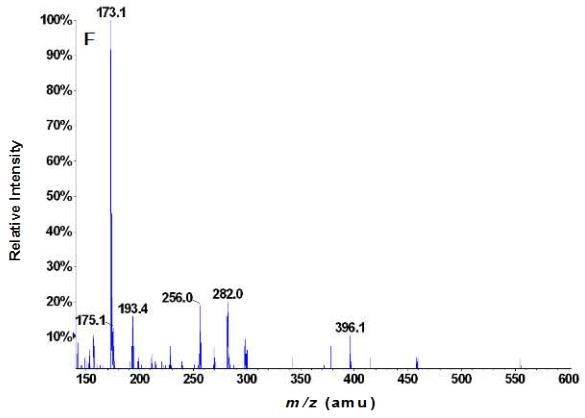
F
173.1
193.4
256.0
282.0
175.1
396.1
Relative Intensity
m/z (amu)

Figure 3.7 ESI-MS/MS of selected oligosaccharides from chondroitinase ABC digestion of DS

Oligosaccharides resulting from limited chondroitinase ABC digestion of DS were purified by size-exclusion chromatography, derivatised with PMP, identified by ESI-MS and then further characterised by ESI-MS/MS. Panel A shows the product ion spectrum at CE -24 of the DS tetrasaccharide, ΔUA-GalNAc-IdoA-GalNAc (+2S), which eluted from the column in fraction 45 (180 mL), with the $[M-2H]^{-2}$ ion at *m/z* 623.3. Major product ions were observed at *m/z* 496.1, 536.3 and 634.0. Panel B shows the product ion spectrum of the same DS tetrasaccharide, ΔUA-GalNAc-IdoA-GalNAc (+2S), but at CE -68. Major product ions were observed at *m/z* 173.4, 256.4, 282.0 and 300.1. Panel C shows the product ion spectrum at CE -28 of the DS pentasaccharide, ΔUA-$[GalNAc-IdoA]_2$ (+2S), which eluted from the column in fraction 41 (164 mL), with the $[M-2H]^{-2}$ ion at *m/z* 711.7. Major product ions were observed at *m/z* 331.1, 624.3 and 837.3. Panel D shows the product ion spectrum at CE -24 of the DS hexasaccharide, ΔUA-GalNAc-$[IdoA-GalNAc]_2$ (+3S), which eluted from the column in fraction 41 (164 mL), with the $[M-3H]^{-3}$ ion at *m/z* 568.5. Major product ions were observed at *m/z* 173.1, 483.5, 510.0, 546.2 and 725.8. Panel E shows the product ion spectrum of the same DS hexasaccharide, ΔUA-GalNAc-$[IdoA-GalNAc]_2$ (+3S), but at CE -60. Major product ions were observed at *m/z* 173.1, 175.4, 238.6, 256.1, 281.9 and 300.0. Panel F shows the product ion spectrum at CE -28 of the DS octasaccharide, ΔUA-GalNAc-$[IdoA-GalNAc]_3$ (+3S), which eluted from the column in fraction 37 (148 mL), with the $[M-3H]^{-3}$ ion at *m/z* 694.5. Major product ions were observed at *m/z* 173.1, 298.1, 610.7, 637.0, 735.5 and 916.3.

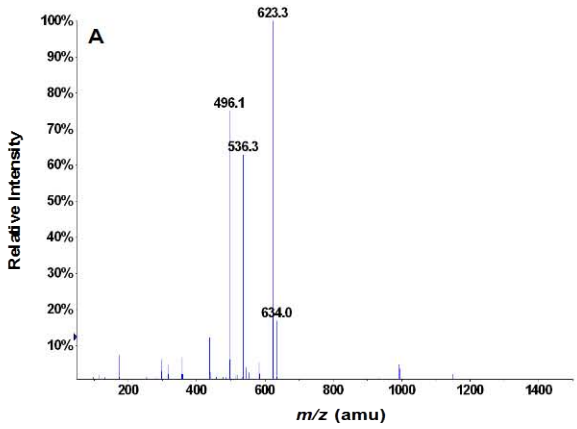
A
623.3
496.1
536.3
634.0
Relative Intensity
m/z (amu)

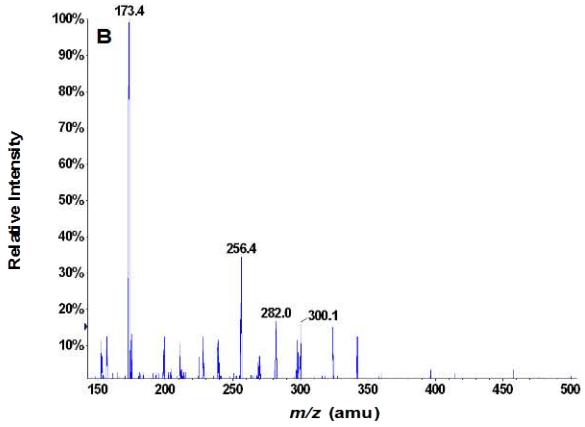
B
173.4
256.4
282.0
300.1
Relative Intensity
m/z (amu)

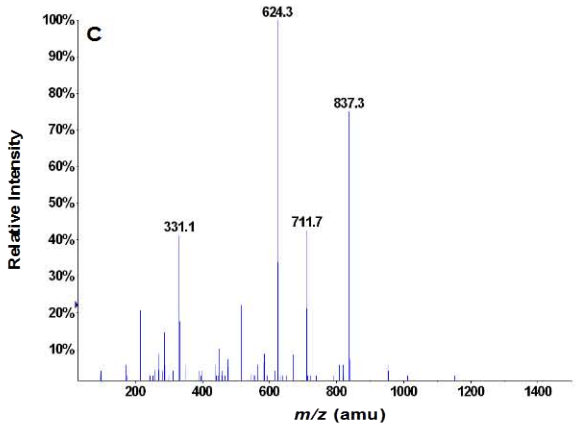
C
624.3
837.3
331.1
711.7
Relative Intensity
m/z (amu)

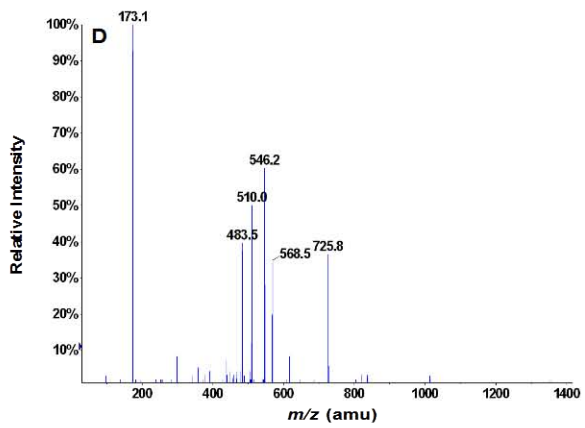
D
173.1
546.2
510.0
483.5
568.5
725.8
Relative Intensity
m/z (amu)

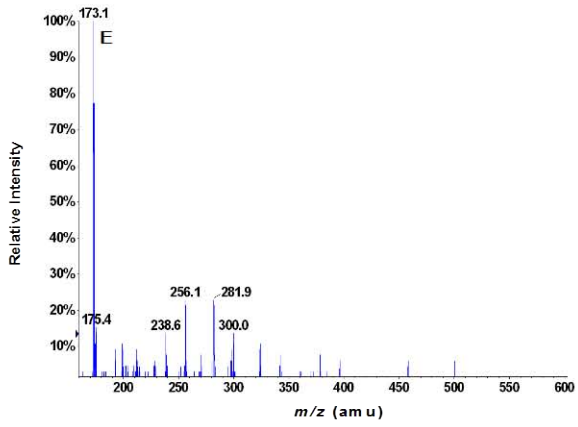
E
173.1
256.1
281.9
175.4
238.6
300.0
Relative Intensity
m/z (amu)

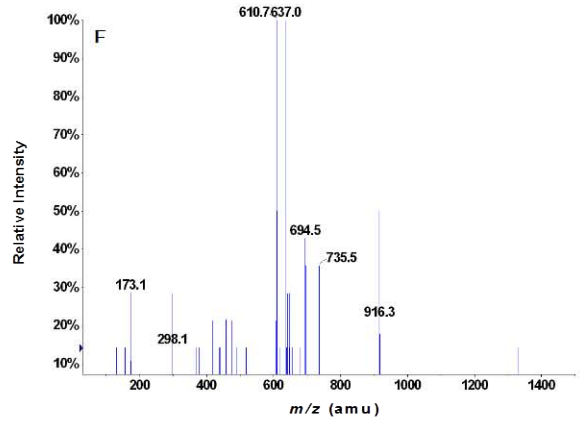
F
610.7637.0
694.5
735.5
173.1
916.3
298.1
Relative Intensity
m/z (amu)

3.3 DISCUSSION

A series of oligosaccharide substrates was prepared by BTH and chondroitinase ABC digestion of CS-A from bovine trachea and DS from porcine intestinal mucosa. These particular polysaccharide preparations were selected for depolymerisation as they: 1) have extremely simple structures, comprising > 90% GlcA-GalNAc(4S) and IdoA-GalNAc(4S) repeating disaccharides, respectively (Muthusamy *et al.* 2004, Sudo *et al.* 2001); and 2) generate oligosaccharide substrates representative of the putative physiological substrates derived from the GlcA-rich and the IdoA-rich domains of DS. The oligosaccharides produced from BTH and chondroitinase ABC digestion were size-fractionated on a Bio-Gel P6 column and then analysed as PMP-derivatives using a combination of negative ion ESI-MS and ESI-MS/MS.

Bio-Gel P6 was selected for size-fractionation of the various oligosaccharides resulting from enzyme digestion, as its broad fractionation range of up to 6 kDa enables the separation of GAG oligosaccharides of up to ~hexadecasaccharide in length, thus facilitating the preparation of the larger structures required to characterise the substrate specificities of the DS-degrading endoglycosidases. Similar to previous reports on the use of Bio-Gel P6 for separation of GAG oligosaccharides (Thonar *et al.* 1983, Muthusamy *et al.* 2004, Mason *et al.* 2006), a partial separation of hexadeca- to disaccharides was achieved in this case. However, the octa-, hexa-, tetra- and disaccharides, which eluted from the column from fraction 40 (160 mL) onwards, were more clearly resolved than the hexadeca-, tetradeca-, dodeca- and decasaccharides, which eluted between fractions 31 (124 mL) and 37 (148 mL) (Figure 3.2). The choice of Bio-Gel P6 for oligosaccharide purification therefore represented a compromise between: 1) its broad fractionation range and ability to rapidly and inexpensively process large sample quantities (hundreds of mg of GAG) without the need for specialised equipment or reagents; and 2) the relatively poor resolution of the decasaccharide and larger oligosaccharides. Although the oligosaccharides could conceivably have been further purified

by HPLC or capillary electrophoresis, these methods are generally not convenient for preparation of the large quantities of oligosaccharides required for the present study.

The negative ion ESI-MS spectra of the oligosaccharides eluted from the Bio-Gel P6 column were complex (Figures 3.3 to 3.5), with most molecules represented by multiple *m/z*, resulting from the presence of ions in various charge states due to differing degrees of oligosaccharide sulphation and proton abstraction. This is particularly evident in the spectra of the larger oligosaccharides, as these structures contain many sites for sulphation and deprotonation. Nevertheless, almost all of the major peaks in the ESI-MS spectra could be assigned to oligosaccharide structures by comparing the *m/z* values of the peaks observed to those of the variously charged ions predicted from oligosaccharides of the anticipated monoisotopic masses and structures. The oligosaccharides identified in this manner were composed of repeating UA-GalNAc disaccharide subunits and ranged in size from hexadeca- to disaccharides, with up to the equivalent of one sulphate per disaccharide (Tables 3.1 to 3.3). These structures are consistent with the uniform GlcA-GalNAc(4S) and IdoA-GalNAc(4S) disaccharide sequences that are reported to account for over 90% of the polysaccharide CS-A from bovine trachea and DS from porcine intestinal mucosa, respectively (Muthusamy *et al.* 2004, Sudo *et al.* 2001). The UA residues of the DS and CS-A oligosaccharides were designated as IdoA and GlcA, respectively, based upon these published structures, which further predict that the sulphates are positioned predominantly at C4 of the GalNAc residues. However, given that stereoisomers cannot be distinguished by *m/z* in ESI-MS scans, the presence of occasional GlcA residues in the DS oligosaccharides is acknowledged.

Product ion scans were performed on the oligosaccharides identified in the ESI-MS scans to: 1) confirm the structural assignments made by ESI-MS; 2) identify the reducing residue; and 3) for selected oligosaccharides, also identify a suitable product ion for MRM. In product ion scans, an oligosaccharide of interest (the parent oligosaccharide) is fragmented by

collision-induced dissociation to produce ions that represent the products of specific bond breakages within the oligosaccharide. The structural characterisation of the oligosaccharides by product ion scans was facilitated by PMP-derivatisation, which results in the addition of two PMP molecules to the reducing terminus, with a concomitant loss of H_2O, such that the molecular weight is increased by 330 Da (Pitt and Gorman 1997) (Figure 3.8). The presence of PMP at the reducing terminus of an oligosaccharide produces a number of characteristic product ions upon collision-induced dissociation. It was observed that each of the oligosaccharides from the BTH and chondroitinase ABC digests of CS-A and DS produced spectra containing multiple *m/z* peaks, indicative of numerous oligosaccharide dissociation events (Figures 3.6 and 3.7). The most prevalent of the product ions observed corresponded to the *m/z* of the parent compound, minus one PMP molecule and/or one sulphate group; this fragmentation was seen in almost all the product spectra and enabled rapid confirmation of the identity of the parent compound as a sulphated PMP-oligosaccharide. The fragmented PMP molecule *per se* was observed as an ion at *m/z* 173 in many spectra, e.g. in those of the CS-A tetra- and hexasaccharides (Figures 3.6D-F) and those of the DS tetra-, hexa- and octasaccharides (Figures 3.7B and D-F).

It has previously been reported that PMP-oligosaccharides with GalNAc and UA at the reducing end will fragment to give characteristic product ions at *m/z* 256 and 331, respectively, corresponding to a fragmented GalNAc with one PMP moiety and an intact UA with a PMP (Fuller *et al.* 2004a) (Figures 3.9A and B). This enabled the reducing end residue of the oligosaccharides to be confirmed as either GalNAc, as in the tetra- and hexasaccharides from CS-A (Figures 3.6D and F) and from DS (Figures 3.7B and E); or GlcA/IdoA, as in the CS-A tri- and pentasaccharides (Figures 3.6 A and B) and the DS pentasaccharide (Figure 3.7C). The presence of an additional product ion at *m/z* 282 in the spectra from the oligosaccharides terminating in GalNAc (Figures 3.6D and F and 3.7B and E), proposed as

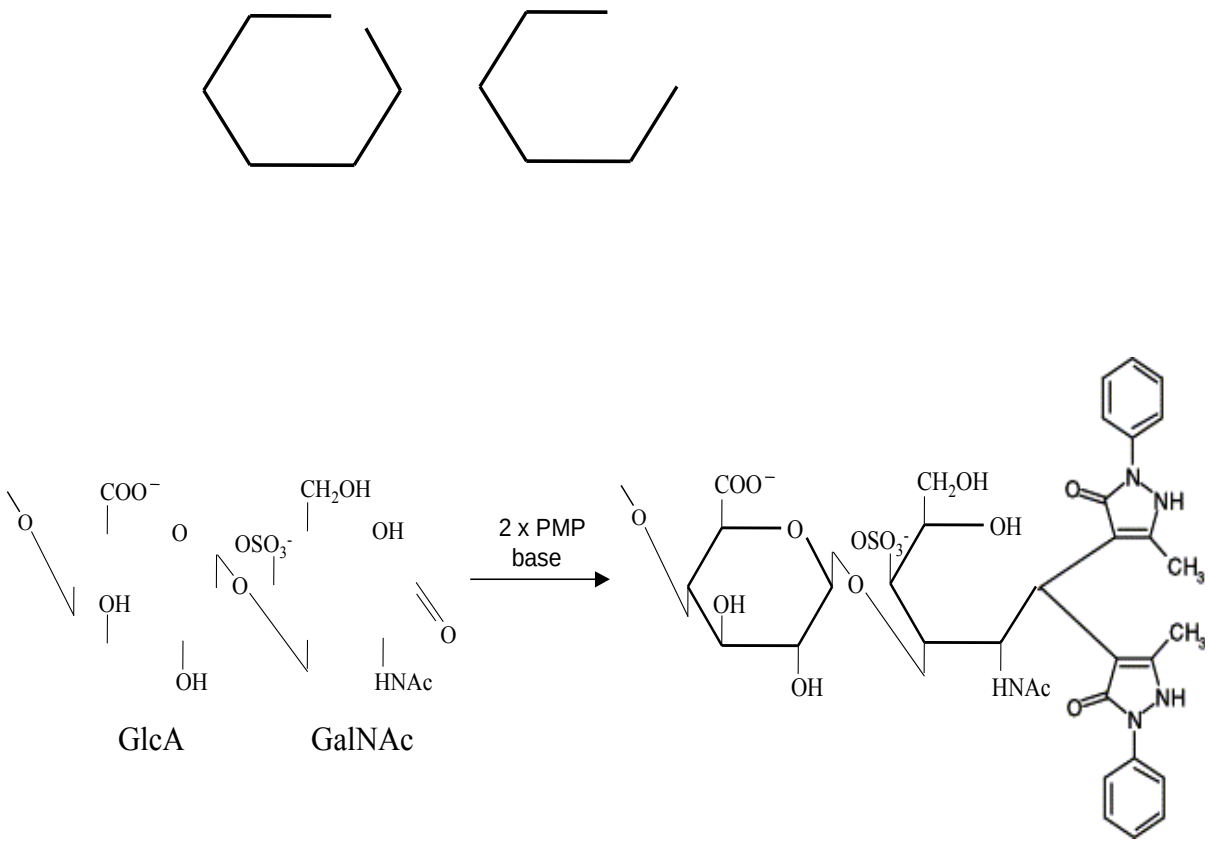

Figure 3.8 Oligosaccharide derivatisation with 1-phenyl-3-methyl-5-pyrazolone (PMP) Schematic illustrating the derivatisation of a representative CS-A oligosaccharide with PMP, which results in the addition of two PMP molecules to the reducing terminus. GlcA, glucuronic acid; GalNAc, *N*-acetylgalactosamine. Adapted from Ramsay *et al.* (2003).

the $[M-H]^{-1}$ ion of an intact reducing end GalNAc (+S) residue (Figure 3.9C), further confirmed these assignments.

All of the oligosaccharides from the BTH digestion of CS-A fragmented to give a product ion at *m/z* 193 and/or 175, as observed in the tetra- and hexasaccharides (Figures 3.6D and F), corresponding to a GlcA fragmented from the non-reducing end (Fuller *et al.* 2004a) (Figure 3.9D). However, ions corresponding to a similar fragmentation (i.e. a loss of ΔUA from the non-reducing end) were not observed at *m/z* 175 and/or 157 in the product spectra of the oligosaccharides from the chondroitinase ABC digests (Figure 3.7). This may indicate that the subtle structural change in non-reducing end UA induced by the removal of H_2O by chondroitinase ABC to form ΔUA reduces the ionisation efficiency of this residue, such that it is rendered undetectable when fragmented from the parent oligosaccharide in product ion scans. It was not possible to identify the fragmentation that resulted in a product ion at *m/z* 300, which was also observed from many of the oligosaccharides, such as the tetrasaccharide from CS-A (Figure 3.6D) and the tetra- and hexasaccharides from DS (Figures 3.7B and E). This product ion may represent an oligosaccharide fragment produced from multiple internal bond cleavages.

Each product ion scan also displayed unique ions detailing structural information about the oligosaccharide. For example, the product ion spectrum of the CS-A pentasaccharide, GlcA-[GalNAc-GlcA]$_2$ (+2S) (Figure 3.6B), showed a strong peak at *m/z* 855.3, corresponding to the $[M-H]^{-1}$ ion of the non-reducing end tetrasaccharide fragment resulting from breakage of the ultimate reducing end glycosidic bond, i.e. [GlcA-GalNAc]$_2$ (+S). The monosulphated nature of this non-reducing tetrasaccharide fragment indicates that the second sulphate of the parent pentasaccharide is located on the reducing end GlcA residue, however, the only ion in this spectrum that corresponds to a reducing end GlcA residue is seen at *m/z* 331.0 and is thus unsulphated. Taken together, these data indicate the presence of up to three pentasaccharide isomers that are distinguished by the positioning of the two

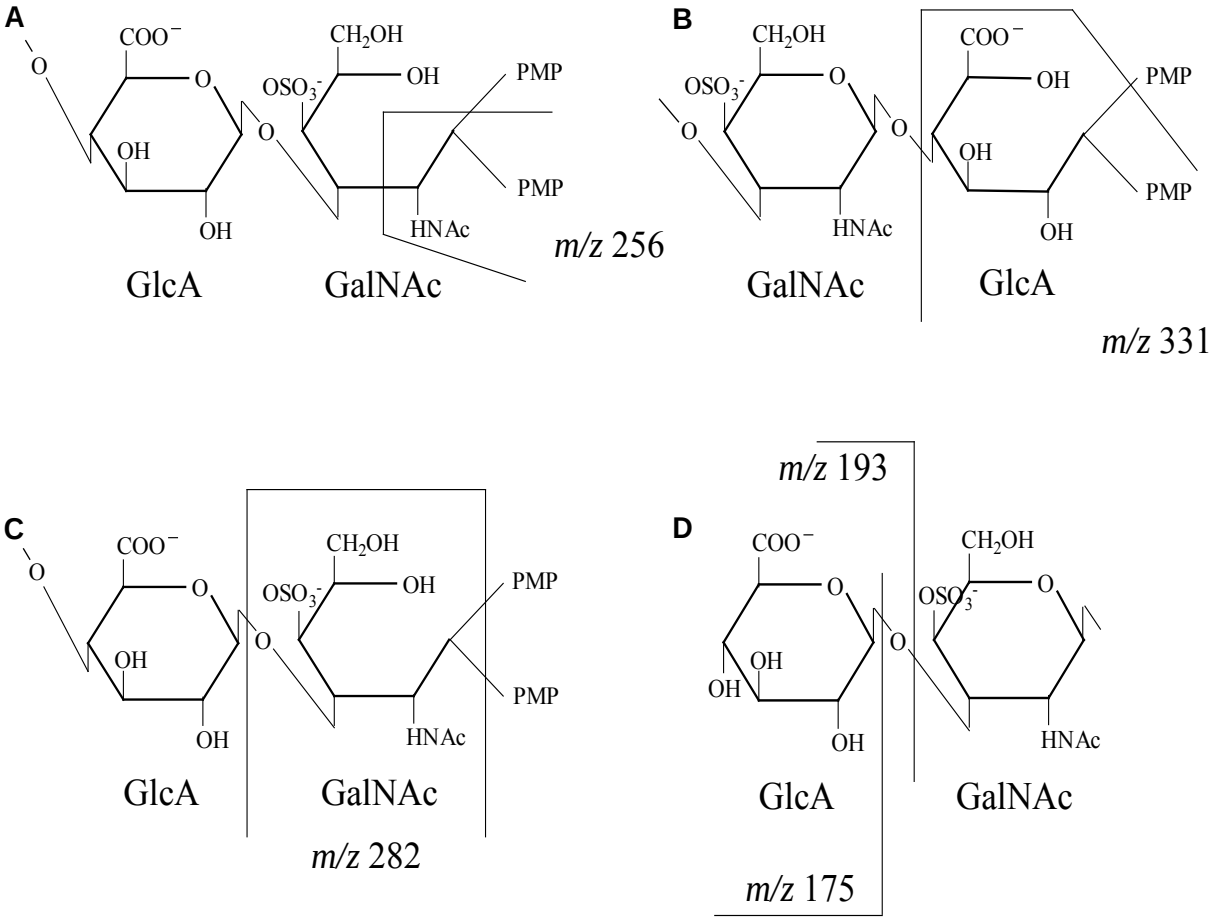

Figure 3.9 Proposed CS-A oligosaccharide fragmentations during ESI-MS/MS analysis

Proposed fragmentation patterns for PMP-derivatised CS-A oligosaccharides during ESI-MS/MS (product ion) analysis. Panel A shows fragmentation of a reducing end GalNAc residue to give the product ion at *m/z* 256. Panel B shows cleavage of an intact reducing end GlcA with a PMP to generate the product ion at *m/z* 331. Panel C illustrates the loss of an intact reducing end GalNAc to produce the ion at *m/z* 282. Panel D demonstrates fragmentation of GlcA from the non-reducing end to give the product ions at *m/z* 175 and/or 193. Similar fragmentations are proposed for PMP-derivatised DS oligosaccharides. GlcA, glucuronic acid; GalNAc, *N*-acetylgalactosamine.

sulphate esters, with two such isomers containing a sulphate on the reducing end GlcA residue (Figure 3.10). The sulphated GlcA residue is extremely rare in bovine tracheal CS-A (Muthusamy *et al.* 2004).

Based upon the well-established substrate specificities of BTH and chondroitinase ABC for GalNAc-UA bonds (Yamagata *et al.* 1968, Kreil 1995), even oligosaccharides with non-reducing end UA and reducing end GalNAc residues (i.e. the di-, tetra-, hexasaccharides etc.) were expected. However, the odd oligosaccharides with UA at the non-reducing end and GlcA or IdoA at the reducing end (i.e. the tri-, penta-, heptasaccharides etc.) cannot be the products of BTH and chondroitinase ABC. The odd oligosaccharides terminating in GlcA presumably represent the products of source tissue endo-β-glucuronidase activity (see section 1.5.1), and/or decomposition of the polysaccharide chains during commercial processing, that have been further depolymerised by BTH and chondroitinase ABC. As a DS-degrading endo-α-L-iduronidase enzyme has hitherto not been reported, the odd oligosaccharides terminating in IdoA most likely result from GAG chain decomposition exclusively. An oligosaccharide structure corresponding to the CS-A trisaccharide, ΔUA-GalNAc-GlcA (+S), has previously been observed after digestion of CS with chondroitinase ABC (Sugahara *et al.* 1994, Lauder *et al.* 2000). The oligosaccharides from the enzyme digests of CS-A and DS that eluted in the fractions from the Bio-Gel P6 column were not further purified and were used as substrates for the endoglycosidase product assay in chapter four.

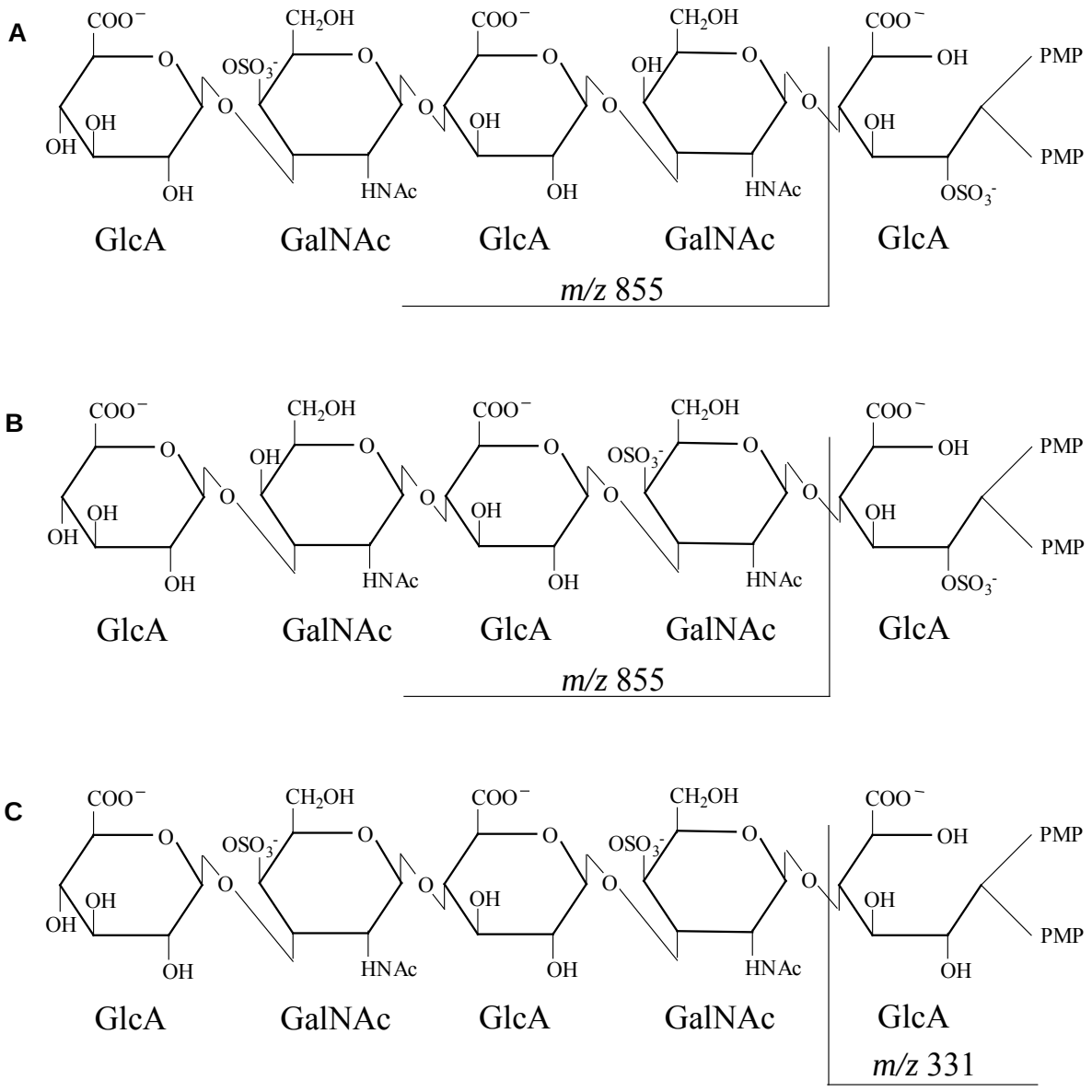

Figure 3.10 Proposed structures of pentasaccharides from BTH digest of CS-A

Potential structures for the disulphated pentasaccharide isolated from the BTH digest of CS-A, GlcA-[GalNAc-GlcA]$_2$ (+2S), based upon product ions observed during ESI-MS/MS analysis. Panels A and B show the pentasaccharide with one sulphate at C2 of the reducing end GlcA residue, and the second at C4 of the first and second GalNAc residues from the non-reducing end, respectively. These structures fragmented during ESI-MS/MS analysis to give the product ion at *m/z* 855. Panel C shows the pentasaccharide with a sulphate at C4 of each of the first and second GalNAc residues from the non-reducing end. This structure gave the product ion at *m/z* 331. GlcA, glucuronic acid; GalNAc, *N*-acetylgalactosamine.

CHAPTER FOUR

DEVELOPMENT OF

ENDOGLYCOSIDASE PRODUCT ASSAY

4.1 INTRODUCTION

Chapter three described the synthesis of a series of structurally defined oligosaccharides, to be used as substrates for evaluating the DS-degrading endoglycosidases. These oligosaccharides were composed of either GlcA-GalNAc or IdoA-GalNAc disaccharides, and were designed to reflect the predicted structures of the physiological substrates derived from the GlcA-rich and the IdoA-rich domains of DS polysaccharide, respectively. As outlined in sections 1.5.1 and 1.6, two different endoglycosidases have been implicated in the intra-cellular degradation of DS and are likely active towards these substrates. Hyal-1 is an acid-active hyaluronidase (endo-β-*N*-acetylhexosaminidase) of the somatic tissues that will cleave the GalNAc-GlcA glycosidic linkages of CS, in addition to the *N*-acetylglucosamine-GlcA bonds of its principal substrate, hyaluronan, to generate small oligosaccharides (di- to octasaccharides) as the main reaction products (Stern 2003, Hofinger *et al.* 2008). An acid-active endo-β-glucuronidase that degrades the GlcA-GalNAc bonds of CS has also been described (Takagaki *et al.* 1988b). While the apparent specificity of these enzymes for glycosidic linkages containing GlcA suggests that they would be active only towards the GlcA-rich domains of DS, their substrate specificities and catalytic mechanisms with respect to the specific degradation of DS oligosaccharides have not been studied in detail. Moreover, there have been no reports of endoglycosidase activities that will cleave the glycosidic linkages of DS that contain IdoA.

This chapter describes the development of an assay to measure endoglycosidase activities and determine their substrate specificities by quantifying specific oligosaccharide products. The oligosaccharides prepared in the previous chapter were incubated with CHO-K1 homogenate (a reported source of endoglycosidase activity) (Bame *et al.* 1998), and relative levels of the even (endo-β-*N*-acetylhexosaminidase) and odd (endohexuronidase) products derived from the non-reducing end of the substrate were measured by ESI-MS/MS. Assay parameters (sample and substrate concentration, pH and buffer conditions) were optimised for maximum product generation, and the effects of divalent cations, NaCl,

detergent, protease inhibitors and potential enzyme inhibitors upon the endoglycosidase activities were assessed. Using this approach, the substrate specificities and functional properties of the DS-degrading endoglycosidases were characterised.

4.2 RESULTS

4.2.1 Selection of oligosaccharides for use as assay substrates

In order to measure endoglycosidase activities, oligosaccharide substrates that would not be degraded by lysosomal exoenzyme activities were required. To determine whether the oligosaccharides prepared in the previous chapter were substrates for lysosomal exoenzymes, the tetrasaccharide from the BTH digest of CS-A, $[GlcA\text{-}GalNAc]_2$ (+2S), and its counterpart from the chondroitinase ABC digest of CS-A, ΔUA-GalNAc-GlcA-GalNAc (+2S) (prepared as described in section 2.2.4), were each incubated with bovine liver β-glucuronidase (section 2.2.4.3), and the levels of these oligosaccharides were then determined by ESI-MS/MS (section 2.2.12.2). Each oligosaccharide was also incubated in the absence of enzyme as a negative control. Figure 4.1 shows that the relative level of $[GlcA\text{-}GalNAc]_2$ (+2S) did not change relative to the negative control following incubation with β-glucuronidase at enzyme concentrations between 1 mU/mL and 1 U/mL. However, a 65% reduction in the level of $[GlcA\text{-}GalNAc]_2$ (+2S) was observed upon increasing the enzyme concentration from 1 to 10 U/mL, and $[GlcA\text{-}GalNAc]_2$ (+2S) was not detected at all upon subsequent 10-fold increases in enzyme concentration (100U-10kU/mL), indicating that the non-reducing GlcA residue of $[GlcA\text{-}GalNAc]_2$ (+2S) was a substrate for β-glucuronidase. In contrast, the relative level of ΔUA-GalNAc-GlcA-GalNAc (+2S) was unaltered following incubation with β-glucuronidase at all of the enzyme concentrations tested (Figure 4.1), suggesting that the non-reducing ΔUA residue of this oligosaccharide was resistant to cleavage by β-glucuronidase. Hence, the oligosaccharides containing this residue (i.e. those from the chondroitinase ABC digests of

CS-A and DS) were selected for use as substrates for development of the endoglycosidase product assay.

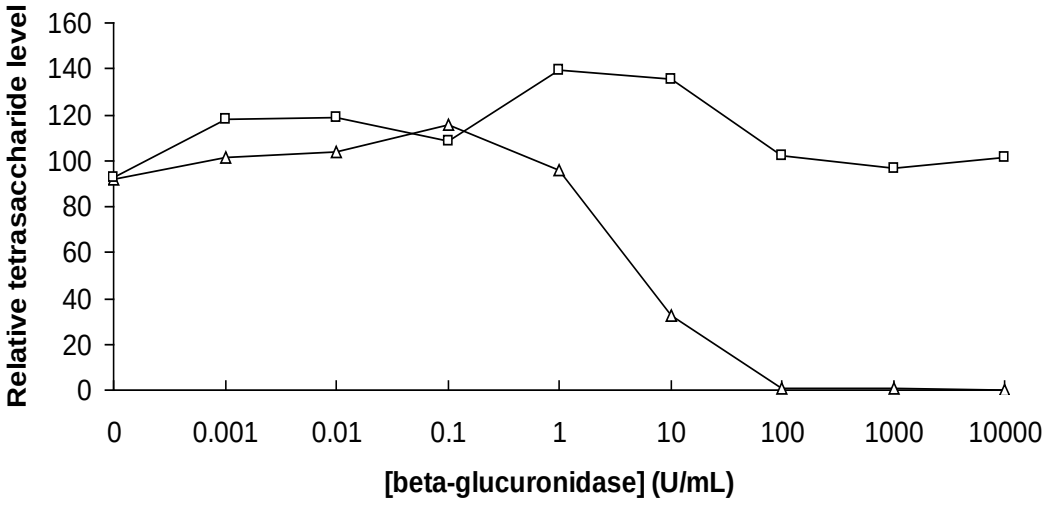

Figure 4.1 Relative tetrasaccharide levels following digestion with β-glucuronidase

The CS-A tetrasaccharides, $[GlcA\text{-}GalNAc]_2$ (+2S) (open triangles) and ΔUA-GalNAc-GlcA-GalNAc (+2S) (open squares), were individually incubated with bovine liver β-glucuronidase (1 mU-10 kU/mL) for 16 hr, and their relative levels were then measured by ESI-MS/MS.

4.2.2 Endo-β-*N*-acetylhexosaminidase activity towards oligosaccharide substrates

To demonstrate endo-β-*N*-acetylhexosaminidase activity towards the oligosaccharides selected in section 4.2.1, the tetra- to tetradecasaccharides from the chondroitinase ABC digests of CS-A and DS (prepared as described in section 2.2.4) were individually incubated with CHO-K1 homogenate (source of endoglycosidase activity) (section 2.2.6), and relative levels of the even di- to octasaccharide products generated from the non-reducing end of the substrate were then determined by ESI-MS/MS (section 2.2.12.2). The structures of the oligosaccharide substrates and products and the abbreviations used in reference to them are summarised in Table 4.1. Figure 4.2A shows that after incubation with the GlcA-rich CS-A Δtetra(+2S) substrate, no products were detected, i.e. CS-A Δtetra(+2S) was not digested. However, the slightly larger CS-A Δhexa(+3S) substrate was digested, generating a small amount of Δdi(+S) product exclusively. Increasing the length of the substrate by one disaccharide (CS-A Δhexa(+3S) to Δocta(+4S)) resulted in a seven-fold increase in Δdi(+S) product and the appearance of minor Δtetra(+2S) product. The addition of another disaccharide to the length of the substrate did not further alter the level of Δdi(+S) product, but did result in a nine-fold increase in Δtetra(+2S) product. The amounts of both Δdi(+S) and Δtetra(+2S) products were unchanged with subsequent disaccharide increases in substrate length. Small quantities of Δhexa(+2S), Δhexa(+3S), and Δocta(+3S) products were also detected from CS-A Δdodeca(+6S) substrate. The levels of these products increased slightly as substrate length was increased by another disaccharide (to CS-A Δtetradeca(+7S)). Incubation with IdoA-rich substrate (DS Δdodeca(+6S)) produced Δdi(+S), Δtetra(+2S), Δhexa(+2S) and Δhexa(+3S) in quantities equivalent to only 14%, 7%, 8% and 16%, respectively, of those generated from CS-A Δdodeca(+6S) (Figure 4.2B).

Table 4.1 Structures of CS-A/DS oligosaccharide substrates/products

Oligosaccharide[a]	Abbreviation
ΔUA-GalNAc (+S)	Δdi(+S)
ΔUA-GalNAc-UA (+S)	Δtri(+S)
ΔUA-GalNAc-UA-GalNAc (+2S)	Δtetra(+2S)
ΔUA-[GalNAc-UA]$_2$ (+2S)	Δpenta(+2S)
ΔUA-GalNAc-[UA-GalNAc]$_2$ (+2-3S)	Δhexa(+2-3S)
ΔUA-[GalNAc-UA]$_3$ (+3S)	Δhepta(+3S)
ΔUA-GalNAc-[UA-GalNAc]$_3$ (+3-4S)	Δocta(+3-4S)
ΔUA-[GalNAc-UA]$_4$ (+4S)	Δnona(+4S)
ΔUA-GalNAc-[UA-GalNAc]$_4$ (+3-5S)	Δdeca(+3-5S)
ΔUA-[GalNAc-UA]$_5$ (+4-5S)	Δundeca(+4-5S)
ΔUA-GalNAc-[UA-GalNAc]$_5$ (+4-6S)	Δdodeca(+4-6S)
ΔUA-[GalNAc-UA]$_6$ (+5-6S)	Δtrideca(+5-6S)
ΔUA-GalNAc-[UA-GalNAc]$_6$ (+5-7S)	Δtetradeca(+5-7S)

[a]ΔUA, unsaturated uronic acid; UA, uronic acid; GalNAc, *N*-acetylgalactosamine; S, sulphate

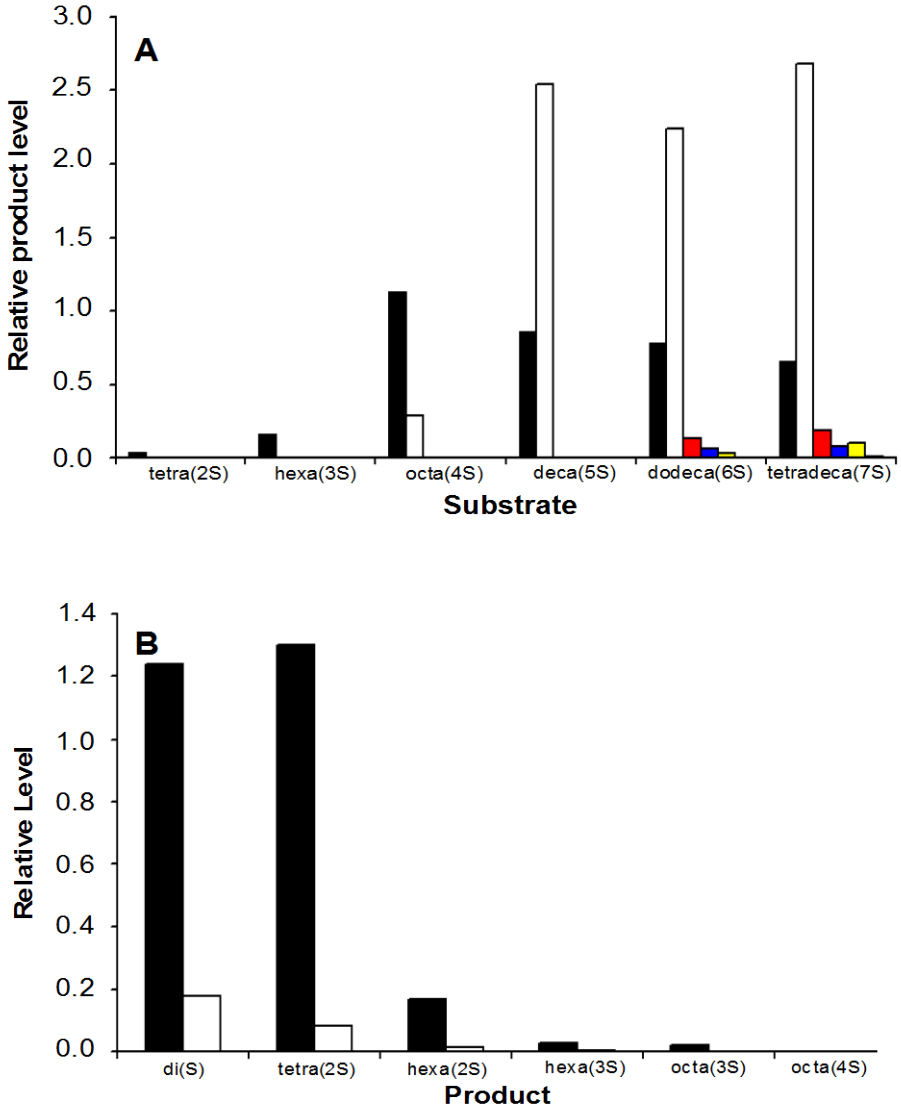

Figure 4.2 Relative levels of endo-β-*N*-acetylhexosaminidase products following endohydrolysis of oligosaccharide substrates

Oligosaccharide substrates were individually incubated with CHO-K1 homogenate (25 mg/mL protein equivalents) in 100 mM sodium formate, pH 3.5, for 24 hr, and relative levels of the even products derived from the non-reducing end of the substrate were then measured by ESI-MS/MS. Panel A shows the relative levels of the products, Δdi(+S) (black bar), Δtetra(+2S) (white bar), Δhexa(+2S) (red bar), Δhexa(+3S) (blue bar), Δocta(+3S) (yellow bar) and Δocta(+4S) (pink bar) following endohydrolysis of tetra- to tetradecasaccharide substrates from CS-A. Panel B shows the relative levels of these products following endohydrolysis of dodecasaccharide substrate from CS-A (black bar) and DS (white bar).

Based on these findings, the sensitivities of the *N*-acetylhexosaminic linkages of the oligosaccharide substrates to endo-β-*N*-acetylhexosaminidase cleavage were established (Table 4.2). Whereas the activity cleaved CS-A Δhexa(+3S) at the ultimate non-reducing end *N*-acetylhexosaminic bond exclusively, the larger CS-A substrates were also cleaved at the penultimate, and CS-A Δdodeca(+6S) and Δtetradeca(+7S) were further degraded at the antepenultimate and preantepenultimate linkages. Minor cleavage of DS Δdodeca(+6S) occurred at each of the ultimate, penultimate and antepenultimate *N*-acetylhexosaminic linkages from the non-reducing end.

4.2.3 Endohexuronidase activity towards oligosaccharide substrates

To demonstrate endohexuronidase cleavage of the selected oligosaccharides, the hexa- to tetradecasaccharides from the chondroitinase ABC digests of CS-A and DS (prepared as described in section 2.2.4) were individually incubated with CHO-K1 homogenate (source of endoglycosidase activity) (section 2.2.6), and relative levels of the odd di- to octasaccharide products generated from the non-reducing end of the substrate were then determined by ESI-MS/MS (section 2.2.12.2). The use of CS-A Δtetra(+2S) as a substrate for the endohexuronidase activity was prevented by high levels of Δtri(+S) impurities in the CS-A Δtetra(+2S) substrate preparation. These impurities resulted from co-elution of Δtri(+S) and Δtetra(+2S) from the Bio-Gel P6 column (Figures 3.2B and 3.4E; Table 3.2). Figure 4.3A illustrates that when the GlcA-rich CS-A Δhexa(+3S) was used as substrate, no digestion was observed, and that whilst both CS-A Δocta(+4S) and Δdeca(+5S) generated exclusively Δtri(+S), seven-fold more was detected from the latter. Further increasing the length of the substrate had no effect upon the level of Δtri(+S). However, it did result in the generation of Δpenta(+2S) and Δhepta(+3S) products. The quantities of Δpenta(+2S) and Δhepta(+3S) products increased marginally as substrate length was increased by a disaccharide (CS-A

Δdodeca(+6S) to Δtetradeca(+7S)). The IdoA-rich DS Δdodeca(+6S) produced Δtri(+S) and Δpenta(+2S) in amounts equivalent to 6% and 19%, respectively, of those generated from CS-A Δdodeca(+6S) (Figure 4.3B).

Table 4.2 indicates the uronidic linkages in the oligosaccharides that were degraded by the endohexuronidase activity. While CS-A Δocta(+4S) and Δdeca(+5S) were digested only at the penultimate non-reducing end uronidic bond, the larger CS-A substrates were additionally cleaved at the antepenultimate and preantepenultimate linkages. Some degradation of DS Δdodeca(+6S) occurred at the penultimate and antepenultimate non-reducing uronidic linkages.

4.2.4 Optimisation of assay conditions

To determine the optimum assay parameters for measurement of endoglycosidase products, oligosaccharide substrates (prepared as described in section 2.2.4) were incubated with CHO-K1 homogenate under a range of conditions and relative levels of the non-reducing end products were determined by ESI-MS/MS (section 2.2.12.2). The parameters evaluated included sample and substrate concentration, pH and buffer conditions, and the effects of NaCl, divalent cations, detergent and protease inhibitors. The CS-A substrates larger than Δocta(+4S) were selected for these experiments, since these were of sufficient length for maximum generation of the major endo-β-*N*-acetylhexosaminidase and endohexuronidase products, i.e. Δtetra(+2S) and Δtri(+S), respectively (Figures 4.2A and 4.3A).

Figures 4.4 and 4.5 show that generation of Δtetra(+2S) and Δtri(+S) products was proportional to sample concentration up to 25 mg/mL protein, and proportional to substrate concentration up to 500 μM, and hence all subsequent assays were performed with a substrate concentration of 500 μM. Both products were generated only within a narrow acidic pH range, with maximum product generation occurring at around pH 3.5 and none above pH 4.0

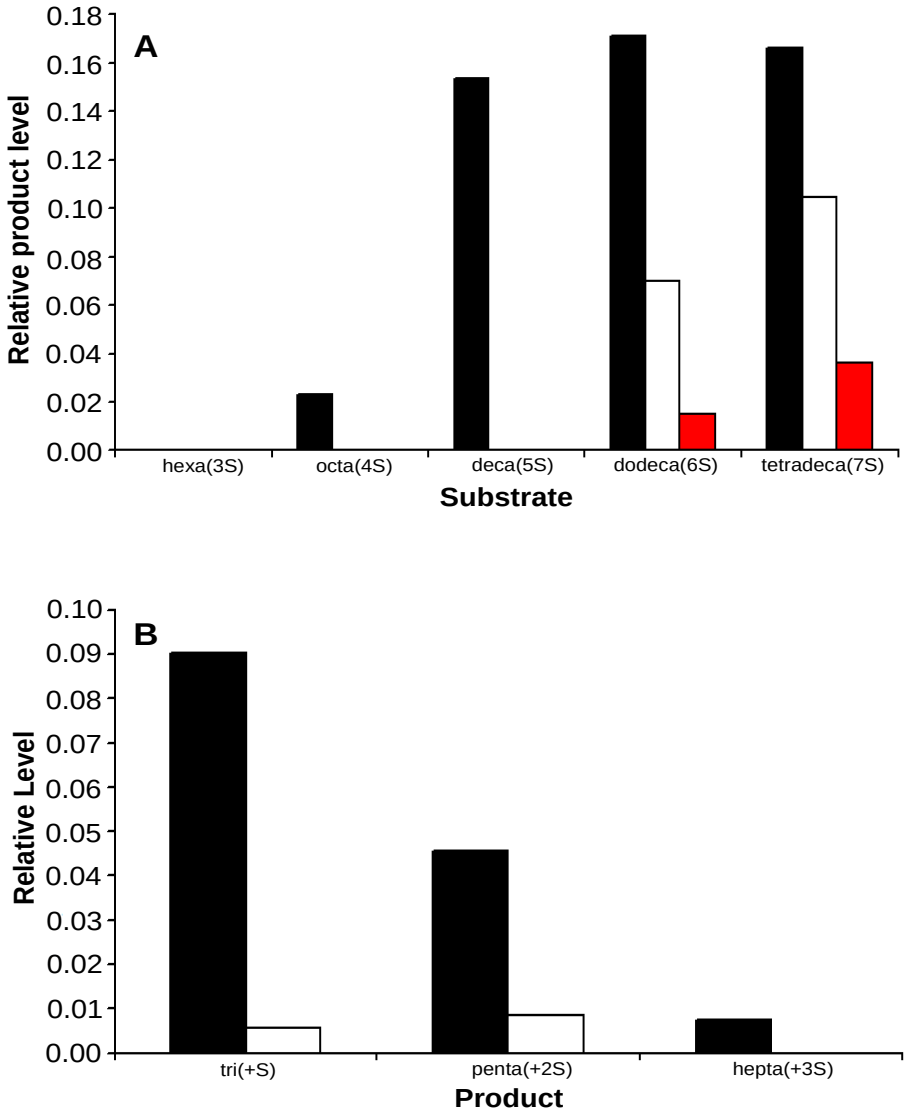

Figure 4.3 Relative levels of endohexuronidase products following endohydrolysis of oligosaccharide substrates

Oligosaccharide substrates were individually incubated with CHO-K1 homogenate (25 mg/mL protein equivalents) in 100 mM sodium formate, pH 3.5, for 24 hr, and relative levels of the odd products derived from the non-reducing end of the substrate were then measured by ESI-MS/MS. Panel A shows the relative levels of the products, Δtri(+S) (black bar), Δpenta(+2S) (white bar) and Δhepta(+3S) (red bar) following endohydrolysis of hexa- to tetradecasaccharide substrates from CS-A. Panel B shows the relative levels of these products following endohydrolysis of dodecasaccharide substrate from CS-A (black bar) and DS (white bar).

Table 4.2 Sensitivities of oligosaccharides to endo-β-*N*-acetylhexosaminidase and endohexuronidase activities

Oligosaccharide	Structure[a]
CS-A Δtetra(+2S)	ΔUA[b]-GalNAc-UA-GalNAc
CS-A Δhexa(+3S)	ΔUA[b]-GalNAc[c]-UA-GalNAc-UA-GalNAc
CS-A Δocta(+4S)	ΔUA[b]-GalNAc[c]-UA[d]-GalNAc[c]-UA-GalNAc-UA-GalNAc
CS-A Δdeca(+5S)	ΔUA[b]-GalNAc[c]-UA[d]-GalNAc[c]-UA-GalNAc-UA-GalNAc-UA[b]-GalNAc
CS-A Δdodeca(+6S)	ΔUA[b]-GalNAc[c]-UA[d]-GalNAc[c]-UA[d]-GalNAc[c]-UA[d]-GalNAc[c]-UA[b]-GalNAc[b]-UA[b]-GalNAc
CS-A Δtetradeca(+7S)	ΔUA[b]-GalNAc[c]-UA[d]-GalNAc[c]-UA[d]-GalNAc[c]-UA[d]-GalNAc[c]-UA[b]-GalNAc[b]-UA[b]-GalNAc[b]-UA[b]-GalNAc
DS Δdodeca(+6S)	ΔUA[b]-GalNAc[c]-UA[d]-GalNAc[c]-UA[d]-GalNAc[c]-UA-GalNAc-UA[b]-GalNAc[b]-UA[b]-GalNAc

[a]ΔUA, unsaturated uronic acid; UA, uronic acid; GalNAc, *N*-acetylgalactosamine; S, sulphate

[b]not monitored

[c]endo-β-*N*-acetylhexosaminidase cleavage site

[d]endohexuronidase cleavage site

(Figure 4.6). Product generation was maximum when substrate was incubated in the presence of sodium formate, compared to sodium acetate and 3,3-dimethylglutaric acid (DMG) buffers (Table 4.3). Increasing the ionic strength of the sodium formate and DMG buffers from 50 to 100 mM increased the generation of these products, however their levels were considerably reduced when the strength of the sodium acetate buffer was correspondingly increased (Table 4.3). The addition of protease inhibitors to the incubation mixture almost tripled and doubled the generation of the Δtetra(+2S) and Δtri(+S) products, respectively, compared to control experiments performed in their absence, whereas the presence of NaCl had a slightly inhibitory effect upon the generation of these products, which was augmented by the inclusion of detergent (Table 4.4).

Figure 4.7 shows that $MnCl_2$ had no effect upon product generation when present at concentrations of 100 μM or 1 mM, but at 10 mM increased the generation of Δtetra(+2S) and Δtri(+S) products to levels 73% and 37% higher, respectively, than those generated from a control digest performed in the absence of cation (panel A). $MgCl_2$ had little effect upon product generation at each of the three concentrations tested (panel B). $CoCl_2$ slightly inhibited the generation of Δtri(+S) product when present at a concentration of 100 μM, but at 1 mM increased the production of Δtetra(+2S) and Δtri(+S) to levels 27% and 18% higher than the control, respectively (panel C). An additional increase in the generation of Δtetra(+2S) to a level 47% above the control occurred as the concentration of $CoCl_2$ was further increased to 10 mM, but no corresponding increase in the level of Δtri(+S) was observed. $CaCl_2$ increased the generation of Δtetra(+2S) and Δtri(+S) by ~60% and ~35-60% relative to the control, respectively, when included at concentrations of 100 μM and 1 mM, however, product generation decreased back to control levels as the $CaCl_2$ concentration was further increased to 10 mM (panel D).

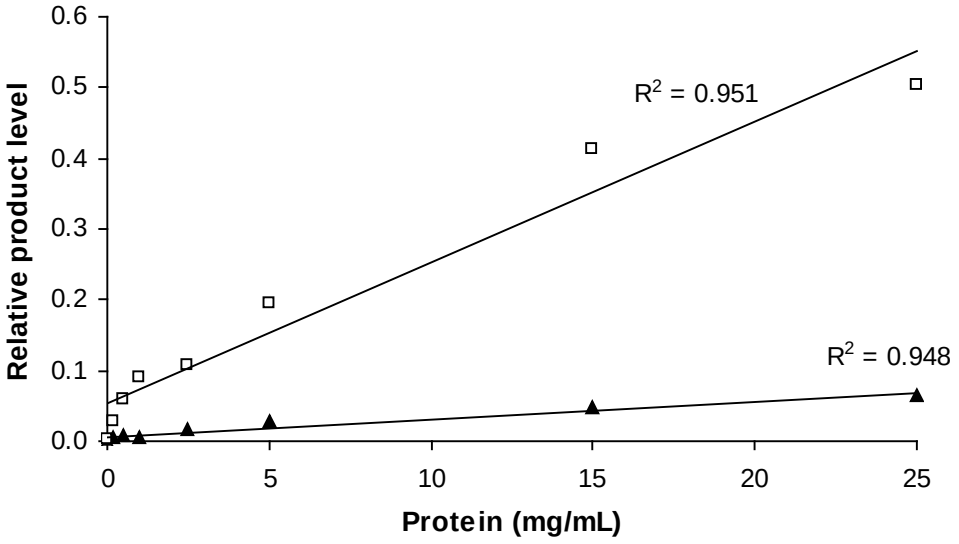

Figure 4.4 Effect of sample concentration on relative product levels following endohydrolysis of CS-A

Tetradecasaccharide substrate from CS-A was incubated with CHO-K1 homogenate (0.20-25 mg/mL protein equivalents) in 100 mM sodium formate, pH 3.5, for 24 hr, and relative levels of the products derived from the non-reducing end of the substrate were then measured by ESI-MS/MS. Relative levels of the products, Δtetra(+2S) (open squares) and Δtri(+S) (filled triangles) are shown.

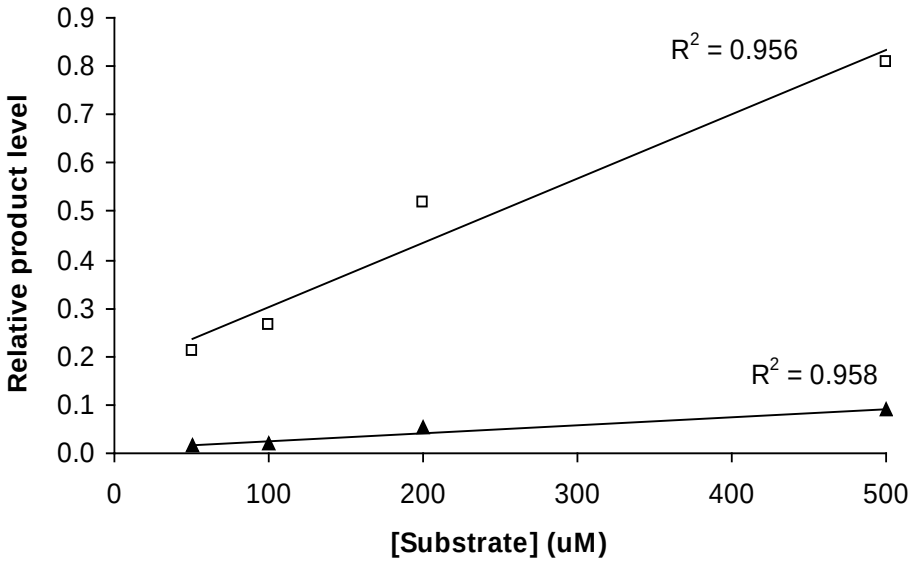

Figure 4.5 Effect of substrate concentration on relative product levels following endohydrolysis of CS-A

Dodecasaccharide substrate from CS-A (5-50 nmol) was incubated with CHO-K1 homogenate (25 mg/mL protein equivalents) in 100 mM sodium formate, pH 3.5, for 24 hr, and relative levels of the products derived from the non-reducing end of the substrate were then measured by ESI-MS/MS. Relative levels of the products, Δtetra(+2S) (open squares) and Δtri(+S) (filled triangles) are shown.

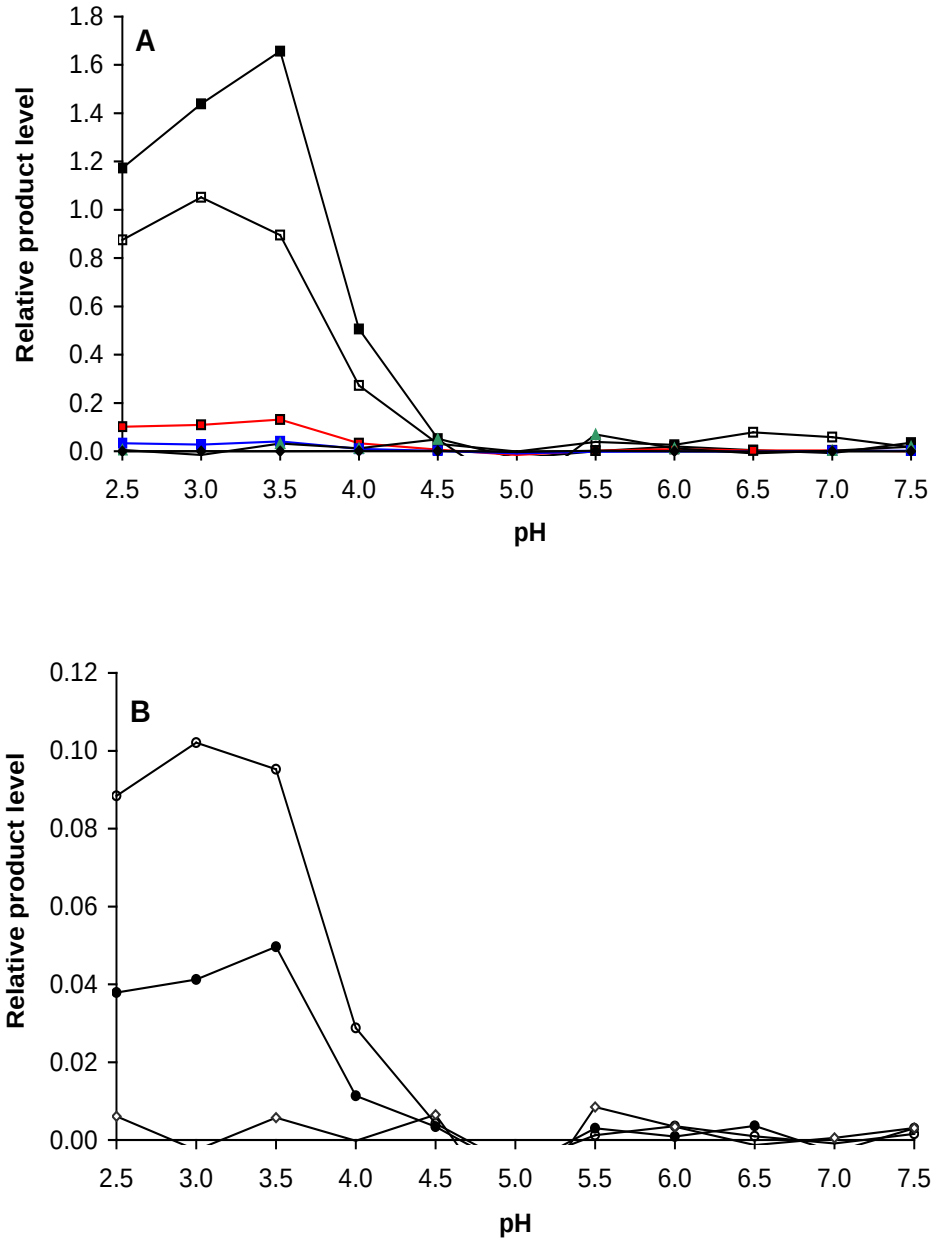

Figure 4.6 Effect of pH on relative product levels following endohydrolysis of CS-A

Dodecasaccharide substrate from CS-A was incubated with CHO-K1 homogenate (25 mg/mL protein equivalents) in 100 mM DMG buffer, pH 2.5-7.5, for 24 hr, and relative levels of the even (panel A) and odd (panel B) products derived from the non-reducing end of the substrate were then measured by ESI-MS/MS. Relative levels of the products, Δdi(+S) (white squares), Δtetra(+2S) (black squares), Δhexa(+2S) (red s quares), Δhexa(+3S) (blue s quares), Δocta(+3S) (green triangles), Δocta(+4S) (black di amonds), Δtri(+S) (ope n circles), Δpenta(+2S) (black circles) and Δhepta(+3S) (open diamonds) are shown.

Table 4.3 Comparison of relative product levels following endohydrolysis of CS-A Δdeca(+5S) substrate in sodium formate, sodium acetate and DMG buffers

	Δtri(+S)		
	HCOONa	DMG	CH_3COONa
50 mM	57	39	13
100 mM	100	54	5
	Δtetra(+2S)		
	HCOONa	DMG	CH_3COONa
50 mM	65	37	13
100 mM	100	62	5

Relative product levels are expressed as a percentage of product generated in 100 mM sodium formate buffer. Buffers were at pH 3.5.

Table 4.4 Comparison of relative product levels following endohydrolysis of CS-A Δdodeca(+6S) substrate in the presence of NaCl, Triton X-100 and protease inhibitors

	NaCl (0.15 M)	NaCl (0.15 M) + Triton (0.1% (v/v))	Protease Inhibitors[a]
Δtri (+S)	81	52	179
Δtetra(+2S)	92	77	284

Incubations were performed in 100 mM sodium formate, pH 3.5. Relative product levels are expressed as a percentage of product generated in this buffer alone.

[a]one tablet Complete Mini protease inhibitor cocktail/10 mL and 1 μM pepstatin

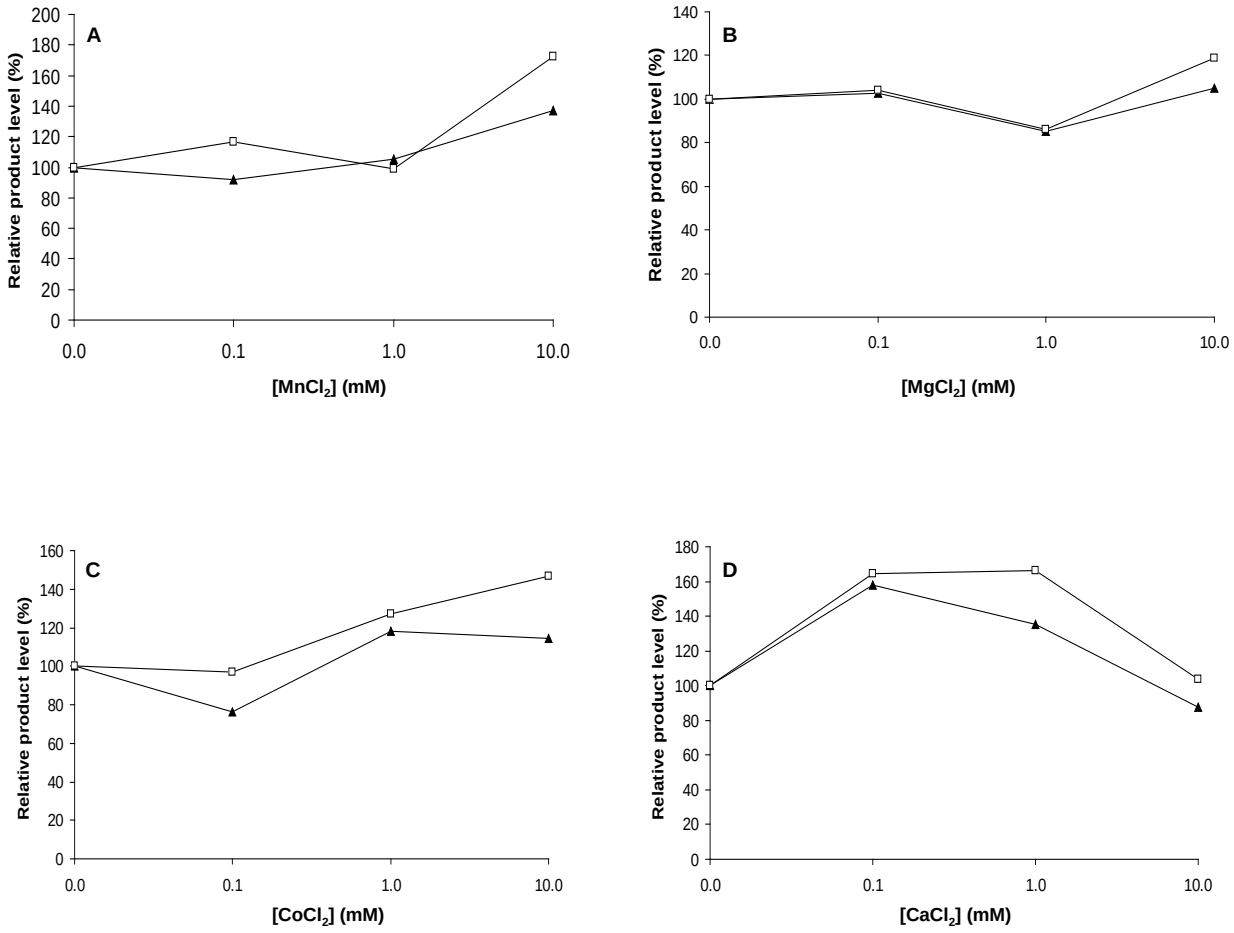

Figure 4.7 Effect of divalent metal cations on relative product levels following endohydrolysis of CS-A

Oligosaccharide substrates from CS-A were incubated with CHO-K1 homogenate (25 mg/mL protein equivalents) in 100 mM sodium formate containing metal cations, pH 3.5, for 24 hr, and relative levels of the products derived from the non-reducing end of the substrate were then measured by ESI-MS/MS. Panels A and B show the relative levels of the products, Δtetra(+2S) (open squares) and Δtri(+S) (filled triangles) following endohydrolysis of dodecasaccharide substrate in the presence of 0.1, 1 and 10 mM $MnCl_2$ and $MgCl_2$, respectively. Panels C and D show the relative levels of these products following endohydrolysis of decasaccharide substrate in the presence of 0.1, 1 and 10 mM $CoCl_2$ and $CaCl_2$, respectively. Relative product levels are expressed as a percentage of product generated in 100 mM sodium formate, pH 3.5.

4.2.5 Attempted inhibition of endo-β-*N*-acetylhexosaminidase activity

To enable the measurement of endohexuronidase activity independently of endo-β-*N*-acetylhexosaminidase activity, an attempt was made to inhibit the endo-β-*N*-acetylhexosaminidase activity in the CHO-K1 homogenates by competitive inhibition, using the reported hyaluronidase inhibitor, apigenin, and small oligosaccharides. Figure 4.8 shows that both endoglycosidase activities were unaffected by the presence of apigenin at concentrations of up to 100 μg/mL, however, slight inhibition of the activities was observed at concentrations of 250 and 500 μg/mL, as evidenced by a ~30-40% reduction in the generation of both Δtetra(+2S) and Δtri(+S) products compared to control experiments performed in the absence of the inhibitor. Further increasing the apigenin concentration from 500 to 1000 μg/mL resulted in restoration of the endoglycosidase activities to control levels (Figure 4.8). In contrast, the presence of an excess (1 mM) of the CS-A tetrasaccharide (CS-A Δtetra(+2S)) completely abolished the generation of Δtetra(+2S) and Δtri(+S) products, indicating that complete inhibition of both endo-β-*N*-acetylhexosaminidase and endohexuronidase activities had occurred (data not shown).

4.3 DISCUSSION

An ESI-MS/MS assay was developed to measure endoglycosidase activities and determine their substrate specificities by quantifying specific oligosaccharide products. The oligosaccharides prepared from the chondroitinase ABC digests of CS-A and DS were selected for use as assay substrates, since: 1) these oligosaccharides are representative of the putative physiological substrates derived from the GlcA-rich and IdoA-rich domains of DS, respectively; 2) the complete resistance of the non-reducing ΔUA residue of these oligosaccharides to digestion by bovine liver β-glucuronidase (Figure 4.1) suggested that they were not substrates for lysosomal exoenzymes; 3) the presence of this residue further enabled

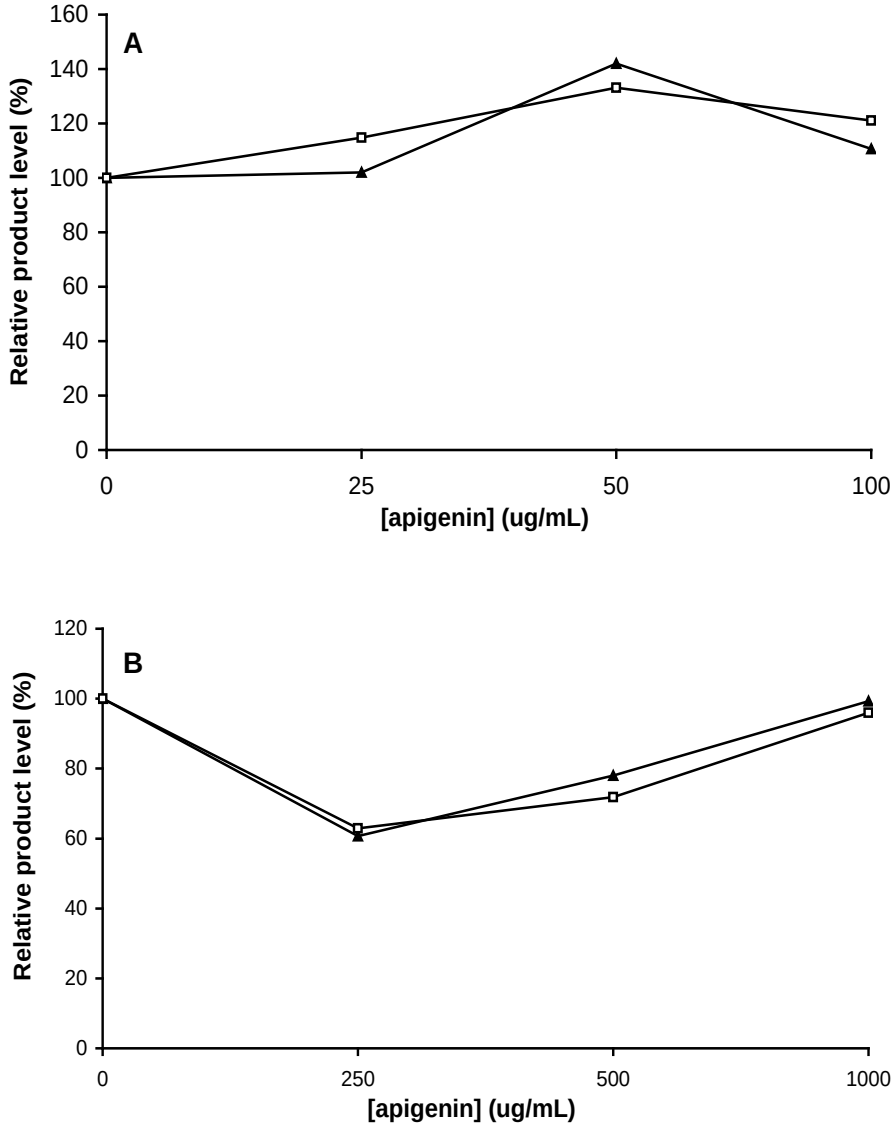

Figure 4.8 Effect of apigenin on relative product levels following endohydrolysis of CS-A

Decasaccharide substrate from CS-A was incubated with CHO-K1 homogenate (25 mg/mL protein equivalents) in 100 mM sodium formate containing apigenin (prepared in DMSO and added to the buffer so that the final concentration of the solvent did not exceed 0.1%), pH 3.5, for 24 hr, and relative levels of the products derived from the non-reducing end of the substrate were then measured by ESI-MS/MS. Relative levels of the products, Δtetra(+2S) (open squares) and Δtri(+S) (filled triangles) are shown following endohydrolysis of substrate in the presence of 25-100 μg/mL (panel A) or 250-1000 μg/mL (panel B) apigenin. Relative product levels are expressed as a percentage of product generated in 100 mM sodium formate/0.1% (v/v) DMSO, pH 3.5.

the selective monitoring by ESI-MS/MS of even (endo-β-*N*-acetylhexosaminidase) and odd (endohexuronidase) non-reducing products, which differed in mass from their reducing side counterparts by 18 amu (i.e. one H_2O molecule); and 4) both endo-β-*N*-acetylhexosaminidase and endohexuronidase activities were detected towards these substrates (Figures 2 and 3). Analysis of the specific products of the CHO-K1 endoglycosidase activities towards the oligosaccharide substrates enabled several novel aspects of the substrate specificities, catalytic mechanisms and functional properties of the DS-degrading endoglycosidases to be determined.

4.3.1 Substrate specificity of endo-β-*N*-acetylhexosaminidase activity

The endo-β-*N*-acetylhexosaminidase activity showed a marked preference for oligosaccharide substrates rich in GlcA, compared to IdoA, as evidenced by the relative resistance of IdoA-rich DS oligosaccharide to digestion (Figure 4.2 B). This most likely reflects specificity for GalNAc-GlcA rather than GalNAc-IdoA glycosidic linkages, with the small amounts of products observed after incubation with the DS oligosaccharide reflecting the specific cleavage of the approximately one in ten GalNAc-UA linkages of porcine intestinal mucosa DS that contain GlcA (Sudo *et al.* 2001). However, as the structures of the products derived from the reducing side of the endo-β-*N*-acetylhexosaminidase cleavage sites are not apparent from these data, the non-reducing products observed from the DS oligosaccharide could conceivably also result from, for example, a slow cleavage of the GalNAc-IdoA linkages, or from cleavage at specific, infrequent subsets of such linkages. In any case, these findings indicate that endohydrolysis of polysaccharide DS occurs predominantly in the GlcA-rich domains, where the GalNAc-GlcA linkages are concentrated.

The ultimate reducing end *N*-acetylhexosaminic linkage of each CS-A oligosaccharide was resistant to cleavage by the endo-β-*N*-acetylhexosaminidase activity (Table 4.2), which implies an absolute requirement for a minimum of two disaccharides on the reducing side of

the target GalNAc, and the minimum-sized substrate requirement was thus a hexasaccharide (Figure 4.2A). Maximum generation of a specific product required at least three disaccharides on the reducing side of the target GalNAc. For example, although some Δdi(+S) product could be liberated from CS-A Δhexa(+3S) substrate by endohydrolysis of the first GalNAc-UA linkage from the non-reducing end according to the two-disaccharide minimum requirement, production of Δdi(+S) reached a maximum when at least three disaccharides were present to the reducing side of this linkage, i.e. in the Δocta(+4S) and larger substrates (Figure 4.2A).

As deuterated internal standards were not available for each of the oligosaccharide species under investigation, the levels of the oligosaccharide products were calculated relative to a disaccharide internal standard, ΔUA-GlcNAc(6S)(d_3). Direct comparison between the relative levels of different oligosaccharides is complicated by their varying response factors when determined by ESI-MS/MS (Rozaklis *et al.* 2002). Analysis of the CS-A oligosaccharide substrates showed that each disaccharide addition to an oligosaccharide resulted in a successive decrease in response of approximately 50% (data not shown). Therefore, to allow a more accurate comparison between product levels, the relative levels of the products larger than Δdi(+S) were successively doubled for each disaccharide equivalent increase in chain length. After this correction for approximate response factors, the major endo-β-*N*-acetylhexosaminidase product from CS-A Δhexa(+3S) and Δocta(+4S) substrates was Δdi(+S), and from the CS-A substrates larger than Δocta(+4S), the major product was Δtetra(+2S) (Figure 4.9 A). This indicates that notwithstanding restrictions imposed by the length of the substrate, as discussed above, the endo-β-*N*-acetylhexosaminidase activity preferentially cleaves the second *N*-acetylhexosaminic linkage from the non-reducing end of oligosaccharide substrates rather than other *N*-acetylhexosaminic bonds to liberate tetrasaccharides as the main reaction products.

The endo-β-*N*-acetylhexosaminidase activity towards GalNAc-UA linkages described here is consistent with the reported ability of the Hyal-1 hyaluronidase enzyme to cleave the GalNAc-GlcA linkages of CS (Stern 2003). Although the minimum-sized hyaluronan substrate requirement of recombinant human Hyal-1 was recently reported as an octasaccharide (Hofinger *et al.* 2007a), this may simply reflect substrate-specific size minima. These data indicate that Hyal-1 preferentially hydrolyses tetrasaccharides from the non-reducing end of oligosaccharide substrates, similar to a mechanism previously described for the PH20 hyaluronidase from bovine testes (i.e. BTH) (Takagaki *et al.* 1994).

4.3.2 Substrate specificity of endohexuronidase activity

Likewise, the endohexuronidase activity preferentially cleaved oligosaccharide substrates rich in GlcA, compared to IdoA (Figure 4.3B), indicating that activity towards DS polysaccharide would be directed principally to the GlcA-rich domains. This suggests specificity for GlcA-GalNAc rather than IdoA-GalNAc glycosidic linkages, but as the reducing residue of the oligosaccharide products measured could not be distinguished by ESI-MS/MS, this cannot be stated absolutely. No less than five monosaccharides was required on the reducing side of the target UA for endohydrolysis of CS-A substrate (Table 4.2), and the minimum-sized substrate requirement was thus a octasaccharide (Figure 4.3A). Although unlikely, the endohexuronidase activity could conceivably have cleaved the first glycosidic linkage from the non-reducing end of the substrates to liberate the monosaccharide, ΔUA, which was not monitored in these experiments as monosaccharides would not bind to the solid phase extraction columns used to extract GAGs from the digestion mixtures. Maximum generation of a specific product required at least seven monosaccharides on the reducing side of the target UA (Figure 4.3A). Correction of the endohexuronidase product levels for their approximate response factors, as described above, indicated that digestion of CS-A Δocta(+4S) and Δdeca(+5S) generated only Δtri(+S). Subsequent additions to the length of the

substrate resulted in increased production of Δpenta(+2S) and Δhepta(+3S) also, such that Δtri(+S), Δpenta(+2S) and Δhepta(+3S) products were detected in equal amounts from Δtetradeca(+7S) substrate (Figure 4.9 B). However, the combined levels of the products of endohexuronidase digestion of CS-A Δtetradeca(+7S) represented only ~15% of that of the Δtetra(+2S) produced by endo-β-*N*-acetylhexosaminidase (compare Figures 4.9A and B). Therefore, the endohexuronidase activity appears a relatively minor activity that randomly cleaves UA-GalNAc linkages when unrestricted by substrate length. The substrate specificity of the endohexuronidase activity described here is consistent with the CS-degrading endo-β-glucuronidase enzyme described by Takagaki *et al.* (1988b).

4.3.3 Properties of endoglycosidase activities

The pH profiles of the endo-β-*N*-acetylhexosaminidase and endohexuronidase activities (Figure 4.6) closely resembled those previously reported for Hyal-1 (Hofinger *et al.* 2007b, Muckenschnabel *et al.* 1998, Orkin and Toole 1980) and endo-β-glucuronidase (Takagaki *et al.* 1988b) and suggested an acidic milieu (i.e. lysosome or late endosome) for both activities. Inhibition of Hyal-1 by sodium acetate and NaCl (Tables 4.3 and 4.4) has previously been reported (Gold 1982, Afify *et al.* 1993, Orkin and Toole 1980) and may result from an affinity of the acetate and chloride ions for the active site of the enzyme, or possibly from a "salting out" of substrate-protein complexes that may have formed in the CHO-K1 homogenates and caused the CS-A oligosaccharide to be a more suitable substrate for Hyal-1 degradation. The results of the present study indicate that the endo-β-glucuronidase enzyme is similarly affected by these anions, and that both enzymes are also repressed by the presence of detergent (Table 4.4). Therefore, the common practice of including detergent and/or NaCl in enzyme digestion buffers should be avoided for these endoglycosidases.

As the optimum assay condition for both the endo-β-*N*-acetylhexosaminidase and the endohexuronidase activities was 100 mM sodium formate, pH 3.5 (Figure 4.6 and Table 4.3),

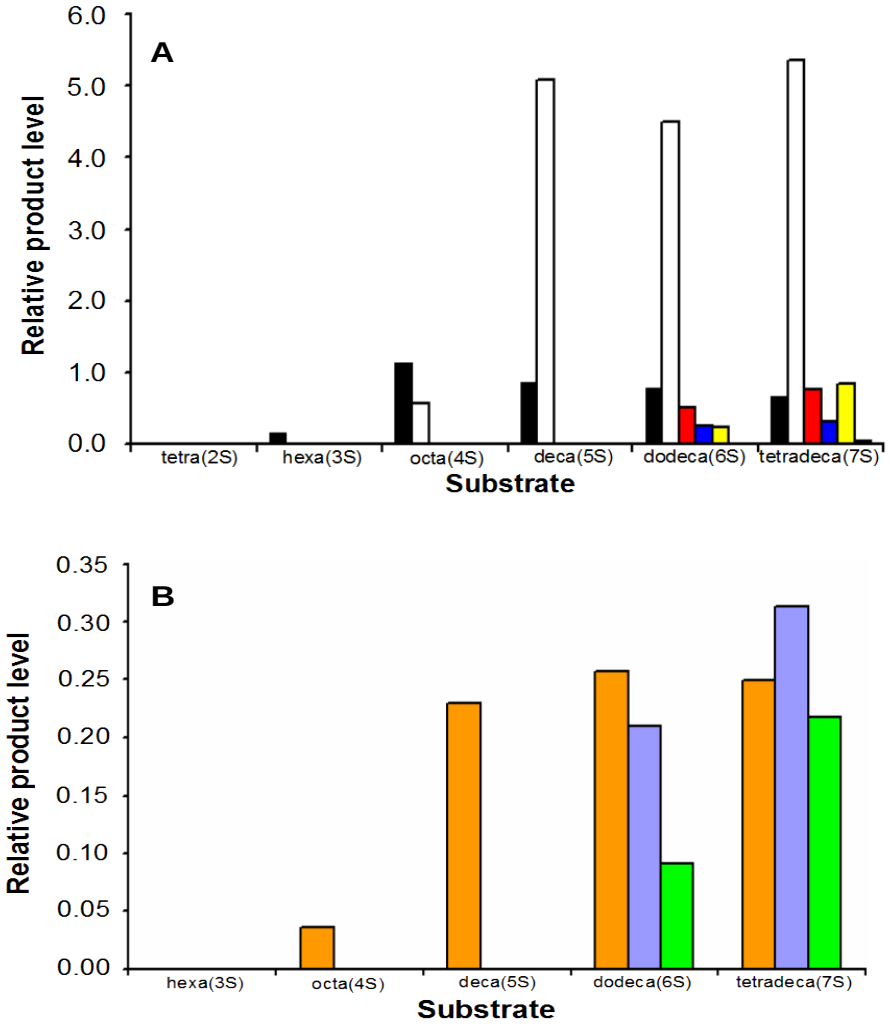

Figure 4.9 Relative levels of endo-β-*N*-acetylhexosaminidase and endohexuronidase products following endohydrolysis of oligosaccharide substrates, corrected for approximate ESI-MS/MS response factors

Tetra- to tetradecasaccharide substrates from CS-A were individually incubated with CHO-K1 homogenate (25 mg/mL protein equivalents) in 100 mM sodium formate, pH 3.5, for 24 hr. Relative levels of the even (endo-β-*N*-acetylhexosaminidase) (panel A) and odd (endohexuronidase) (panel B) products derived from the non-reducing end of the substrate were then measured by ESI-MS/MS and corrected for their approximate response factors. Corrected relative levels of the products, Δdi(+S) (black bar), Δtetra(+2S) (white bar), Δhexa(+2S) (red bar), Δhexa(+3S) (blue bar), Δocta(+3S) (yellow bar), Δocta(+4S) (pink bar), Δtri(+S) (orange bar), Δpenta(+2S) (blue bar) and Δhepta(+3S) (green bar) are shown.

and as their responses to the presence of NaCl, detergent, protease inhibitors and divalent cations were similar (Table 4.4 and Figure 4.7), the analysis of these activities in biological samples may be complicated by the fact that each activity is analysed in the presence of the other, under conditions where both are active. Hence, the products of oligosaccharide digestion could conceivably result from the concerted action of both activities, rather than necessarily one activity in isolation. To address this, an attempt was made to inhibit the endo-β-*N*-acetylhexosaminidase activity in CHO-K1 homogenate by competitive inhibition using the plant flavonoid, apigenin, and with an excess of small oligosaccharide. Apigenin has been shown to almost completely inhibit the sperm PH20-type hyaluronidase (BTH) (Hunnicutt *et al.* 1996) and an acid-active hyaluronidase secreted by human tumour cell lines (Podyma *et al.* 1997), but in this case only slightly reduced CHO-K1 endo-β-*N*-acetylhexosaminidase activity across the range of concentrations tested, and moreover reduced the endohexuronidase activity similarly (Figure 4.8). Likewise, the inclusion of C S-A tetrasaccharide (previously shown to inhibit PH20 *in vitro*) (Tatemoto *et al.* 2005) in the assay mixture abolished both activities (data not shown), and hence it was not possible to selectively inhibit the CHO-K1 endo-β-*N*-acetylhexosaminidase activity.

The assay developed in this chapter, utilising ESI-MS/MS for the determination of specific endoglycosidase product oligosaccharides, provides a convenient tool to measure these activities and determine their substrate specificities. In the following section, the assay is applied to study endo-β-*N*-acetylhexosaminidase and endohexuronidase activities in the DS-storing MPSs, which are hypothesised to be altered as a consequence of the excess DS that accumulates.

CHAPTER FIVE

ENDOGLYCOSIDASE ACTIVITIES IN THE MUCOPOLYSACCHARIDOSES

5.1 INTRODUCTION

Low-molecular-weight DS oligosaccharide fragments have been shown to accumulate in cultured skin fibroblasts from MPS I patients, as a consequence of the deficiency in α-L-iduronidase (Fuller *et al.* 2004a). These stored DS fragments are presumably the products of endoglycosidase activities, followed by exoenzyme activities that terminate at the first IdoA residue. DS-derived di- and trisaccharides containing IdoA at the non-reducing end and GalNAc or UA at the reducing terminus were identified, confirming the presence of endo-β-*N*-acetylhexosaminidase and endohexuronidase activities towards the GalNAc-UA and UA-GalNAc linkages of DS, respectively, in these cells. Both the di- and trisaccharide contained a single sulphate, positioned on the GalNAc residue, which indicated that the fibroblast endoglycosidase activities have specificity for the poorly sulphated, GlcA-rich domains of DS (Fuller *et al.* 2004a). These specificities are consistent with the Hyal-1- and endo-β-glucuronidase-like enzyme activities described in section 1.5.1 and in the previous chapter.

In this section, an attempt was made to compare Hyal-1- and endo-β-glucuronidase-like activities and substrate specificities in normal skin fibroblasts and in fibroblasts from MPS patients where DS is known to accumulate, using the ESI-MS/MS assay developed in the previous chapter. Skin fibroblasts from two of the DS-storing MPSs (section 1.6) were selected for this study: MPS I, where cells have already been shown to accumulate the products of putative Hyal-1 and endo-β-glucuronidase activities towards DS (Fuller *et al.* 2004a); and MPS VI, where a deficiency in the exosulphatase, *N*-acetylgalactosamine-4-sulphatase, results in storage of DS without the concurrent accumulation of heparan sulphate that occurs in MPS I (Neufeld and Muenzer 2001). It was hypothesised that the excess DS that accumulates in MPS I and VI fibroblasts as a consequence of the exoenzyme deficiency provides a positive feedback signal to the cell to up-regulate the synthesis and/or activities of Hyal-1 and endo-β-glucuronidase, to assist in the degradation of the excess DS. Previous reports have shown that Hyal-1 expression in cultured human skin fibroblasts is confluence-

dependent, with the highest levels of activity occurring in quiescent, post-confluent cells (Stair-Nawy *et al.* 1999), and hence the Hyal-1- and endo-β-glucuronidase-like activities were assessed in both rapidly-dividing (80% confluent) and 3 weeks post-confluent MPS and control fibroblasts for this study. Furthermore, as Hyal-1 activity in cultured human skin fibroblasts is so low as to be undetectable using some methodologies (Stair-Nawy *et al.* 1999) (such that at one point it was concluded that no such activity existed (Arbogast *et al.* 1975, Klein and von Figura 1980)), the endoglycosidases were also assessed in a range of mouse tissues (including whole skin) to confirm the ability of the ESI-MS/MS assay to detect and measure these activities.

5.2 RESULTS

5.2.1 Endoglycosidase activity in skin fibroblasts

To measure endoglycosidase activity towards oligosaccharide substrates in MPS skin fibroblasts, octa- to hexadecasaccharide substrates from CS-A (prepared as described in section 2.2.4) were individually incubated with MPS I, MPS VI and unaffected control fibroblast homogenates (section 2.2.6), and relative levels of the di- to octasaccharide products generated from the non-reducing end of the substrate were then determined by ESI-MS/MS (section 2.2.12.2). Since these substrates were demonstrated in the previous chapter to be successfully degraded by the Hyal-1- and endo-β-glucuronidase-like activities that are present in CHO-K1 cells, each substrate was also incubated with CHO-K1 homogenate serving as a positive control. Generation of the major Hyal-1- and endo-β-glucuronidase-like activity products (i.e. Δtetra(+2S) and Δtri(+S)[1]) was below the detection limit of the assay (defined as 10% of the product generation detected in the positive control) in each of the skin fibroblast homogenates, using CS-A Δocta(+4S), Δtetradeca(+7S) and Δhexadeca(+8S) as substrates. The absence of endoglycosidase activity towards the substrates was independent of the state of confluence of the fibroblasts, with no detectable product generation occurring

[1]the abbreviations used in reference to the oligosaccharide substrates/products were outlined in Table 4.1 (p. 85)

from CS-A Δtetradeca(+7S) substrate in homogenates from either rapidly-dividing cells harvested at 80% confluence or from cells harvested at confluence and at 3 weeks post-confluence (data not shown).

To exclude the possibility that the lack of detectable endoglycosidase activity in the skin fibroblast homogenates was due to endogenous inhibitors of the Hyal-1- and endo-β-glucuronidase-like activities, CS-A Δtetradeca(+7S) substrate was incubated with CHO-K1/skin fibroblast homogenate mixtures that were prepared by spiking MPS I and control fibroblast homogenates into CHO-K1 homogenates, and with CHO-K1 and skin fibroblast homogenates alone. Figure 5.1 illustrates that incubation of CS-A Δtetradeca(+7S) substrate with control fibroblast homogenate alone resulted in no detectable increase in the level of Δtetra(+2S) and Δtri(+S) products above the substrate blank, and that incubation with MPS I fibroblast homogenate alone generated Δtetra(+2S) and Δtri(+S) to levels only 6% and 60%, respectively, of those generated following incubation with CHO-K1 homogenate alone. However, incubation of CS-A Δtetradeca(+7S) substrate with control skin fibroblast/CHO-K1 homogenate mixture and with MPS I skin fibroblast/CHO-K1 homogenate mixture generated Δtetra(+2S) and Δtri(+S) to levels similar to those generated following incubation with CHO-K1 homogenate alone.

5.2.2 Endoglycosidase product oligosaccharides in skin fibroblasts

Hyal-1- and endo-β-glucuronidase-like activities were not detected towards oligosaccharide substrates in MPS and control skin fibroblast homogenates, as described in section 5.2.1. To confirm the presence of these activities in skin fibroblasts, MPS I, MPS VI and unaffected control fibroblast homogenates were screened by ESI-MS/MS for the presence of a series of oligosaccharide structures terminating in both *N*-acetylhexosamine (HNAc) and UA, corresponding to the products of Hyal-1- and endo-β-glucuronidase-like activities towards endogenous DS, respectively (section 2.2.12.2). The oligosaccharides measured were the

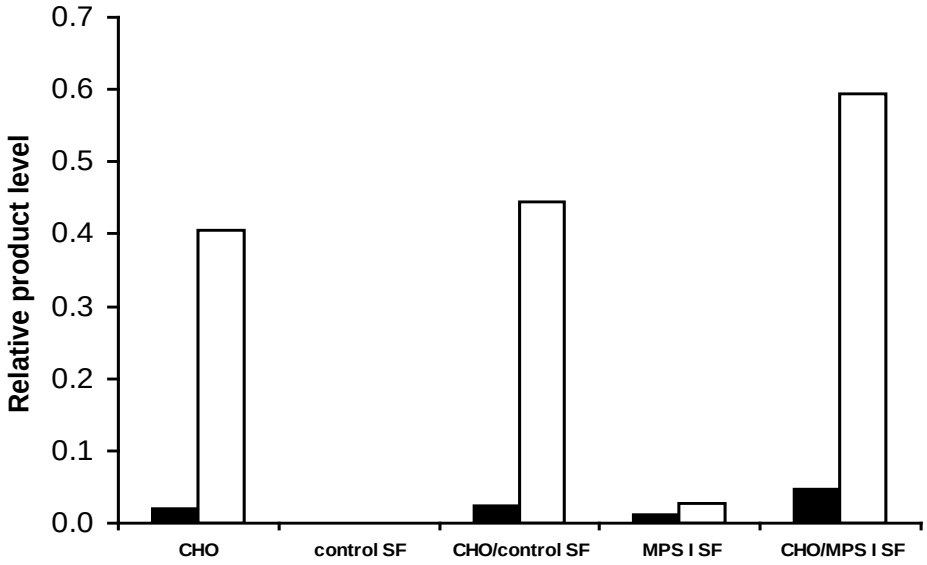

Figure 5.1 Relative product levels following endohydrolysis of CS-A in CHO-K1/skin fibroblast mixtures

Tetradecasaccharide substrate from CS-A was incubated with 4 mg/mL protein equivalents each of unaffected control skin fibroblast (SF) homogenate, MPS I SF homogenate, CHO-K1 homogenate, and a mixture (4 mg/mL protein equivalents each) of CHO-K1 and SF homogenates in 100 mM sodium formate containing protease inhibitors (one tablet Complete Mini protease inhibitor cocktail/10 mL and 1 μM pepstatin), pH 3.5, for 24 hr. Relative levels of the products derived from the non-reducing end of the substrate were then measured by ESI-MS/MS. Relative levels of the products, Δtetra(+2S) (open bars) and Δtri(+S) (filled bars) are shown.

monosaccharides, HNAc (+1-2S), which have been previously reported elevated in MPS VI urine (Ramsay *et al.* 2003); and the di-, tri-, tetra-, penta- and hexasaccharides, UA-HNAc (+S), UA-HNAc-UA (+S), $[UA\text{-}HNAc]_2$ (+2S), UA-$[HNAc\text{-}UA]_2$ (+2S) and $[UA\text{-}HNAc]_3$ (+2-3S), which have been reported elevated in MPS I urine and/or skin fibroblasts (Fuller *et al.* 2004a). As the elevations in the DS oligosaccharides reported by Fuller *et al.* in skin fibroblasts increased with time post-confluence, all cells were analysed when 3 weeks post-confluent.

Figure 5.2 shows that of the oligosaccharides measured, the control fibroblasts contained only the monosulphated monosaccharide, HNAc (+S), which was present at the modest relative level of 144. In contrast, the MPS I cells had varying amounts of all the oligosaccharides measured. The disaccharide, UA-HNAc (+S), and the trisaccharide, UA-HNAc-UA (+S), were detected at the highest relative levels in the MPS I cells (514 and 856, respectively), followed by HNAc (+S) (relative level of 117), the trisulphated hexasaccharide, $[UA\text{-}HNAc]_3$ (+3S) (relative level of 83), the tetrasaccharide, $[UA\text{-}HNAc]_2$ (+2S) (relative level of 59), the disulphated monosaccharide, HNAc (+2S) (relative level of 47), the disulphated hexasaccharide, $[UA\text{-}HNAc]_3$ (+2S) (relative level of 36), and the pentasaccharide, UA-$[HNAc\text{-}UA]_2$ (+2S) (relative level of 29) (Figure 5.2). The MPS VI fibroblasts contained an abundance of HNAc (+S) (relative level of 4570, corresponding to a 32- and 39-fold increase over the amount detected in the control and MPS I fibroblasts, respectively), and also a minor amount of HNAc (+2S) (relative level of 35), but no detectable amounts of the di- to hexasaccharides measured (Figure 5.2).

5.2.3 Sub-cellular localisation of oligosaccharides in skin fibroblasts

To determine the sub-cellular location of the endogenous DS oligosaccharides that were detected in the skin fibroblasts (section 5.2.2), Percoll density gradient fractionation was performed on MPS I, MPS VI and unaffected control cells (section 2.2.3). Each gradient

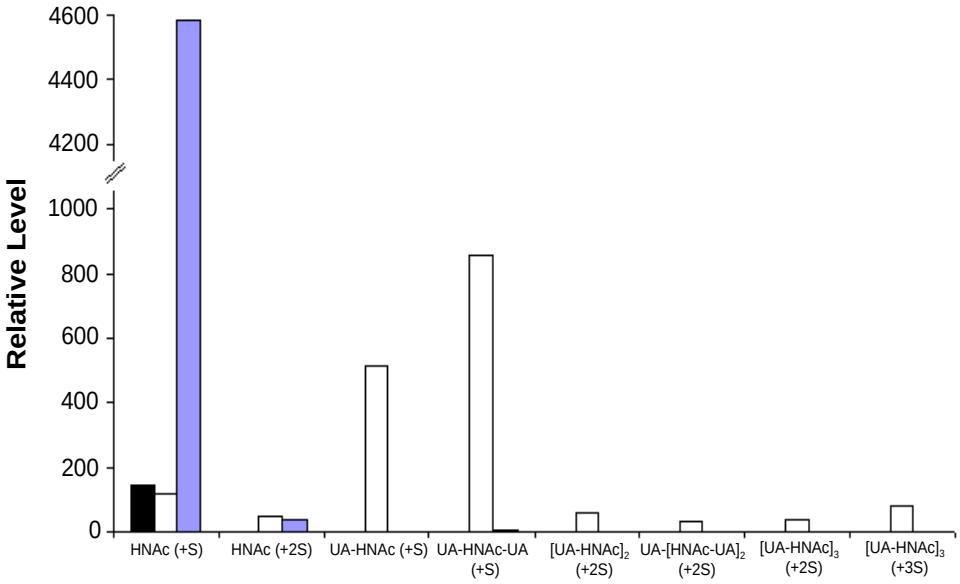

Figure 5.2 Relative levels of oligosaccharides in skin fibroblasts

Skin fibroblasts were harvested at 3 weeks post-confluence and analysed for oligosaccharides by ESI-MS/MS. Relative levels of HNAc (+S), HNAc (+2S), UA-HNAc (+S), UA-HNAc-UA (+S), $[UA\text{-}HNAc]_2$ (+2S), UA-$[HNAc\text{-}UA]_2$ (+2S), $[UA\text{-}HNAc]_3$ (+2S) and $[UA\text{-}HNAc]_3$ (+3S) per mg of cell protein in control (black bar), MPS I (white bar) and MPS VI (blue bar) fibroblasts are shown.

fraction was assayed for the organelle marker enzymes, β-hexosaminidase (found predominantly in the lysosomes) and acid phosphatase (found in both lysosomes and endosomes) (section 2.2.9), to confirm the location of these organelles, and then analysed for oligosaccharides by ESI-MS/MS (section 2.2.12.2). To assess the effect of state of confluence on the accumulation and distribution of the endoglycosidase product oligosaccharides, cells were analysed both when rapidly-dividing (80% confluent) and when 3 weeks post-confluent. Consistent with the absence of the measured di- to hexasaccharides in the control skin fibroblast homogenate (Figure 5.2), the density gradient fractions from both the rapidly-dividing and post-confluent control skin fibroblasts contained no appreciable amounts of these oligosaccharides (data not shown). The monosulphated monosaccharide, HNAc (+S), which was present at low levels in the control skin fibroblast homogenate (Figure 5.2), was also not detected in the density gradient fractions prepared from these cells (data not shown).

Figure 5.3 shows the sub-cellular distributions of the oligosaccharides that were detected in the density gradient fractions from the MPS I fibroblasts. A small amount of the disulphated monosaccharide, HNAc (+2S), was present in the lysosomes (fractions 13 to 20) of the rapidly-dividing MPS I cells, with the highest relative level of 0.0029 occurring in fraction 18. This distribution did not change when the MPS I cells were left for 3 weeks post-confluence. The monosulphated disaccharide, UA-HNAc (+S), was scattered unevenly at low relative levels (generally < 0.002) across the density gradient from the rapidly-dividing MPS I fibroblasts, however, a small amount of UA-HNAc (+S) localised to the lysosomes (fractions 13 to 20) in the confluent MPS I skin fibroblast gradient, with the highest relative level (0.003) occurring in fraction 17. A substantial amount of the monosulphated trisaccharide, UA-HNAc-UA (+S), was clearly localised to the fractions containing the lysosomes in the gradients from the MPS I fibroblasts, both when rapidly-dividing and confluent. The quantity of UA-HNAc-UA (+S) in the lysosomal fractions of the MPS I cell gradients was dependent upon state of confluence, increasing from a relative level of 0.026 in fraction 17 of the

rapidly-dividing cells, to 0.11 in the corresponding fraction of the confluent cells. Likewise, the relative levels of the di- and trisulphated hexasaccharides, $[UA\text{-}HNAc]_3$ (+2-3S), were confluence-dependent, as evidenced by a 3- and 2-fold increase in confluent cells, respectively. Of the two hexasaccharide species detected in the lysosomes of the MPS I cells (i.e. $[UA\text{-}HNAc]_3$ (+2S) and $[UA\text{-}HNAc]_3$ (+3S)), the trisulphated species was the more abundant, being 5-fold and 3-fold higher than the disulphated in cells rapidly-dividing and confluent, respectively. The monosulphated monosaccharide, HNAc (+S), the disulphated tetrasaccharide, $[UA\text{-}HNAc]_2$ (+2S), and the disulphated pentasaccharide, $UA\text{-}[HNAc\text{-}UA]_2$ (+2S), which were all detected at low levels in the MPS I fibroblast homogenate (Figure 5.2), were either sporadically distributed in small quantities (relative levels < 0.001) across the gradients from the rapidly-dividing and confluent MPS I skin fibroblasts, or were not detected at all (data not shown).

The distributions of the two monosaccharides found in the density gradient fractions from the MPS VI skin fibroblasts are shown in Figure 5.4. The monosulphated monosaccharide, HNAc (+S), was evenly dispersed at a low relative level (0.03-0.13) across the density gradient fractions from the rapidly-dividing MPS VI fibroblasts, with no apparent localisation with lysosomes or endosomes. However, the distribution profile of HNAc (+S) across the gradient from the confluent MPS VI cells shows a clear clustering of the monosaccharide into two peaks comprising the early gradient fractions (1 to 6) and the gradient fractions corresponding to the lysosomes (12 to 20), with the highest relative levels (~0.40) occurring in fractions 2 and 18, respectively. Similarly, storage of the disulphated monosaccharide, HNAc (+2S), was confluence-dependent in the MPS VI fibroblasts, as no specific localisation of the monosaccharide was observed in rapidly-dividing cells, whereas a clear, specific accumulation of HNAc (+2S) (relative level 0.002-0.006) occurred in the lysosomes of confluent cells. As expected from their absence from the MPS VI skin fibroblast homogenate (Figure 5.2), the density gradient fractions prepared from the rapidly-dividing

Figure 5.3 Relative levels of oligosaccharides in MPS I skin fibroblast density gradient fractions

Percoll density gradient fractionation was performed on MPS I skin fibroblasts. Each fraction was assayed for the organelle marker enzymes, β-hexosaminidase (open squares) and acid phosphatase (closed triangles) (y_2-axis), and analysed for oligosaccharides by ESI-MS/MS (y_1-axis). Relative levels of the monosaccharide, HNAc (+2S), the disaccharide, UA-HNAc (+S), the trisaccharide, UA-HNAc-UA (+S), and the hexasaccharides, $[UA\text{-}HNAc]_3$ (+2-3S), in fractions from rapidly-dividing (80% confluent) and 3 weeks post-confluent MPS I fibroblasts are shown.

80% confluent | **3 weeks post-confluent**

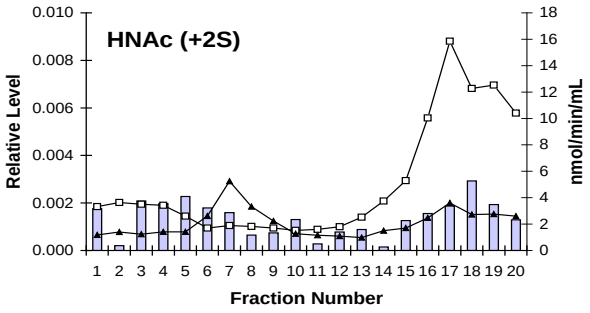

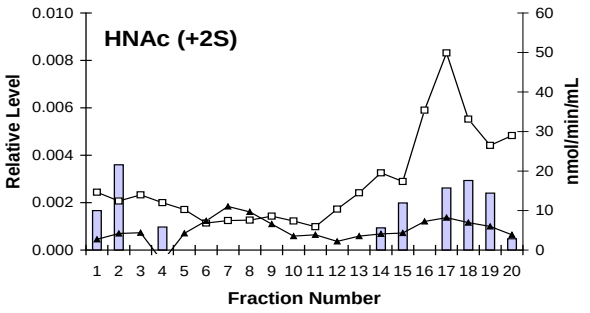

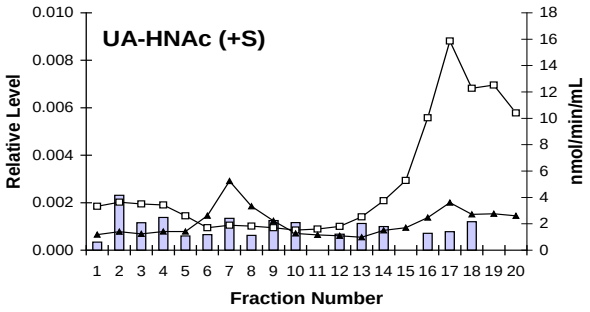

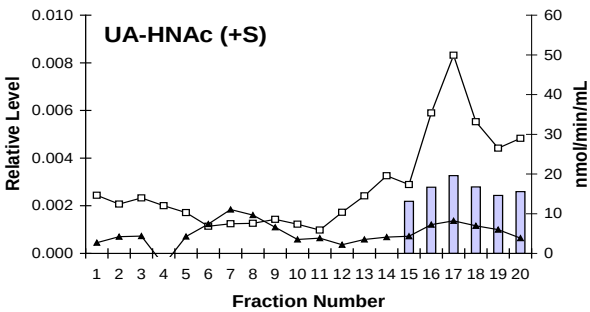

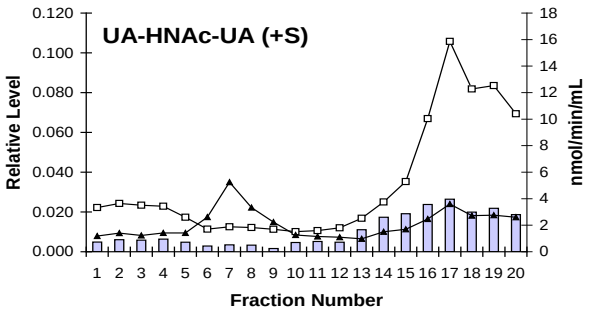

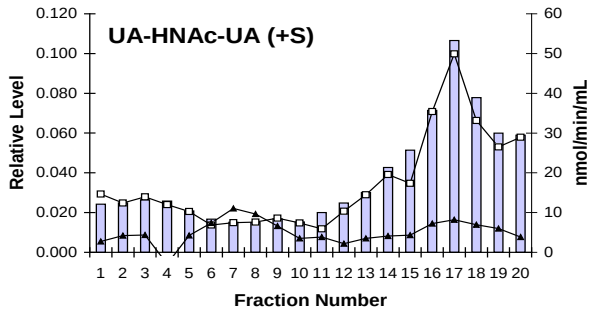

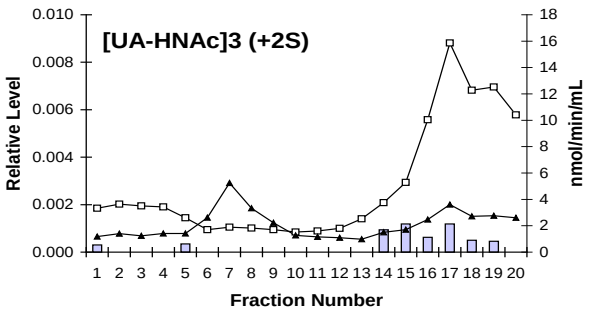

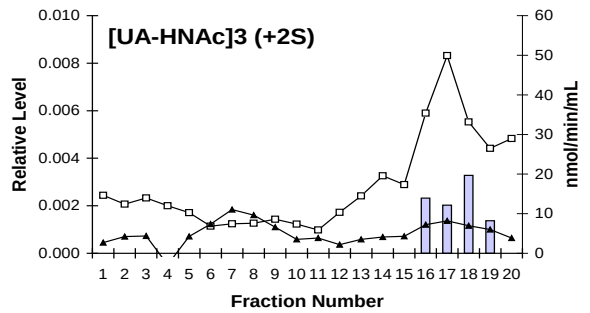

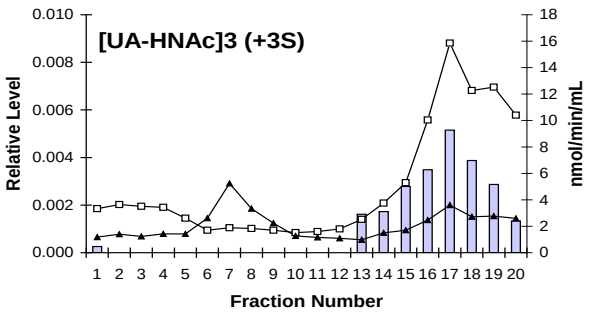

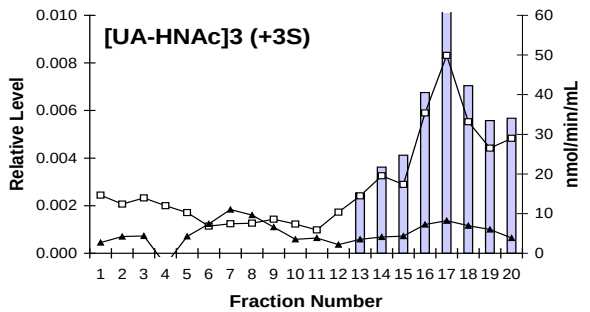

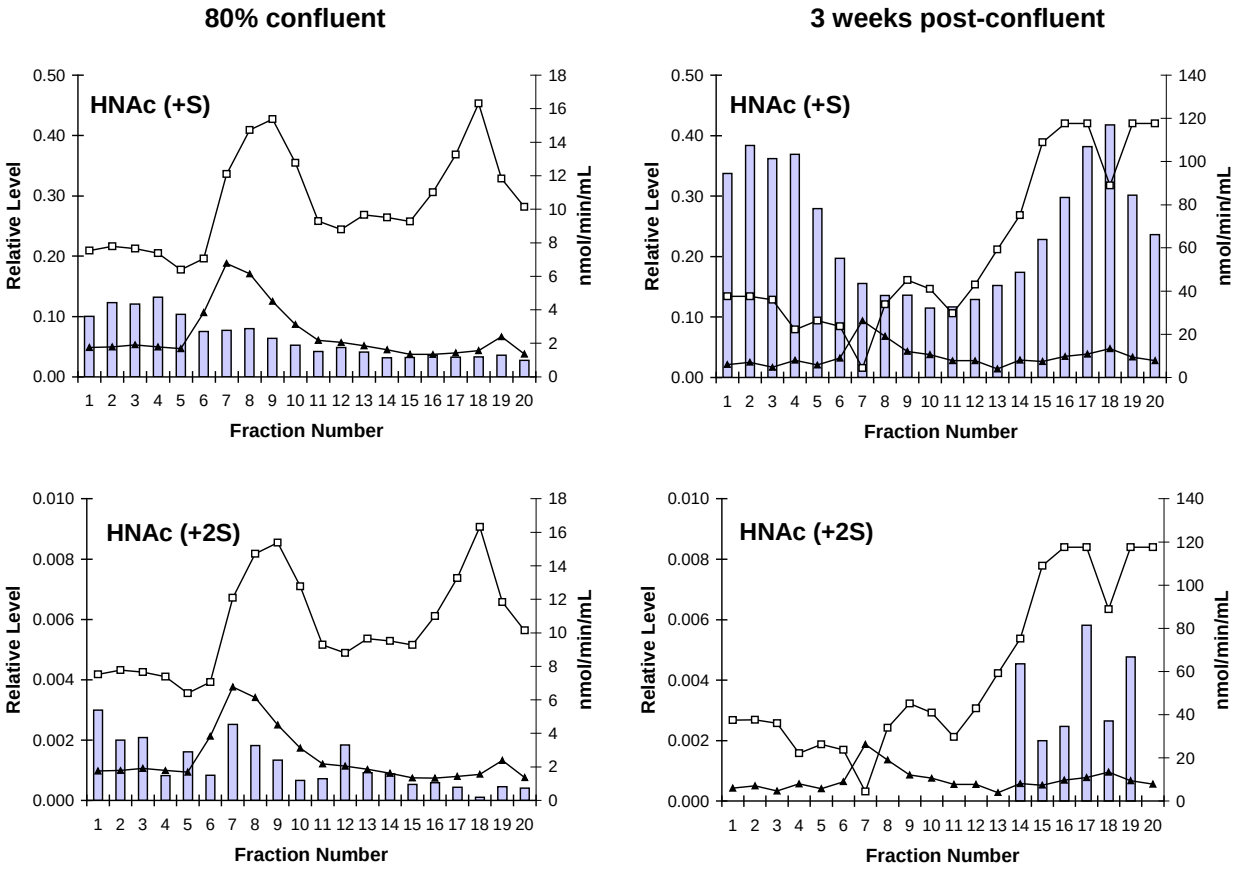

Figure 5.4 Relative levels of monosaccharides in MPS VI skin fibroblast density gradient fractions

Percoll density gradient fractionation was performed on MPS VI skin fibroblasts. Each fraction was assayed for the organelle marker enzymes, β-hexosaminidase (open squares) and acid phosphatase (closed triangles) (y_2-axis), and analysed for oligosaccharides by ESI-MS/MS (y_1-axis). Relative levels of the monosaccharides, HNAc (+1-2S), in fractions from rapidly-dividing (80% confluent) and 3 weeks post-confluent MPS VI fibroblasts are shown.

and confluent MPS VI cells contained no appreciable amounts of the di- to hexasaccharides measured (data not shown).

5.2.4 Endoglycosidase activity in fibroblast lysosomes

Sub-cellular localisation of the endogenous DS oligosaccharides in skin fibroblasts indicated that the DS-degrading endoglycosidase activities are restricted to the lysosome (section 5.2.3). To assess whether endoglycosidase activities could be detected towards exogenous oligosaccharide substrates in concentrated lysosomal fractions, the lysosomal fractions from the MPS I, MPS VI and control skin fibroblast density gradients prepared in section 5.2.3 were each pooled and concentrated (section 2.2.5). Each concentrated lysosomal preparation was incubated with dodecasaccharide substrate from CS-A (prepared as described in section 2.2.4) as outlined in section 2.2.6, and relative levels of the di- to octasaccharide products generated from the non-reducing end of the substrate were determined by ESI-MS/MS (section 2.2.12.2). As a positive control, tetradecasaccharide substrate from CS-A was incubated with concentrated microsomal, endosomal and lysosomal fractions prepared by sub-cellular fractionation of CHO-K1 cells (sections 2.2.3 and 2.2.5). Generation of Δtetra(+2S) and Δtri(+S) by the Hyal-1- and endo-β-glucuronidase-like activities was below the detection limit of the assay in the control, MPS I and MPS VI fibroblast lysosomal preparations, irrespective of whether the lysosomes were prepared from rapidly-dividing (80% confluent) or 3 weeks post-confluent fibroblasts (data not shown). In contrast, both activities were detected in the microsomal, endosomal and lysosomal preparations from CHO-K1 cells, with product generation in the lysosomal preparation approximately 3- to 7-fold and 2-fold higher than in the microsomal and endosomal preparations, respectively (Figure 5.5).

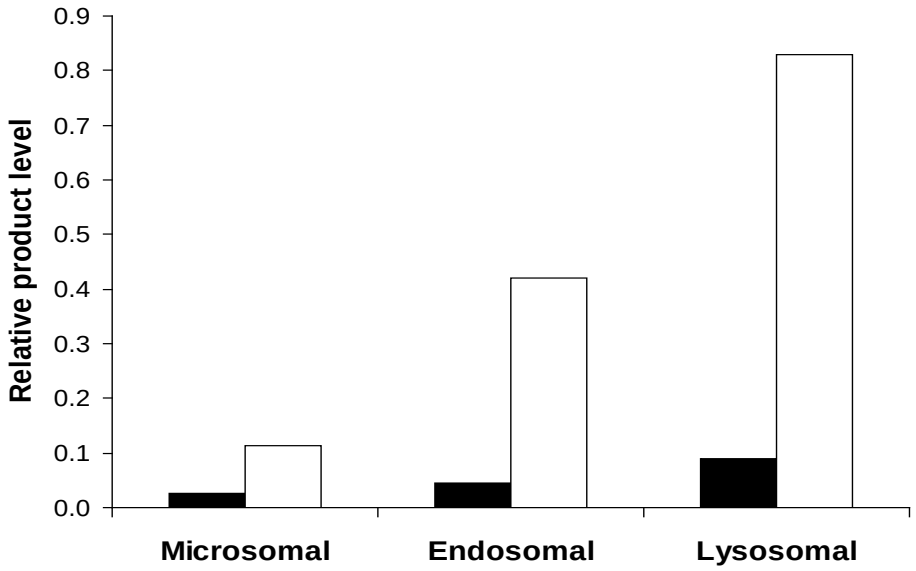

Figure 5.5 Relative product levels following endohydrolysis of CS-A in microsomal, endosomal and lysosomal preparations from CHO-K1 cells

Percoll density gradient fractionation was performed on CHO-K1 cells, and each gradient fraction was assayed for the organelle marker enzymes, β-hexosaminidase and acid phosphatase. The fractions containing microsomes (1 to 4), endosomes (5 to 10) and lysosomes (13 to 20) were pooled and concentrated. Each combined organelle fraction was incubated with tetradecasaccharide substrate from CS-A for 24 hr, and relative levels of the products derived from the non-reducing end of the substrate were then measured by ESI-MS/MS. Relative levels of the products, Δtetra(+2S) (open bars) and Δtri(+S) (filled bars) are shown.

5.2.5 Endoglycosidase activity in mouse tissues

Hyal-1- and endo-β-glucuronidase-like activities were detected in ovary-derived CHO-K1 cells but not skin fibroblasts, suggesting that expression of these activities may be cell- or tissue-specific and/or that the ESI-MS/MS assay may not be sufficiently sensitive to detect these activities in fibroblasts. To examine the tissue distribution of the endoglycosidase activities and demonstrate the ability of the ESI-MS/MS assay to detect Hyal-1- and endo-β-glucuronidase-like activities in a range of different samples, dodecasaccharide substrate from CS-A (prepared as described in section 2.2.4) was incubated with homogenates of mouse skin, liver, kidney, ovary, brain and lung (section 2.2.6), and relative levels of the di- to octasaccharide products generated from the non-reducing end of the substrate were then determined by ESI-MS/MS (section 2.2.12.2). Figure 5.6 illustrates that Hyal-1- and endo-β-glucuronidase-like activities were detected in each of the tissues evaluated, with the highest production of Δtetra(+2S) and Δtri(+S) occurring in the ovaries. Generation of both products in lung and skin was approximately 35% and 20-30% of that detected in ovary, respectively; and in liver, kidney and brain, was approximately 13%, 7% and 10% of that detected in ovary, respectively.

5.3 DISCUSSION

The present study was undertaken to determine the substrate specificities of the endoglycosidase activities that act upon DS in skin fibroblasts, and to test the hypothesis that these activities are up-regulated in the MPSs to degrade the excess DS that accumulates as a result of the exoenzyme deficiency. The absence of detectable endoglycosidase activity in the control and MPS skin fibroblast homogenates (section 5.2.1) was therefore unexpected. This most likely reflects non-recognition of the exogenous oligosaccharide substrates tested, rather than an absence of endoglycosidase activities in fibroblasts, since: 1) Hyal-1 activity, albeit at very low levels, has previously been detected in cultured human skin fibroblasts using

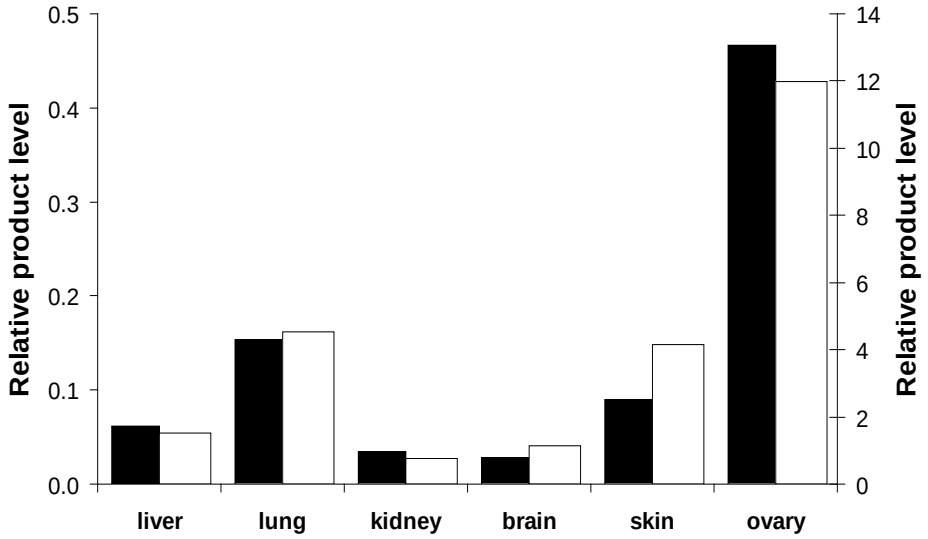

Figure 5.6 Relative product levels following endohydrolysis of CS-A in tissue homogenates

Dodecasaccharide substrate from CS-A was incubated with tissue homogenates in 100 mM sodium formate containing protease inhibitors (one tablet Complete Mini protease inhibitor cocktail/10 mL and 1 μM pepstatin), pH 3.5, for 24 hr, and relative levels of the products derived from the non-reducing end of the substrate were then measured by ESI-MS/MS. Relative levels of the products, Δtetra(+2S) (open bars) (y_2-axis) and Δtri(+S) (closed bars) (y_1-axis) per mg of tissue protein are shown.

hyaluronan substrate gel zymography (Stair-Nawy *et al.* 1999); 2) the presence of an endogenous inhibitor of the endoglycosidase activities in skin fibroblasts was ruled out by the finding that CHO-K1 Hyal-1- and endo-β-glucuronidase-like activities towards exogenous substrate were unaltered in the presence of fibroblast homogenate (section 5.2.1); 3) what appear to be the oligosaccharide products of Hyal-1- and endo-β-glucuronidase-like activities towards endogenous DS could be detected in the lysosomes of the MPS I fibroblasts (section 5.2.3); 4) endoglycosidase activity was not detected towards exogenous substrate in concentrated lysosomal fractions prepared from the skin fibroblasts, despite the fact that relatively high levels of these activities were detected in the corresponding fractions prepared from CHO-K1 cells (section 5.2.4); and 5) MRM was sensitive enough to detect traces of Δtetra(+2S) and Δtri(+S) impurities in each of the CS-A oligosaccharide substrate preparations tested (data not shown). As these Δtetra(+2S) and Δtri(+S) impurities correspond to the major Hyal-1- and endo-β-glucuronidase-like enzyme activity product oligosaccharides, this necessitated the subtraction of a substrate blank from the level of the Δtetra(+2S) and Δtri(+S) products attributed to the Hyal-1- and endo-β-glucuronidase-like activities in each experiment. Even slight endoglycosidase activity would have resulted in an increase in the level of Δtetra(+2S) and Δtri(+S) above the assay detection limit. The detection of both activities towards exogenous substrate in each of the mouse tissues evaluated (including whole skin) (section 5.2.5) further indicates that the absence of detectable activity in the fibroblast homogenates is not the result of a lack of assay sensitivity.

Based upon the inactivity of the Hyal-1- and endo-β-glucuronidase-like activities towards the exogenous oligosaccharide substrates tested, the following substrate recognition properties of the fibroblast endoglycosidases are proposed. Firstly, they may have larger minimum substrate requirements than the oligosaccharides tested here (i.e. larger than a hexadecasaccharide). Although the CHO-K1 Hyal-1- and endo-β-glucuronidase-like activities were demonstrated in the previous chapter to have CS-A hexa- and octasaccharide substrate

minima, respectively, and the minimum hyaluronan substrate requirement of recombinant human Hyal-1 is an octasaccharide (Hofinger *et al.* 2007a), there have been no explicit studies on the substrate specificities of human skin fibroblast Hyal-1 and endo-β-glucuronidase using small CS-A oligosaccharide substrates similar to those tested here. Second, the fibroblast endoglycosidases may not recognise the ΔUA residue at the non-reducing end of the substrate oligosaccharides, as this residue is not found in the normal mammalian physiological substrate, although this did not appear to inhibit substrate recognition by the CHO-K1 endoglycosidases (previous chapter). Finally, since the activity of Hyal-1 from chick embryo skin- and muscle-derived fibroblasts towards CS-C (which differs from CS-A only in the position of the single sulphate on the GalNAc residue) has been shown to be only 25% of that detected towards hyaluronan (Orkin and Toole 1980), the possibility that the fibroblast Hyal-1 enzyme is inactive towards CS-A cannot be ruled out. These suggestions, if correct, point to the existence of fibroblast-specific Hyal-1 and endo-β-glucuronidase isoforms with unique substrate specificities. The cleavage of exogenous oligosaccharide by both enzyme activities in whole skin homogenate (Figure 5.6), which likely contains a mixture of other cell types in addition to fibroblasts (e.g. keratinocytes, melanocytes, macrophages, adipocytes), is consistent with this hypothesis.

As mentioned above, the argument for the presence of Hyal-1- and endo-β-glucuronidase-like activities in skin fibroblasts is supported by the identification of DS oligosaccharides terminating in both HNAc (the di-, tetra- and hexasaccharides) and UA (the tri- and pentasaccharide) in MPS I skin fibroblast homogenate (Figure 5.2), and the subsequent localisation of most of these oligosaccharides to the lysosomes (section 5.2.3), where the bulk of the DS-degrading endoglycosidase activities were shown to reside (Figure 5.5). These oligosaccharides are suggested to result from Hyal-1- and endo-β-glucuronidase-like activities towards endogenous DS. Although it could be argued that some or all of these stored oligosaccharides are non-DS stereoisomers derived from endoglycosidase action upon

the second GAG stored as a result of the α-L-iduronidase deficiency, heparan sulphate, this is unlikely for three reasons: 1) oligosaccharides corresponding to the tri-, tetra-, penta- and hexasaccharides measured here have been enzymatically sequenced in the urine of an MPS I patient and shown to derive from DS (Fuller *et al.* 2004a); 2) the very high abundance of DS in the skin (Trowbridge and Gallo 2002) makes it more likely that the oligosaccharides in the MPS I fibroblasts are derived from DS rather than heparan sulphate; and 3) the overall structure of heparan sulphate dictates that the stored oligosaccharides derived from this GAG would probably contain a free glucosamine rather than an *N*-acetylglucosamine residue adjacent to the non-reducing end IdoA residue (Maccarana *et al.* 1996). The apparent non-localisation of the monosulphated monosaccharide and the tetra- and pentasaccharide to the lysosomes (section 5.2.3) following their detection in the MPS I fibroblast homogenate (Figure 5.2) may result from the dilution of what are already scarce oligosaccharides in these cells across the 5-6 lysosomal fractions of the density gradient, such that they are undetectable by ESI-MS/MS.

The sulphated HNAc monosaccharides detected in the lysosomes of the MPS VI fibroblasts (Figure 5.4) are not the direct products of a Hyal-1-like activity towards endogenous DS, but rather result from an alternate catabolic pathway for DS whereby β-hexosaminidase will cleave non-reducing end sulphated GalNAc residues *en bloc*, in addition to its normal action upon unsulphated GalNAc residues (Hopwood and Elliott 1985). However, given the evidence presented above for the presence of lysosomal endoglycosidase activities towards endogenous DS in MPS I fibroblasts (i.e. the presence of the putative products of these activities), it is highly likely that this alternate β-hexosaminidase activity is preceded in the degradation of DS in MPS VI fibroblasts, firstly by endoglycosidases, and then by other exoenzymes up to the first GalNAc(4S, ±6S) residue. The small amounts of sulphated monosaccharides detected in the control and MPS I fibroblast homogenates (Figure 5.2) likely reflect the basal level of the alternate β-hexosaminidase pathway in cells where DS

fragments with non-reducing end GalNAc(4S, ±6S) residues do not accumulate; with the exception of the disulphated species in MPS I (Figure 5.3), these monosaccharides were of such low abundance in the control and MPS I fibroblasts that they were undetectable when diluted across the lysosomal density gradient fractions (section 5.2.3). The presence of HNAc (+S) in the earlier, lower-density fractions of the confluent MPS VI fibroblast gradient (Figure 5.4) results from unavoidable lysis of the lysosomes during cell fractionation, as these organelles become increasingly fragile in response to the hypertrophy that accompanies oligosaccharide accumulation.

Based upon their acidic pH optima and likely proximity to the lysosomal exoenzymes required for the final stage of GAG catabolism, the Hyal-1- and endo-β-glucuronidase-like enzyme activities were suggested in the previous chapter to reside in the lysosomes and/or late endosomes, which collectively are known to contain the bulk of the acid hydrolase pool in most cell types (Claus *et al*. 1998, Storrie 1988), and this was confirmed here in CHO-K1 cells by sub-cellular fractionation (Figure 5.5). The localisation of the Hyal-1- and endo-β-glucuronidase-like enzyme activities to the lysosomes is consistent with the presence of the putative oligosaccharide products of their action upon endogenous DS in the lysosomes of the MPS I and MPS VI skin fibroblasts (Figures 5.3 and 5.4), with the absence of DS oligosaccharides in the endosomal fractions of the MPS fibroblasts probably reflecting an inability to clearly discriminate late endosomes from lysosomes using β-hexosaminidase and acid phosphatase activities exclusively. The endoglycosidase activity detected in the CHO-K1 microsomal preparation (Figure 5.5) presumably represents newly-synthesised enzyme originating from the ER *en route* to the Golgi complex.

As mentioned, Hyal-1- and endo-β-glucuronidase-like activities were detected in each of the mouse organ homogenates tested (Figure 5.6), suggesting a broad distribution of the enzymes across the somatic tissues. However, as in CHO-K1 cells, product generation by the endo-β-glucuronidase-like activity was only 2-5% that of the Hyal-1-like activity in each

tissue, indicating that the endo-β-glucuronidase-like activity may have a relatively minor overall role in the degradation of DS. The elevated endoglycosidase activity levels observed in lung, skin and ovary (Figure 5.6) likely reflect a higher content in these tissues of the specific GAGs that are the substrates for these enzymes, i.e. CS, DS and hyaluronan. In particular, skin is known to be very rich in these GAGs (Trowbridge and Gallo 2002, Reed *et al.* 1988).

In line with reports showing a gradual, progressive accumulation of DS oligosaccharides in MPS cells aged post-confluence (Fuller *et al.* 2004a), the putative oligosaccharide products of the Hyal-1- and endo-β-glucuronidase-like activities towards endogenous DS were generally more abundant in the lysosomes of the MPS I skin fibroblasts harvested when 3 weeks post-confluent, compared to those rapidly-dividing (Figure 5.3). This progressive accumulation with time post-confluence may result from a combination of factors, including a lack of dilution of the lysosomal contents by cell division; a lower rate of lysosomal exocytosis (a process shown to deliver storage material to the culture medium in exoenzyme-deficient cells (Klein *et al.* 2005)); and the increased Hyal-1 activity that occurs in skin fibroblasts upon reaching confluence (Stair-Nawy *et al.* 1999), which may in itself be the result of, or augmented by, a lower rate of lysosomal exocytosis, given that cultured human skin fibroblasts secrete significant amounts of Hyal-1 activity into the culture medium (Stair-Nawy *et al.* 1999). The role of exocytosis in the progressive lysosomal accumulation of DS oligosaccharides in cultured MPS fibroblasts might be further investigated by analysing the culture medium of these cells for a concurrent reduction in the levels of lysosome-derived endoglycosidase activities and/or DS fragments.

SUMMARY AND CONCLUSIONS

The catabolism of DS is a multi-step process that commences with endohydrolysis of the polysaccharide to oligosaccharides. At the commencement of this study, both Hyal-1 hyaluronidase (endo-β-*N*-acetylhexosaminidase) and endo-β-glucuronidase activities towards DS had been proposed, based upon the identification of DS oligosaccharide fragments terminating in GalNAc and UA in the urine of MPS patients (Fuller *et al*. 2004a and 2006) (see section 1.6), but the specific roles of these enzymes in the intra-cellular degradation of DS were not well understood. This was primarily due to a lack of convenient methods to study endoglycosidase activities and their substrates. The overall aim of this thesis was thus to develop novel ESI-MS/MS methodology for the identification and characterisation of endoglycosidase activities towards DS. An ESI-MS/MS assay was designed to measure specific products resulting from enzyme activity upon structurally defined oligosaccharide substrates. The distinct advantages of this assay were that: 1) multiple products differing in structure by as little as one sulphate group could be resolved and relative levels measured simultaneously by MRM, without prior chromatography; 2) the preparation of oligosaccharide substrates containing the mammalian exoenzyme-resistant ΔUA residue at the non-reducing end, introduced through the eliminative action of chondroitinase ABC (chapter three), was simple and enabled the selective monitoring of even (endo-β-*N*-acetylhexosaminidase) and odd (endohexuronidase) non-reducing end products; and 3) enzyme specificities and relative activities could be determined in a single experiment. Using this approach, several novel aspects of the substrate specificities and catalytic mechanisms of the DS-degrading endoglycosidases were elucidated.

CHO-K1 cells were selected as the source of endoglycosidase activity for assay development, as these cells grow extremely rapidly in culture and have been shown to contain GAG-degrading endo- and exoglycosidases (Bame *et al.* 1998, Brooks *et al.* 2001). Even and odd non-reducing products were detected following incubation of CHO-K1 homogenate with oligosaccharide substrate, confirming the presence of endo-β-*N*-acetylhexosaminidase and

endohexuronidase activities in these cells (chapter four). Consistent with the properties of the aforementioned Hyal-1 and endo-β-glucuronidase enzymes (Orkin and Toole 1980, Takagaki *et al.* 1988b), the CHO-K1 endoglycosidases displayed acidic pH optima, were modestly inhibited by the presence of NaCl, and were preferentially active towards GlcA-rich substrate, with only minor activity detected towards IdoA-rich substrate.

Analysis of the specific even and odd non-reducing end products of CHO-K1 endoglycosidase activity towards different-sized oligosaccharide substrates provided insight into the substrate recognition properties and mechanisms of action of the putative Hyal-1 and endo-β-glucuronidase activities (chapter four). For example, as the largest non-reducing end product of the Hyal-1-like activity was always a minimum of two disaccharides smaller than its parent substrate, it was deduced that cleavage by this enzyme is absolutely dependent upon the presence of a minimum of two disaccharide units on the reducing side of the target glycosidic linkage, such that the minimum substrate requirement is a hexasaccharide. Maximum generation of a given product by the Hyal-1-like activity was shown to depend upon the presence of a minimum of three disaccharides to the reducing side of the target glycosidic linkage. Furthermore, as decasaccharide and larger oligosaccharide substrates generated predominantly tetrasaccharide product, it was established that this activity acts exo-endolytically upon oligosaccharide substrates by sequentially removing tetrasaccharides from the non-reducing end.

The CS-A hexasaccharide minimum substrate requirement observed here for the Hyal-1-like activity was in accord with previous predictions based upon the minimum substrate of the related enzyme, BTH (Stern 2003, Stern and Jedrzejas 2006), but at odds with the hyaluronan octasaccharide minimum recently reported for recombinant human Hyal-1 (Hofinger *et al.* 2007a). Since the CS-A hexasaccharide substrate preparation contained no traces of contaminating octasaccharide (Figure 3.4d), this suggested that enzyme recognition is influenced by the subtle structural difference between the GalNAc and *N*-

acetylglucosamine residues of CS-A and hyaluronan oligosaccharides, respectively, and/or by the presence of sulphate groups, which do not adorn hyaluronan. Future work might involve a comparative study of the substrate specificity of Hyal-1 with respect to CS-A and hyaluronan oligosaccharides. A substantial reduction in Hyal-1 activity was previously observed when macromolecular CS was used as substrate in the place of hyaluronan (Orkin and Toole 1980).

The finding that the Hyal-1-like activity sequentially removes tetrasaccharides from the non-reducing end of oligosaccharide substrates, and therefore acts in an exo-endolytic, processive fashion similar to that previously reported for BTH (Takagaki *et al.* 1994), was one of the more intriguing of this study. Given that this mechanism would preclude access to the internal GlcA-rich domains of macromolecular DS, since enzyme action would slow considerably, if not cease, upon reaching the first IdoA-rich domain from the non-reducing terminus, it is postulated that the catalytic mechanism of Hyal-1 towards DS differs according to substrate size, such that macromolecular DS is instead attacked *via* the endolytic, "random-bite" (i.e. non-processive) mechanism proposed by Stern and Jedrzejas (2006); and/or that the initial internal clipping of macromolecular DS is performed predominantly by endo-β-glucuronidase (which appears non-processive in action (see below)) and possibly also Hyal-2, which has been shown to degrade high-molecular-weight hyaluronan to intermediate-sized fragments of about 20 kDa (50 disaccharide units) (Lepperdinger *et al.* 2001) (see section 1.5.1). Although the apparently low relative activities of Hyal-2 (Lepperdinger *et al.* 2001) and endo-β-glucuronidase (see below) would limit the overall contribution of Hyal-1 to DS endodegradation by the latter model, it must be kept in mind that Hyal-1 activity towards CS/DS is secondary to its principal role in the catabolism of hyaluronan, a GAG composed entirely of GlcA-*N*-acetylglucosamine disaccharides that could theoretically be degraded by Hyal-1 entirely in the exo-endolytic fashion. A comparison of the catalytic mechanisms of Hyal-1, Hyal-2 and endo-β-glucuronidase towards macromolecular and oligosaccharide DS substrates would therefore be of intrinsic interest.

Although the endo-β-*N*-acetylhexosaminidase and endohexuronidase activities described here shared a number of biochemical properties and were active at the same relative levels across the range of cells and tissues tested, it is likely that the endohexuronidase activity represents that of the discrete endo-β-glucuronidase enzyme reported by Takagaki *et al.* (1988b) rather than one enzyme with dual specificity, since a recent report on the catalytic behaviour of recombinant human Hyal-1 showed no evidence of endo-β-glucuronidase activity towards hyaluronan oligosaccharides (Hofinger *et al*. 2007a). This thesis represents the first detailed study of the substrate specificity of this endo-β-glucuronidase enzyme since its initial description twenty years ago. Based upon its activity towards oligosaccharide substrates, the CHO-K1 endo-β-glucuronidase appears to have an absolute requirement for a minimum of five monosaccharides on the reducing side of the target glycosidic linkage and hence a minimum substrate requirement of an octasaccharide (chapter four). Maximum generation of a particular product by this enzyme was shown to require a minimum of seven monosaccharides to the reducing side of the target linkage. However, since generation of the different-sized non-reducing end oligosaccharide products of this activity approached parity as substrate length was progressively extended, it appears that, in contrast to the exo-endolytic mechanism observed for the Hyal-1-like activity, this enzyme acts randomly on substrates larger than a decasaccharide. From the very low level of product generation observed by the endo-β-glucuronidase-like activity relative to the Hyal-1-like activity in both CHO-K1 cells (chapter four) and mouse tissue samples (chapter five), it may be further speculated that the overall role of this endoglycosidase in the intra-cellular degradation of DS is minor.

Sub-cellular fractionation confirmed that the Hyal-1- and endo-β-glucuronidase-like activities are predominantly lysosomal (chapter five). However, a significant amount of enzyme activity was also detected in the endosomes, indicating that the degradation of DS may actually commence in a late endosomal compartment. The intra-cellular degradation pathway of DS could be more clearly defined by pulse-chase experiments, using a

combination of sub-cellular fractionation and ESI-MS/MS to monitor the progress of DS fragments through the endosome/lysosome network of cultured cells following uptake of radiolabelled DSPG precursors. A number of protein markers have been shown to discretely localise throughout the endosome/lysosome network (such as Rabs 4 and 5 for the early endosomes, Rabs 7 and 9 for the late endosomes, and the lysosome-associated membrane proteins (LAMPs) for the lysosomes (Miaczynska and Zerial 2002, Winchester 2001)) and would enable greater discrimination of the sub-organelles believed to comprise the DS-degradation pathway.

Taken together, the results discussed above suggest that both endo-β-*N*-acetylhexosaminidase and a minor endohexuronidase activity, probably representing the Hyal-1 and endo-β-glucuronidase enzymes described previously, act in concert to degrade the low-sulphate, GlcA-rich domains of DS but are less active towards the highly sulphated regions containing IdoA. Endohydrolysis of DS appears to commence in the late endosome and/or lysosome with cleavages by endo-β-glucuronidase, and possibly Hyals-1 and -2, to generate two types of oligosaccharide intermediates. The first type of intermediate is GlcA-rich and results from cleavages within the susceptible domains of the polysaccharide; these GlcA-rich oligosaccharides are further endohydrolysed by Hyal-1 and endo-β-glucuronidase, prior to complete degradation by lysosomal exohydrolases. The second type of intermediate is larger, IdoA-rich and represents the regions of the polysaccharide resistant to the initial cleavages; this type of oligosaccharide is not a good substrate for endohydrolysis and is predominantly degraded by the lysosomal exohydrolases.

A central hypothesis of this thesis was that endoglycosidase activities are up-regulated in the MPSs to degrade the excess DS that accumulates as a consequence of the exoenzyme deficiency. Unexpectedly, however, endoglycosidase activity was not detected towards exogenous octa- to hexadecasaccharide substrates in MPS I and MPS VI skin fibroblast homogenates, despite the fact that what appear to be the products of Hyal-1 and endo-β-

glucuronidase activities towards endogenous DS could be localised to the lysosomes of the MPS I cells (chapter five). This absence of detectable activity suggested that the fibroblast endoglycosidases did not recognise the exogenous substrates tested and hence have substrate specificities that differ radically from those previously reported for these enzymes (Hofinger *et al.* 2007a, Stern 2003, Takagaki *et al.* 1988b, chapter four). Based upon the structures of the oligosaccharides that were not recognised, the fibroblast endoglycosidases may: 1) have a minimum substrate requirement larger than a hexadecasaccharide; 2) recognise only hyaluronan oligosaccharides, with no activity towards CS/DS oligosaccharides; and 3) be inhibited by the ΔUA residue that was present at the non-reducing end of the substrates tested (see section 5.3). A more detailed analysis of the fibroblast endoglycosidase specificities might be facilitated by the synthesis of more appropriate oligosaccharide substrates which, considering the apparent limitations of enzyme recognition discussed above, would: 1) be larger than a hexadecasaccharide; 2) contain a GlcA rather than a ΔUA residue at the non-reducing end; and 3) be derived from CS-C and/or hyaluronan rather than, or in addition to, CS-A. However, further evidence that the lack of detectable endoglycosidase activity in the skin fibroblasts was the result of enzyme non-recognition of the exogenous substrates tested rather than an absence of these activities *per se* could be obtained more immediately by assessing the cell culture medium for activity towards these substrates, as cultured human skin fibroblasts have been shown to secrete the vast majority of their Hyal-1 activity (Stair-Nawy *et al.* 1999). PCR (Stair-Nawy *et al.* 1999) and/or immunohistochemistry using an anti-Hyal-1 antibody (Kramer *et al*. 2009) could also be performed to further confirm the presence of Hyal-1 mRNA and protein, respectively, within these cells.

Although the substrates tested here were not recognised by the skin fibroblast Hyal-1- and endo-β-glucuronidase-like activities, they may nonetheless still prove useful for a comparison of endoglycosidase activities in other MPS cells and tissues, given that they were readily digested by the Hyal-1- and endo-β-glucuronidase-like activities present in a range of

mouse tissues (chapter five). A number of murine MPS models that are deficient in DS-degrading exoenzymes have been described and would be useful for these studies, including MPS I (α-L-iduronidase deficiency) (Ohmi *et al.* 2003), MPS II (iduronate-2-sulphatase deficiency) (Muenzer *et al.* 2002) and MPS VII (β-glucuronidase deficiency) (Vogler *et al.* 2001). Likewise, an examination of Hyal-1-deficient MPS IX human skin fibroblasts (Natowicz *et al.* 1996) and/or mouse tissues (Martin *et al.* 2008) for an up-regulation of endo-β-glucuronidase-like activity would be of interest. The detection of Hyal-1- and endo-β-glucuronidase-like activities towards exogenous substrate in whole skin preparation indicates that the atypical substrate specificities discussed above may not apply to other cells present in the skin except for fibroblasts.

While oligosaccharides corresponding to the products of Hyal-1- and endo-β-glucuronidase-like activities towards endogenous DS were detected in the lysosomes of MPS I skin fibroblasts, as mentioned above, such oligosaccharides were not found in MPS VI skin fibroblasts which, in contrast, contained large quantities of sulphated monosaccharides exclusively (chapter five). This may indicate that the ability of β-hexosaminidase to cleave non-reducing sulphated GalNAc residues from DS *en bloc* (Hopwood and Elliot 1985, Hepbildikler *et al.* 2002) enables the near-complete digestion of endoglycosidase product oligosaccharides in MPS VI fibroblasts, such that only the non-reducing GalNAc(4S, ±6S) monosaccharides liberated from DS *via* this alternate β-hexosaminidase pathway are stored as a consequence of the *N*-acetylgalactosamine-4-sulphatase deficiency. Notwithstanding this, a broad heterogeneity of DS oligosaccharide fragments has been identified in MPS VI urine and tissues (ranging in size from high-molecular-weight structures down to small tetra- and hexasaccharides) (Byers *et al.* 1998), suggesting that the alternate β-hexosaminidase activity is unable to completely prevent the accumulation of larger DS oligosaccharides in other cell types.

One complication with the study of the individual Hyal-1- and endo-β-glucuronidase-like enzyme activities towards DS that was identified in the course of this work was that as these activities in biological samples share a number of common biochemical properties (most notably, pH and anion optima), each is assayed for in the presence of the other under conditions where both are active (chapter four). Therefore, the products of oligosaccharide digestion may result from the concerted action of both activities, rather than necessarily one activity in isolation. This complication is, however, not a limitation of the ESI-MS/MS assay *per se* and would apply equally to any other assay used to measure endoglycosidase activity towards CS/DS in biological samples. An attempt to address this issue here by inhibiting the putative Hyal-1 activity in CHO-K1 homogenates using the reported hyaluronidase inhibitor, apigenin (Hunnicutt *et al.* 1996, Podyma *et al.* 1997), successfully reduced activity by a modest ~ 40%, however this inhibition was non-selective and accompanied by a corresponding decrease in endo-β-glucuronidase-like activity (chapter four). Future work might be concerned with testing a battery of other known hyaluronidase inhibitors, such as ascorbic acid and glycyrrhizic acid (reviewed in Mio and Stern (2002)); investigating endo-β-glucuronidase-like activity in Hyal-1-deficient (MPS IX) human skin fibroblasts (Natowicz *et al.* 1996); or attempting to purify the two activities. The partial inhibition of the CHO-K1 endo-β-glucuronidase-like activity by apigenin indicates that the plant-derived flavonoids (of which this compound is a member) may be useful inhibitors of this enzyme.

To enable the efficient processing of the large quantities of oligosaccharides required for the development of the endoglycosidase product assay, the oligosaccharides prepared from the enzymatic digestions of CS-A and DS for use as assay substrates were purified by large-format column chromatography on a Bio-Gel P6 column which, as expected, resulted in relatively poor resolution of the larger oligosaccharide species (Figure 3.2). Given that the optimum conditions for the endoglycosidase product assay have now been established, the substrate specificities of the DS-degrading endoglycosidases might be further probed using

more highly purified oligosaccharides prepared by methods such as HPLC or capillary electrophoresis. In particular, strong anion exchange (SAX)-HPLC has been used for the separation, to near homogeneity, of oligosaccharides derived from porcine intestinal mucosa DS of up to dodecasaccharide in length (Yang *et al.* 2000).

As discussed above, the CHO-K1 Hyal-1- and endo-β-glucuronidase-like enzyme activities preferentially degraded substrate rich in GlcA, compared to IdoA, which suggested that these enzymes have specificity for glycosidic linkages containing GlcA (i.e. GalNAc-GlcA and GlcA-GalNAc rather than GalNAc-IdoA and IdoA-GalNAc linkages, respectively) (chapter four). However, as GlcA and IdoA units are stereoisomeric and hence have identical mass, the individual UA residues of the oligosaccharide substrates and their products could not be distinguished as GlcA/IdoA by ESI-MS/MS, and hence the specificities of the endoglycosidases for linkages containing GlcA or IdoA cannot be stated absolutely here. The GlcA/IdoA content of the oligosaccharide substrates/products might be ascertained in future by assessing their susceptibility to digestion with the chondroitinase AC and B enzymes, which are specific for GalNAc-GlcA and GalNAc-IdoA glycosidic linkages, respectively (Yamagata *et al.* 1968); by ^{1}H NMR analysis, which has been reported to clearly distinguish GlcA/IdoA residues in DS (Sudo *et al.* 2001, Yang *et al.* 2000); or by definitive sequencing with recombinant exoenzymes. With more highly defined substrates, the ESI-MS/MS assay developed here would be ideal for quickly resolving the GlcA/IdoA enzyme specificity issue. Of note, there are no reports of DS-degrading endo-α-L-iduronidase enzymes in the literature.

The endo-β-*N*-acetylhexosaminidase and endohexuronidase activities characterised here in CHO-K1 cells were referred to throughout as "Hyal-1-like" and "endo-β-glucuronidase-like" activities, respectively, in reference to the fact that their substrate recognition properties and responses to changes in assay parameters were similar to those previously reported for these enzymes. Further evidence that the CHO-K1 endoglycosidase activities indeed represent the Hyal-1 and endo-β-glucuronidase enzymes could be obtained

by testing the cells for the presence of Hyal-1 mRNA and protein using PCR (Stair-Nawy *et al.* 1999) and immunohistochemistry (Kramer *et al*. 2009), respectively.

This study has demonstrated the usefulness of ESI-MS/MS as a tool for the study of endoglycosidase activities towards DS. The assay developed herein enables the identification, measurement and characterisation of the different endoglycosidase activities present in biological samples, and may be useful for the study of conditions where endoglycosidase activities are known to be aberrant, such as certain cancers (Lokeshwar *et al*. 1999, Franzmann *et al.* 2003), and/or for the evaluation of putative enzyme inhibitors that may have application for treating such conditions. Furthermore, as discussed above, the assay may yet be applied to test the hypothesis that endoglycosidase activities are up-regulated in the MPSs using tissue samples and/or cells other than fibroblasts, given that both Hyal-1- and endo-β-glucuronidase-like activities could be detected in mouse tissue samples. While the focus of this thesis was DS, the strategy adopted here could easily be adapted for the study of endoglycosidase activities towards other GAGs such as heparan sulphate and hyaluronan, which have likewise been shown to exert numerous biological effects.

REFERENCES

Afify, A.M., Stern, M., Guntenhoner, M. and Stern, R. (1993) Purification and characterization of human serum hyaluronidase *Arch. Biochem. Biophys.* **305(2)**: 434-441

Arbogast, B., Hopwood, J.J. and Dorfman, A. (1975) Absence of hyaluronidase in cultured human skin fibroblasts *Biochem. Biophys. Res. Commun.* **67(1)**: 376-382

Ashton, L.J., Brooks, D.A., McCourt, P.A., Muller, V.J., Clements, P.R. and Hopwood, J.J. (1992) Immunoquantification and enzyme kinetics of alpha-L-iduronidase in cultured fibroblasts from normal controls and mucopolysaccharidosis type I patients *Am. J. Hum. Genet.* **50(4)**: 787-794

Bame, K.J., Hassall, A., Sanderson, C., Venkatesan, I. and Sun, C. (1998) Partial purification of heparanase activities in Chinese hamster ovary cells: evidence for multiple intracellular heparanases *Biochem. J.* **336(1)**: 191-200

Bao, X., Muramatsu, T. and Sugahara, K. (2005) Demonstration of the pleiotrophin-binding oligosaccharide sequences isolated from chondroitin sulfate/dermatan sulfate hybrid chains of embryonic pig brains *J. Biol. Chem.* **280(42)**: 35318-35328

Barroso, B., Didraga, M. and Bischoff, R. (2005) Analysis of proteoglycans derived sulphated disaccharides by liquid chromatography/mass spectrometry *J. Chromatogr. A* **1080(1)**: 43-48

Beech, D.J., Madan, A.K. and Deng, N. (2002) Expression of PH-20 in normal and neoplastic breast tissue *J. Surg. Res.* **103(2)**: 203-207

Bernfield, M., Götte, M., Park, P.W., Reizes, O., Fitzgerald, M.L., Lincecum, J. and Zako, M. (1999) Functions of cell surface heparan sulfate proteoglycans *Annu. Rev. Biochem.* **68(1)**: 729-777

Blumenkrantz, N. and Asboe-Hansen, G. (1973) New method for quantitative determination of uronic acids *Anal. Biochem.* **54(2)**: 484-489

Brooks, D.A., Fabrega, S., Hein, L.K., Parkinson, E.J., Durand, P., Yogalingam, G., Matte, U., Giugliani, R., Dasvarma, A., Elsahpazire, J., Henrissat, B., Mornon, J.P., Hopwood, J.J. and Lehn, P. (2001) Glycosidase active site mutations in human alpha-L-iduronidase *Glycobiology* **11(9)**: 741-750

Bunge, S., Kleijer, W.J., Steglich, C., Beck, M., Zuther, C., Morris, C.P., Schwinger, E., Hopwood, J.J., Scott, H.S. and Gal, A. (1994) Mucopolysaccharidosis type I: identification of 8 novel mutations and determination of the frequency of the two common alpha-L-iduronidase mutations (W402X and Q 70X) among European patients *Hum. Mol. Genet.* **3(6)**: 861-866

Byers, S., Rozaklis, T., Brumfield, L.K., Ranieri, E. and Hopwood, J.J. (1998) Glycosaminoglycan accumulation and excretion in the mucopolysaccharidoses: characterization and basis of a diagnostic test for MPS *Mol. Genet. Metab.* **65(4)**: 282-290

Cheng, F., Heinegard, D., Malmstrom, A., Schmidtchen, A., Yoshida, K. and Fransson, L.A. (1994) Patterns of uronosyl epimerization and 4-/6-O-sulphation in chondroitin/dermatan sulphate from decorin and biglycan of various bovine tissues *Glycobiology* **4(5)**: 685-696

Cherr, G.N., Yudin, A.I. and Overstreet, J.W. (2001) The dual functions of GPI-anchored PH-20: hyaluronidase and intracellular signalling *Matrix Biol.* **20(8)**: 515-525

Claus, V., Jahraus, A., Tjelle, T., Berg, T., Kirschke, H., Faulstich, H. and Griffiths, G. (1998) Lysosomal enzyme trafficking between phagosomes, endosomes, and lysosomes in J774 macrophages. Enrichment of cathepsin H in early endosomes *J. Biol. Chem.* **273(16)**: 9842-9851

Crotty, P.L., Braun, S.E., Anderson, R.A. and Whitley, C.B. (1992) Mutation R468W of the iduronate-2-sulfatase gene in mild Hunter syndrome (mucopolysaccharidosis type II) confirmed by in vitro mutagenesis and expression *Hum. Mol. Genet.* **1(9)**: 755-757

Csóka, A.B., Frost, G.I. and Stern, R. (2001) The six hyaluronidase-like genes in the human and mouse genomes *Matrix Biol.* **20(8)**: 499-508

Csóka, A.B., Frost, G.I., Wong, T. and Stern, R. (1997) Purification and microsequencing of hyaluronidase isozymes from human urine *FEBS Lett.* **417**(**3**): 307-310

Csóka, A.B., Scherer, S.W. and Stern, R. (1999) Expression analysis of six paralogous human hyaluronidase genes clustered on chromosomes 3p21 and 7q31 *Genomics* **60**(**3**): 356-361

Culav, E.M., Clark, C.H. and Merrilees, M.J. (1999) Connective tissues: matrix composition and its relevance to physical therapy *Phys. Ther.* **79**(**3**): 308-319

Deng, X., He, Y. and Martin-Deleon, P.A. (2000) Mouse Spam1 (PH-20): evidence for its expression in the epididymis and for a new category of spermatogenic-expressed genes *J. Androl.* **21**(**6**): 822-832

Denti, A., Sini, P., Tira, M.E. and Balduini, C. (1995) Structural heterogeneity of dermatan sulfate chains: correlation with heparin cofactor II activating properties *Thromb. Res.* **79**(**2**): 187-198

Etchison, J.R., Srikrishna, G. and Freeze, H.H. (1995) A novel method to co-localize glycosaminoglycan-core oligosaccharide glycosyltransferases in rat liver Golgi. Co-localization of galactosyltransferase I with a sialyltransferase *J. Biol. Chem.* **270**(**2**): 756-764

Feugaing, D.D., Tammi, R., Echtermeyer, F.G., Stenmark, H., Kresse, H., Smollich, M., Schonherr, E., Kiesel, L. and Götte, M. (2007) Endocytosis of the dermatan sulfate proteoglycan decorin utilizes multiple pathways and is modulated by epidermal growth factor receptor signaling *Biochimie* **89**(**5**): 637-657

Franzmann, E.J., Schroeder, G.L., Goodwin, W.J., Weed, D.T., Fisher, P. and Lokeshwar, V.B. (2003) Expression of tumor markers hyaluronic acid and hyaluronidase (HYAL1) in head and neck tumors *Int. J. Cancer* **106(3)**: 438-445

Frost, G.I., Csóka, A.B., Wong, T. and Stern, R. (1997) Purification, cloning, and expression of human plasma hyaluronidase *Biochem. Biophys. Res. Commun.* **236**(**1**): 10-15

Fuller, M., Chau, A., Nowak, R.C., Hopwood, J.J. and Meikle, P.J. (2006) A defect in exodegradative pathways provides insight into endodegradation of heparan and dermatan sulfates *Glycobiology* **16**(**4**): 318-325

Fuller, M., Meikle, P.J. and Hopwood, J.J. (2004a) Glycosaminoglycan degradation fragments in mucopolysaccharidosis I *Glycobiology* **14**(**5**): 443-450

Fuller, M., Rozaklis, T., Ramsay, S.L., Hopwood, J.J. and Meikle, P.J. (2004b) Disease-specific markers for the mucopolysaccharidoses *Pediatr. Res.* **56**(**5**): 733-738

Gold, E.W. (1982) Purification and properties of hyaluronidase from human liver. Differences from and similarities to the testicular enzyme *Biochem. J.* **205**(**1**): 69-74

Gowda, D.C., Hogue-Angeletti, R., Margolis, R.K. and Margolis, R.U. (1990) Chromaffin granule and PC12 cell chondroitin sulfate proteoglycans and their relation to chromogranin A *Arch. Biochem. Biophys.* **281**(**2**): 219-224

Griffiths, G. and Gruenberg, J. (1991) The arguments for pre-existing early and late endosomes *Trends Cell Biol.* **1**(**1**): 5-9

Halldorsdottir, A.M., Zhang, L. and Tollefsen, D.M. (2006) N-Acetylgalactosamine 4,6-O-sulfate residues mediate binding and activation of heparin cofactor II by porcine mucosal dermatan sulfate *Glycobiology* **16**(**8**): 693-701

Hemming, R., Martin, D.C., Slominski, E., Nagy, J.I., Halayko, A.J., Pind, S. and Triggs-Raine, B. (2008) Mouse Hyal3 encodes a 45- to 56-kDa glycoprotein whose overexpression increases hyaluronidase 1 activity in cultured cells *Glycobiology* **18**(**4**): 280-289

Hepbildikler, S.T., Sandhoff, R., Kolzer, M., Proia, R.L. and Sandhoff, K. (2002) Physiological substrates for human lysosomal beta-hexosaminidase S *J. Biol. Chem.* **277(4)**: 2562-2572

Hochuli, M., Wüthrich, K. and Steinmann, B. (2003) Two-dimensional NMR spectroscopy of urinary glycosaminoglycans from patients with different mucopolysaccharidoses *NMR Biomed.* **16(4)**: 224-236

Hofinger, E.S., Bernhardt, G. and Buschauer, A. (2007a) Kinetics of Hyal-1 and PH-20 hyaluronidases: comparison of minimal substrates and analysis of the transglycosylation reaction *Glycobiology* **17**(**9**): 963-971

Hofinger, E.S., Hoechstetter, J., Oettl, M., Bernhardt, G. and Buschauer, A. (2008) Isoenzyme-specific differences in the degradation of hyaluronic acid by mammalian-type hyaluronidases *Glycoconj. J.* **25(2)**: 101-109

Hofinger, E.S., Spickenreither, M., Oschmann, J., Bernhardt, G., Rudolph, R. and Buschauer, A. (2007b) Recombinant human hyaluronidase Hyal-1: insect cells versus Escherichia coli as expression system and identification of low molecular weight inhibitors *Glycobiology* **17(4)**: 444-453

Hoppe, W., Rauch, U. and Kresse, H. (1988) Degradation of endocytosed dermatan sulfate proteoglycan in human fibroblasts *J. Biol. Chem.* **263**(**12)**: 5926-5932

Hopwood, J.J. and Elliott, H. (1985) Urinary excretion of sulphated N-acetylhexosamines in patients with various mucopolysaccharidoses *Biochem. J.* **229(3)**: 579-586

Hopwood, J.J., Muller, V., Harrison, J.R., Carey, W.F., Elliot, H., Robertson, E.F. and Pollard, A.C. (1982) Enzymatic diagnosis of the mucopolysaccharidoses: experience of 96 cases diagnosed in a five-year period *Med. J. Aust.* **1(6)**: 257-260

Hunnicutt, G.R., Primakoff, P. and Myles, D.G. (1996) Sperm surface protein PH-20 is bifunctional: one activity is a hyaluronidase and a second, distinct activity is required in secondary sperm-zona binding *Biol. Reprod.* **55(1)**: 80-86

Iozzo, R.V. (1998) Matrix proteoglycans: from molecular design to cellular function *Annu. Rev. Biochem.* **67**(**1**): 609-652

Isogai, K., Sukegawa, K., Tomatsu, S., Fukao, T., Song, X.Q., Yamada, Y., Fukuda, S., Orii, T. and Kondo, N. (1998) Mutation analysis in the iduronate-2-sulphatase gene in 43 Japanese patients with mucopolysaccharidosis type II (Hunter disease) *J. Inherit. Metab. Dis.* **21**(**1)**: 60-70

Jonas, A.J. and Jobe, H. (1990) Sulfate transport by rat liver lysosomes *J. Biol. Chem.* **265**(**29)**: 17545-17549

Karamanos, N.K., Syrokou, A., Vanky, P., Nurminen, M. and Hjerpe, A. (1994) Determination of 24 variously sulfated galactosaminoglycan- and hyaluronan-derived disaccharides by high-performance liquid chromatography *Anal. Biochem.* **221**(**1)**: 189-199

Kearns, A.E., Vertel, B.M. and Schwartz, N.B. (1993) Topography of glycosylation and UDP-xylose production *J. Biol. Chem.* **268**(**15)**: 11097-11104

Kitagawa, H., Kinoshita, A. and Sugahara, K. (1995) Microanalysis of glycosaminoglycan-derived disaccharides labelled with the fluorophore 2-aminoacridone by capillary electrophoresis and high-performance liquid chromatography *Anal. Biochem.* **232**(**1)**: 114-121

Kitagawa, H., Tsutsumi, K., Ujikawa, M., Goto, F., Tamura, J., Neumann, K.W., Ogawa, T. and Sugahara, K. (1997a) Regulation of chondroitin sulfate biosynthesis by specific sulfation: acceptor specificity of serum beta-GalNAc transferase revealed by structurally defined oligosaccharides *Glycobiology* **7**(**4)**: 531-537

Kitagawa, H., Ujikawa, M., Tsutsumi, K., Tamura, J., Neumann, K.W., Ogawa, T. and Sugahara, K. (1997b) Characterization of serum beta-glucuronyltransferase involved in chondroitin sulfate biosynthesis *Glycobiology* **7**(**7)**: 905-911

Kjellen, L. and Lindahl, U. (1991) Proteoglycans: structures and interactions *Annu. Rev. Biochem.* **60**(**1)**: 443-475

Klein, D., Büssow, H., Fewou, S.N. and Gieselmann, V. (2005) Exocytosis of storage material in a lysosomal disorder *Biochem. Biophys. Res. Commun.* **327(3)**: 663-667

Klein, U. and von Figura, K. (1980) Characterization of dermatan sulfate in mucopolysaccharidosis VI. Evidence for the absence of hyaluronidase-like enzymes in human skin fibroblasts *Biochim. Biophys. Acta* **630(1)**: 10-14

Kobayashi, M., Sugumaran, G., Liu, J., Shworak, N.W., Silbert, J.E. and Rosenberg, R.D. (1999) Molecular cloning and characterization of a human uronyl 2-sulfotransferase that sulfates iduronyl and glucuronyl residues in dermatan/chondroitin sulfate *J. Biol. Chem.* **274(15)**: 10474-10480

Koketsu, M. and Linhardt, R.J. (2000) Electrophoresis for the analysis of acidic oligosaccharides *Anal. Biochem.* **283(2)**: 136-145

Kolodny, E.H. and Mumford, R.A. (1976) Human leukocyte acid hydrolases: characterization of eleven lysosomal enzymes and study of reaction conditions for their automated analysis *Clin. Chim. Acta* **70(2)**: 247-257

Kramer, M.W., Golshani, R., Merseburger, A.S., Knapp, J., Garcia, A., Hennenlotter, J., Duncan, R.C., Soloway, M.S., Jorda, M., Kuczyk, M.A., Stenzl, A. and Lokeshwar, V.B. (2009) HYAL-1 hyaluronidase: a potential prognostic indicator for progression to muscle invasion and recurrence in bladder cancer *Eur. Urol.* (in press)

Kreil, G. (1995) Hyaluronidases-a group of neglected enzymes *Protein Sci.* **4(9)**: 1666-1669

Lauder, R.M., Huckerby, T.N. and Nieduszynski, I.A. (2000) A fingerprinting method for chondroitin/dermatan sulfate and hyaluronan oligosaccharides *Glycobiology* **10(4)**: 393-401

Leaback, D.H. and Walker, P.G. (1961) Studies on glucosaminidase. 4. The fluorimetric assay of N-acetyl-beta-glucosaminidase *Biochem. J.* **78**: 151-156

Lepperdinger, G., Mullegger, J. and Kreil, G. (2001) Hyal2-less active, but more versatile? *Matrix Biol.* **20(8)**: 509-514

Lepperdinger, G., Strobl, B. and Kreil, G. (1998) HYAL2, a human gene expressed in many cells, encodes a lysosomal hyaluronidase with a novel type of specificity *J. Biol. Chem.* **273(35)**: 22466-22470

Li, F., Shetty, A.K. and Sugahara, K. (2007) Neuritogenic activity of chondroitin/dermatan sulfate hybrid chains of embryonic pig brain and their mimicry from shark liver. Involvement of the pleiotrophin and hepatocyte growth factor signalling pathways *J. Biol. Chem.* **282(5)**: 2956-2966

Liaw, P.C., Becker, D.L., Stafford, A.R., Fredenburgh, J.C. and Weitz, J.I. (2001) Molecular basis for the susceptibility of fibrin-bound thrombin to inactivation by heparin cofactor II in the presence of dermatan sulfate but not heparin *J. Biol. Chem.* **276(24)**: 20959-20965

Lokeshwar, V.B., Young, M.J., Goudarzi, G., Iida, N., Yudin, A.I., Cherr, G.N. and Selzer, M.G. (1999) Identification of bladder tumor-derived hyaluronidase: its similarity to HYAL1 *Cancer Res.* **59(17)**: 4464-4470

Lowry, O.H., Rosebrough, N.J., Farr, A.L. and Randall, R.J. (1951) Protein measurement with the Folin phenol reagent *J. Biol. Chem.* **193(1)**: 265-275

Maccarana, M., Sakura, Y., Tawada, A., Yoshida, K. and Lindahl, U. (1996) Domain structure of heparan sulfates from bovine organs *J. Biol. Chem.* **271(30)**: 17804-17810

Mancini, G.M., de Jonge, H.R., Galjaard, H. and Verheijen, F.W. (1989) Characterization of a proton-driven carrier for sialic acid in the lysosomal membrane. Evidence for a group-specific transport system for acidic monosaccharides *J. Biol. Chem.* **264(26)**: 15247-15254

Martin, D.C., Atmuri, V., Hemming, R.J., Farley, J., Mort, J.S., Byers, S., Hombach-Klonisch, S., Stern, R. and Triggs-Raine, B.L. (2008) A mouse model of human mucopolysaccharidosis IX exhibits osteoarthritis *Hum. Mol. Genet.* **17(13)**: 1904-1915

Mason, K.E., Meikle, P.J., Hopwood, J.J. and Fuller, M. (2006) Characterization of sulfated oligosaccharides in mucopolysaccharidosis type IIIA by electrospray ionization mass spectrometry *Anal. Chem.* **78(13)**: 4534-4542

Meyers, S.A., Yudin, A.I., Cherr, G.N., VandeVoort, C.A., Myles, D.G., Primakoff, P. and Overstreet, J.W. (1997) Hyaluronidase activity of macaque sperm assessed by an in vitro cumulus penetration assay *Mol. Reprod. Dev.* **46(3)**: 392-400

Miaczynska, M. and Zerial, M. (2002) Mosaic organization of the endocytic pathway *Exp. Cell Res.* **272(1)**: 8-14

Miller, M.J., Costello, C.E., Malmstrom, A. and Zaia, J. (2006) A tandem mass spectrometric approach to determination of chondroitin/dermatan sulfate oligosaccharide glycoforms *Glycobiology* **16(6)**: 502-513

Mio, K. and Stern, R. (2002) Inhibitors of the hyaluronidases *Matrix Biol.* **21(1)**: 31-37

Mitropoulou, T.N., Lamari, F., Syrokou, A., Hjerpe, A. and Karamanos, N.K. (2001) Identification of oligomeric domains within dermatan sulfate chains using differential enzymic treatments, derivatization with 2-aminoacridone and capillary electrophoresis *Electrophoresis* **22(12)**: 2458-2463

Moses, J., Oldberg, A., Cheng, F. and Fransson, L.A. (1997) Biosynthesis of the proteoglycan decorin-transient 2-phosphorylation of xylose during formation of the trisaccharide linkage region *Eur. J. Biochem.* **248(2)**: 521-526

Moses, J., Oldberg, A. and Fransson, L.A. (1999) Initiation of galactosaminoglycan biosynthesis. Separate galactosylation and dephosphorylation pathways for phosphoxylosylated decorin protein and exogenous xyloside *Eur. J. Biochem.* **260(3)**: 879-884

Moskowitz, S.M., Tieu, P.T. and Neufeld, E.F. (1993) Mutation in Scheie syndrome (MPS IS): a G-->A transition creates new splice site in intron 5 of one IDUA allele *Hum. Mutat.* **2(2)**: 141-144

Muckenschnabel, I., Bernhardt, G., Spruss, T., Dietl, B. and Buschauer, A. (1998) Quantitation of hyaluronidases by the Morgan-Elson reaction: comparison of the enzyme activities in the plasma of tumor patients and healthy volunteers *Cancer Lett.* **131(1)**: 13-20

Muenzer, J. (2004) The mucopolysaccharidoses: a heterogeneous group of disorders with variable pediatric presentations *J. Pediatr.* **144(5 Suppl)**: S27-34

Muenzer, J., Lamsa, J.C., Garcia, A., Dacosta, J., Garcia, J. and Treco, D.A. (2002) Enzyme replacement therapy in mucopolysaccharidosis type II (Hunter syndrome): a preliminary report *Acta Paediatr. Suppl.* **91(439)**: 98-99

Muthusamy, A., Achur, R.N., Valiyaveettil, M., Madhunapantula, S.V., Kakizaki, I., Bhavanandan, V.P. and Gowda, C.D. (2004) Structural characterization of the bovine tracheal chondroitin sulfate chains and binding of Plasmodium falciparum-infected erythrocytes *Glycobiology* **14(7)**: 635-645

Natowicz, M.R., Short, M.P., Wang, Y., Dickersin, G.R., Gebhardt, M.C., Rosenthal, D.I., Sims, K.B. and Rosenberg, A.E. (1996) Clinical and biochemical manifestations of hyaluronidase deficiency *N. Engl. J. Med.* **335(14)**: 1029-1033

Neufeld, E.F. and Muenzer, J. (2001) The mucopolysaccharidoses *In*: Scriver, C.R., Beaudet, A.L., Sly, W.S. and Valle, D. (eds.) *The metabolic and molecular bases of inherited disease*, 8th ed., McGraw-Hill, New York, pp 3421-3452

Oguma, T., Tomatsu, S., Montano, A.M. and Okazaki, O. (2007) Analytical method for the determination of disaccharides derived from keratan, heparan, and dermatan sulfates in human serum and plasma by high-performance liquid chromatography/turbo ionspray ionization tandem mass spectrometry *Anal. Biochem.* **368(1)**: 79-86

Ohmi, K., Greenberg, D.S., Rajavel, K.S., Ryazantsev, S., Li, H.H. and Neufeld, E.F. (2003) Activated microglia in cortex of mouse models of mucopolysaccharidoses I and IIIB *Proc. Natl. Acad. Sci.* USA **100(4)**: 1902-1907

Orkin, R.W. and Toole, B.P. (1980) Isolation and characterization of hyaluronidase from cultures of chick embryo skin- and muscle-derived fibroblasts *J. Biol. Chem.* **255(3)**: 1036-1042

Otsu, K., Inoue, H., Tsuzuki, Y., Yonekura, H., Nakanishi, Y. and Suzuki, S. (1985) A distinct terminal structure in newly synthesized chondroitin sulphate chains *Biochem. J.* **227**(**1**): 37-48

Penc, S.F., Pomahac, B., Winkler, T., Dorschner, R.A., Eriksson, E., Herndon, M. and Gallo, R.L. (1998) Dermatan sulfate released after injury is a potent promoter of fibroblast growth factor-2 function *J. Biol. Chem.* **273**(**43**): 28116-28121

Pitt, J.J. and Gorman, J.J. (1997) Oligosaccharide characterization and quantitation using 1-phenyl-3-methyl-5-pyrazolone derivatization and matrix-assisted laser desorption/ionization time-of-flight mass spectrometry *Anal. Biochem.* **248**(**1**): 63-75

Podyma, K.A., Yamagata, S., Sakata, K. and Yamagata, T. (1997) Difference of hyaluronidase produced by human tumor cell lines with hyaluronidase present in human serum as revealed by zymography *Biochem. Biophys. Res. Commun.* **241(2)**: 446-452

Prydz, K. and Dalen, K.T. (2000) Synthesis and sorting of proteoglycans *J. Cell Sci.* **113**(**2**): 193-205

Rai, S.K., Duh, F.M., Vigdorovich, V., Danilkovitch-Miagkova, A., Lerman, M.I. and Miller, A.D. (2001) Candidate tumor suppressor HYAL2 is a glycosylphosphatidylinositol (GPI)-anchored cell-surface receptor for jaagsiekte sheep retrovirus, the envelope protein of which mediates oncogenic transformation *Proc. Natl. Acad. Sci. USA* **98**(**8**): 4443-4448

Ramsay, S.L., Meikle, P.J. and Hopwood, J.J. (2003) Determination of monosaccharides and disaccharides in mucopolysaccharidoses patients by electrospray ionisation mass spectrometry *Mol. Genet. Metab.* **78**(**3**): 193-204

Reed, R.K., Lilja, K. and Laurent, T.C. (1988) Hyaluronan in the rat with special reference to the skin *Acta Physiol. Scand.* **134(3)**: 405-411

Rozaklis, T., Ramsay, S.L., Whitfield, P.D., Ranieri, E., Hopwood, J.J. and Meikle, P.J. (2002) Determination of oligosaccharides in Pompe disease by electrospray ionization tandem mass spectrometry *Clin. Chem.* **48(1)**: 131-139

Sango, K., McDonald, M.P., Crawley, J.N., Mack, M.L., Tifft, C.J., Skop, E., Starr, C.M., Hoffmann, A., Sandhoff, K., Suzuki, K. and Proia, R.L. (1996) Mice lacking both subunits of lysosomal beta-hexosaminidase display gangliosidosis and mucopolysaccharidosis *Nat. Genet.* **14**(**3**): 348-352

Scott, H.S., Litjens, T., Hopwood, J.J. and Morris, C.P. (1992a) A common mutation for mucopolysaccharidosis type I associated with a severe Hurler syndrome phenotype *Hum. Mutat.* **1**(**2**): 103-108

Scott, H.S., Litjens, T., Nelson, P.V., Brooks, D.A., Hopwood, J.J. and Morris, C.P. (1992b) alpha-L-iduronidase mutations (Q70X and P533R) associate with a severe Hurler phenotype *Hum. Mutat.* **1**(**4**): 333-339

Scott, H.S., Litjens, T., Nelson, P.V., Thompson, P.R., Brooks, D.A., Hopwood, J.J. and Morris, C.P. (1993a) Identification of mutations in the alpha-L-iduronidase gene (IDUA) that cause Hurler and Scheie syndromes *Am. J. Hum. Genet.* **53**(**5**): 973-986

Scott, H.S., Nelson, P.V., Litjens, T., Hopwood, J.J. and Morris, C.P. (1993b) Multiple polymorphisms within the alpha-L-iduronidase gene (IDUA): implications for a role in modification of MPS-I disease phenotype *Hum. Mol. Genet.* **2**(**9**): 1471-1473

Shuttleworth, T.L., Wilson, M.D., Wicklow, B.A., Wilkins, J.A. and Triggs-Raine, B.L. (2002) Characterization of the murine hyaluronidase gene region reveals complex organization and cotranscription of Hyal1 with downstream genes, Fus2 and Hyal3 *J. Biol. Chem.* **277**(**25**): 23008-23018

Silbert, C.K., Humphries, D.E., Palmer, M.E. and Silbert, J.E. (1991) Effects of sulfate deprivation on the production of chondroitin/dermatan sulfate by cultures of skin fibroblasts from normal and diabetic individuals *Arch. Biochem. Biophys.* **285**(**1**): 137-141

Silbert, J.E. and Reppucci, A.C., Jr. (1976) Biosynthesis of chondroitin sulfate. Independent addition of glucuronic acid and N-acetylgalactosamine to oligosaccharides *J. Biol. Chem.* **251**(**13**): 3942-3947

Silbert, J.E. and Sugumaran, G. (2002) Biosynthesis of chondroitin/dermatan sulfate *IUBMB Life* **54(4)**: 177-186

Simonaro, C.M., Haskins, M.E. and Schuchman, E.H. (2001) Articular chondrocytes from animals with a dermatan sulfate storage disease undergo a high rate of apoptosis and release nitric oxide and inflammatory cytokines: a possible mechanism underlying degenerative joint disease in the mucopolysaccharidoses *Lab. Invest.* **81(9)**: 1319-1328

Stair-Nawy, S., Csóka, A.B. and Stern, R. (1999) Hyaluronidase expression in human skin fibroblasts *Biochem. Biophys. Res. Commun.* **266(1)**: 268-273

Stern, R. (2003) Devising a pathway for hyaluronan catabolism: are we there yet? *Glycobiology* **13(12)**: 105R-115R

Stern, R. and Jedrzejas, M.J. (2006) Hyaluronidases: their genomics, structures, and mechanisms of action *Chem. Rev.* **106(3)**: 818-839

Storrie, B. (1988) Assembly of lysosomes: perspectives from comparative molecular cell biology *Int. Rev. Cytol.* **111**: 53-105

Sudo, M., Sato, K., Chaidedgumjorn, A., Toyoda, H., Toida, T. and Imanari, T. (2001) ^{1}H nuclear magnetic resonance spectroscopic analysis for determination of glucuronic and iduronic acids in dermatan sulfate, heparin, and heparan sulfate *Anal. Biochem.* **297(1)**: 42-51

Sugahara, K. and Kitagawa, H. (2000) Recent advances in the study of the biosynthesis and functions of sulfated glycosaminoglycans *Curr. Opin. Struct. Biol.* **10(5)**: 518-527

Sugahara, K., Masuda, M., Harada, T., Yamashina, I., de Waard, P. and Vliegenthart, J.F. (1991) Structural studies on sulfated oligosaccharides derived from the carbohydrate-protein linkage region of chondroitin sulfate proteoglycans of whale cartilage *Eur. J. Biochem.* **202(3)**: 805-811

Sugahara, K., Takemura, Y., Sugiura, M., Kohno, Y., Yoshida, K., Takeda, K., Khoo, K.H., Morris, H.R. and Dell, A. (1994) Chondroitinase ABC-resistant sulfated trisaccharides isolated from digests of chondroitin/dermatan sulfate chains *Carbohydr. Res.* **255**: 165-182

Sugumaran, G., Katsman, M. and Silbert, J.E. (1992) Effects of brefeldin A on the localization of chondroitin sulfate-synthesizing enzymes. Activities in subfractions of the Golgi from chick embryo epiphyseal cartilage *J. Biol. Chem.* **267(13)**: 8802-8806

Sugumaran, G., Katsman, M. and Silbert, J.E. (1998) Subcellular co-localization and potential interaction of glucuronosyltransferases with nascent proteochondroitin sulphate at Golgi sites of chondroitin synthesis *Biochem. J.* **329(1)**: 203-208

Sugumaran, G., Katsman, M., Sunthankar, P. and Drake, R.R. (1997) Biosynthesis of chondroitin sulfate. Purification of glucuronosyl transferase II and use of photoaffinity labeling for characterization of the enzyme as an 80-kDa protein *J. Biol. Chem.* **272(22)**: 14399-14403

Takagaki, K., Nakamura, T. and Endo, M. (1988a) Demonstration of an endo-beta-galactosidase and an endo-beta-xylosidase that degrade the proteoglycan linkage region *Biochim. Biophys. Acta* **966(1)**: 94-98

Takagaki, K., Nakamura, T., Izumi, J., Saitoh, H., Endo, M., Kojima, K., Kato, I. and Majima, M. (1994) Characterization of hydrolysis and transglycosylation by testicular hyaluronidase using ion-spray mass spectrometry *Biochemistry* **33(21)**: 6503-6507

Takagaki, K., Nakamura, T., Majima, M. and Endo, M. (1985) Demonstration of chondroitin sulfates degrading endo-beta-glucuronidase activity in rabbit liver *FEBS Lett.* **181(2)**: 271-274

Takagaki, K., Nakamura, T., Majima, M. and Endo, M. (1988b) Isolation and characterization of a chondroitin sulfate-degrading endo-beta-glucuronidase from rabbit liver *J. Biol. Chem.* **263(15)**: 7000-7006

Tatemoto, H., Muto, N., Yim, S.-D. and Nakada, T. (2005) Anti-hyaluronidase oligosaccharide derived from chondroitin sulfate A effectively reduces polyspermy during in vitro fertilization of porcine oocytes *Biol. Reprod.* **72(1)**: 127-134

Taylor, K.R. and Gallo, R.L. (2006) Glycosaminoglycans and their proteoglycans: host-associated molecular patterns for initiation and modulation of inflammation *Faseb J.* **20**(**1**): 9-22

Taylor, K.R., Rudisill, J.A. and Gallo, R.L. (2005) Structural and sequence motifs in dermatan sulfate for promoting fibroblast growth factor-2 (FGF-2) and FGF-7 activity *J. Biol. Chem.* **280**(**7**): 5300-5306

Thonar, E.J., Lohmander, L.S., Kimura, J.H., Fellini, S.A., Yanagishita, M. and Hascall, V.C. (1983) Biosynthesis of O-linked oligosaccharides on proteoglycans by chondrocytes from the swarm rat chondrosarcoma *J. Biol. Chem.* **258**(**19**): 11564-11570

Trowbridge, J.M. and Gallo, R.L. (2002) Dermatan sulfate: new functions from an old glycosaminoglycan *Glycobiology* **12**(**9**): 117R-125R

Tsiganos, C.P., Vynios, D.H. and Kalpaxis, D.L. (1986) Rooster comb hyaluronate-protein, a non-covalently linked complex *Biochem. J.* **235**(**1**): 117-123

Velasco, A., Hidalgo, J., Perez-Vilar, J., Garcia-Herdugo, G. and Navas, P. (1988) Detection of glycosaminoglycans in the Golgi complex of chondrocytes *Eur. J. Cell Biol.* **47**(**2**): 241-250

Vertel, B.M., Walters, L.M., Flay, N., Kearns, A.E. and Schwartz, N.B. (1993) Xylosylation is an endoplasmic reticulum to Golgi event *J. Biol. Chem.* **268**(**15**): 11105-11112

Vogler, C., Levy, B., Galvin, N., Sands, M.S., Birkenmeier, E.H., Sly, W.S. and Barker, J. (2001) A novel model of murine mucopolysaccharidosis type VII due to an intracisternal a particle element transposition into the beta-glucuronidase gene: clinical and pathologic findings *Pediatr. Res.* **49(3)**: 342-348

Volpi, N. (2000) Hyaluronic acid and chondroitin sulfate unsaturated disaccharides analysis by high-performance liquid chromatography and fluorimetric detection with dansylhydrazine *Anal. Biochem.* **277**(**1**): 19-24

Volpi, N. and Maccari, F. (2006) Electrophoretic approaches to the analysis of complex polysaccharides *J. Chromatogr. B* **834**(**1-2**): 1-13

Winchester, B.G. (2001) Lysosomal membrane proteins *Eur. J. Paediatr. Neurol.* **5(Suppl. A)**: 11-19

Yamada, M., Hasegawa, E. and Kanamori, M. (1977) Purification of hyaluronidase from human placenta *J. Biochem. (Tokyo)* **81**(**2**): 485-494

Yamagata, T., Saito, H., Habuchi, O. and Suzuki, S. (1968) Purification and properties of bacterial chondroitinases and chondrosulfatases *J. Biol. Chem.* **243**(**7**): 1523-1535

Yang, H.O., Gunay, N.S., Toida, T., Kuberan, B., Yu, G., Kim, Y.S. and Linhardt, R.J. (2000) Preparation and structural determination of dermatan sulfate-derived oligosaccharides *Glycobiology* **10(10)**: 1033-1039

Zaia, J. (2004) Mass spectrometry of oligosaccharides *Mass Spectrom. Rev.* **23**(**3**): 161-227

Zamfir, A., Seidler, D.G., Kresse, H. and Peter-Katalinic, J. (2003) Structural investigation of chondroitin/dermatan sulfate oligosaccharides from human skin fibroblast decorin *Glycobiology* **13**(**11**): 733-742

Zamfir, A., Seidler, D.G., Schonherr, E., Kresse, H. and Peter-Katalinic, J. (2004) On-line sheathless capillary electrophoresis/nanoelectrospray ionization-tandem mass spectrometry for the analysis of glycosaminoglycan oligosaccharides *Electrophoresis* **25**(**13**): 2010-2016

Zhang, H. and Martin-DeLeon, P.A. (2003) Mouse Spam1 (PH-20) is a multifunctional protein: evidence for its expression in the female reproductive tract *Biol. Reprod.* **69**(**2**): 446-454